



Title	Flammability study on electrolyte components in lithium-ion batteries using a wick combustion method
Author(s)	郭, 峰
Citation	北海道大学. 博士(工学) 甲第13786号
Issue Date	2019-09-25
DOI	10.14943/doctoral.k13786
Doc URL	http://hdl.handle.net/2115/80987
Type	theses (doctoral)
File Information	Feng_Guo.pdf



[Instructions for use](#)

Flammability Study on Electrolyte Components in Lithium-ion Batteries Using A Wick Combustion Method

(灯芯燃焼法を用いたリチウムイオン電池用電解液成分の燃焼
性に関する研究)

Feng GUO

Flammability Study on Electrolyte Components in Lithium-ion Batteries Using A Wick Combustion Method

(灯芯燃焼法を用いたリチウムイオン電池用電解液成分の燃焼
性に関する研究)

By
Feng GUO

Submitted to the Division of Mechanical and Space Engineering,
Graduate School of Engineering, Hokkaido University, Japan,
in Partial Fulfillment of the Requirement for the Degree of
Doctor of Philosophy in Mechanical and Space Engineering

June 2019

Abstract

Fire safety becomes one of the most concern in the development of lithium-ion batteries (LIBs). The main contribution of the LIB fire can be traced back to the combustion of electrolytes. To mitigate the fire hazard of electrolytes, safer components (solvent, lithium salt, and additives) are expected. However, due to the conflict between flame retardancy and battery performance, it requires a quantitative flammability evaluation for a balanced electrolyte formula.

To quantify the flammability limits of organic electrolyte solvents used in lithium-ion batteries, a unique wick combustion system was developed in conjunction with limiting oxygen concentration (LOC) of candle-like flame, named wick-LOC method. By controlling the oxygen-nitrogen ratio of external flow of the wick diffusion flame, the flammability limits (LOC) of electrolyte solvents were determined experimentally.

This thesis first validated the reproducibility and reliability of the wick-LOC method. The LOC of single solvents, binary solvents, and solvents with organophosphorus compound (OPC) additives were quantified and discussed. To make an in-depth understanding of the effect of OPC additives in terms of flame extinction, flame stability limits were then studied. The blow-off regime and quenching regime were found in the flammability maps when OPC added. Finally, the influences of three typical lithium salts (LiPF_6 , LiBF_4 , and LiTFSI) on electrolyte combustion and wick flame extinction were investigated. The gas-phase flame inhibition of LiPF_6 addition was first found by the wick-LOC method. Furthermore, the solid-phase reactions due to the salt decomposition provided some inspirations in suppressing the electrolyte fire.

In Chapter 1, a brief overview of the LIB fire and the hazard of electrolyte components

were introduced. Then, the methods of flammability evaluation for electrolytes were reviewed. Finally, the scope and structure of this thesis were presented.

In Chapter 2, the experimental setup of the wick-LOC method was presented. The experimental conditions and procedures to determine the LOC or flame stability limits were specified. The tested solvents, additives, salts and their combinations for each study were listed as well.

In Chapter 3, validations and applications of the wick-LOC method were conducted. To provide reproducible results under specified conditions, the effects of axial flow velocity, exposed wick length and elapsed time after ignition on the wick-LOC were studied, and the proper experimental conditions were selected for further applications. To validate the reliability of wick-LOC in flammability evaluation, correlation analyses to other flammability properties (flash point, auto-ignition temperature, the heat of combustion and other types of LOC) were conducted. The wick-LOC method was then applied to quantify the flammability of mixed solvents. The linear changes of wick-LOC with mixing ratios were found in the mixture of linear and cyclic carbonates, while the non-linear trends were found in carbonate-ether mixed solvents. To evaluate the flame-retardant effectiveness of organophosphorus compounds (OPCs) as additives in electrolyte solvents, a series of tests were conducted. Results showed that small amounts of OPCs had significant flame-retardant effects, but the efficiency decreased with the higher OPC additions. The effectiveness of four OPCs was distinguished as well.

In Chapter 4, in-depth studies on the wick flame extinction affected by OPC additions were conducted. With the wick-LOC method, two modes of stabilized flame are found, namely, wake flame and full flame. In the case of higher OPC addition, two distinct branches of extinction

processes occurred according to the different flame modes near extinction, and there was no transition from the full flame to wake flame. The flame stability limits are measured as a function of OPC addition for both flame modes. The wake flame is shown to be consistently more stable at low levels of OPC addition. However, once the OPC addition exceeds a critical amount, the full flame shows higher stability with a lower LOC than the wake flame. These phenomena in the two regimes are also found in other cases of high OPC addition (different type of OPC and electrolyte solvent). In terms of the most stable flame mode, the regime switches from the wake flame to the full flame with increasing OPC addition, and they are defined correspondingly as “blow-off regime” and “quenching regime”.

In Chapter 5, the dimethyl carbonate (DMC)-based electrolytes with 1M addition of different lithium salts (LiPF_6 , LiBF_4 , and LiTFSI) were studied comparing with pure DMC and trimethyl phosphate (TMP)-added solvents. The three lithium salts gave unique and distinct flame behaviors including flame shapes, colors and the changes of wick surface until self-extinguishing. The wick-LOC results indicated a considerable flame-retardant effect of LiPF_6 , while other salts have minor effects on the flame extinction. Utilizing the flame spectrum and combustion residue analyses, the roles of salts during combustion were characterized. The PF_6 anion played a similar role with the TMP additive in the gas phase flame inhibition. In the cases of LiPF_6 and LiBF_4 , the solid products (LiF) accumulation blocked the fuel supply from the wick to the flame region. The combustion complexity of LiTFSI on the cotton wick charring and heat release were considered as a potential hazard on solid combustible in the real fire cases.

In Chapter 6, conclusions of the present work and recommendations for the future work were summarized.

Keywords: Lithium ion battery, electrolyte, organic solvents, flammability, limiting oxygen concentration, wick flame, organophosphorus compound, flame retardant, flame stability, lithium salts.

Thesis Supervisor: Osamu Fujita

Title: Professor

Acknowledgements

First and foremost, I would like to express my sincere gratitude to my supervisor, Prof. Osamu Fujita, for his valuable guidance, spontaneous encouragement, untiring efforts, keen interest and whole-hearted supervision through my study in Hokkaido University. Prof. Fujita is the greatest mentor and has brought me into the world of combustion science. It has been a great fortune to be his student. He has taught me, not only how to conduct novel researches, but also how to think myself critically.

I would like to thank Prof. Harunori Nagata, Prof. Hideyuki Ogawa, Prof. Nobuyuki Oshima, Prof. Nozomu Hashimoto for their services on my doctoral committee and also for their help on my study and research in the past years. I also appreciate Prof. Masao Watanabe, Prof. Takashi Nakamura, Prof. Motohiro Sato, Prof. Tsuyoshi Totani, Prof. Yutaka Tabe, Prof. Yuichi Murai, Prof. Hiroshi Terashima for reviewing my thesis.

I would like to express my special appreciation to Prof. Nozomu Hashimoto for his generous help and encouragement on my research. I have learnt a lot from him in the numerical calculation in our collaboration project. I also want to thank Ms. Miho Taga for her kind help for dealing a lot of paper works related to my research and business trips.

I want to acknowledge my master-course advisor, Prof. Guoqing Zhu (CUMT, China). He spent lots of efforts on training me to be a researcher during my master course and encouraged me to study aboard for Ph.D. program.

Special thanks to Dr. Katsunori Nishimura (Hitachi, Ltd.) for the professional support on LIB science, and gratitude to the LIB group members Masaya Inatsuki, Wataru Hase, Yu Ozaki, Smriti Rao, Ryo Aoyagi for the contribution to our research exploration.

I also wish to thank Dr. Hui Yan, Dr. Kenichi Sato, Dr. Yongho Chung, Dr. Hadi Bin Khalid, Dr. Ajit Kumar Dubey, Mr. Yusuke Konno, Mr. Nguyen Truong Gia Tri, Mr. Masashi Nagachi, Mr. Yushin Naito, and Mr. Yu Xia for the inspiring discussion in my research and helps in my life. I appreciate all members in our laboratory as well as the former graduate students for their generous help that makes my life smooth in Hokudai.

I have met many good friends in Hokudai. It is hard to acknowledge all of them here. Some of them are Su Wang, Zhao Wang, Ruoyin Feng, Zhong Huang, Jinming Shi and Lianlian Deng. I am grateful to them for their friendship and the parties enjoyed with them in the past years gave me warmth and happiness.

I acknowledge China Scholarship Council (CSC) for supporting me for 3 years.

With great humble and gratitude, I thank my mother Kunling Liu and my grandma Pei Wang, for their endless love and concern. With their support, I am able to fully devote myself to my study.

Finally, my love Jiayu Huang, thank you for your love and companionship.

List of Abbreviations

LIB	: Lithium-ion battery
FR	: Flame retardant
OPC	: Organophosphorus compound
DMC	: Dimethyl carbonate, $C_3H_6O_3$
EMC	: Ethyl methyl carbonate, $C_4H_8O_3$
DEC	: Diethyl carbonate, $C_5H_{10}O_3$
EC	: Ethylene carbonate, $C_3H_4O_3$
PC	: Propylene carbonate, $C_4H_6O_3$
TEGDME	: Tetraethylene glycol dimethyl ether, $C_{10}H_{22}O_5$
DME	: 1,2-dimethoxyethane, $C_4H_{10}O_2$
TMP	: Trimethyl phosphate, $C_3H_9O_4P$
TEP	: Triethyl phosphate, $C_6H_{15}O_4P$
DMMP	: Dimethyl methyl phosphonate, $C_3H_9O_3P$
TMP(i)	: Trimethyl phosphite, $C_3H_9O_3P$
LiPF ₆	: Lithium hexafluorophosphate
LiBF ₄	: Lithium tetrafluoroborate
LiTFSI	: Lithium bis(trifluoromethanesulfonyl)imide
LiFSI	: Lithium bis (fluorosulfonyl) imide
Da	: Damköhler number, flow time scale / chemical time scale
LOC	: Limiting oxygen concentration (vol%)

LOI	: Limiting oxygen index (vol%)
MP	: Melting point (°C)
BP	: Boiling point (°C)
FP	: Flash point (°C)
AIT	: Auto-ignition temperature (°C)
SET	: Self-extinguishing time (s)
LFL	: Lower flammability limit (vol%)
UFL	: Upper flammability limit (vol%)
MW	: Molar weight
ρ	: Density (g/mL)
VP	: Vapor pressure (Pa)
ΔH_c	: Heat of combustion (kJ/g)
ASTM	: American Society for Testing and Materials
ISO	: International Organization for Standardization
vol	: Volume
wt	: Weight
MSDS	: Material Safety Data Sheets
u_a	: Axial flow velocity (cm/s)
S/V	: Surface volume ratio
XRD	: X-ray diffraction
SEM	: Scanning electron microscopy

Table of Contents

Abstract.....	i
Acknowledgements.....	v
List of Abbreviations.....	vii
Table of Contents.....	ix
List of Figures.....	xii
List of Tables.....	xv
Chapter 1. Introduction.....	1
1.1. Background of Lithium-ion battery fire safety	1
1.1.1. Overview of lithium-ion batteries.....	1
1.1.2. LIB fire safety.....	3
1.2. Safety issues of LIB electrolyte components	6
1.2.1. Organic electrolyte solvents	7
1.2.2. Flame retardant (FR) additives	10
1.2.3. Lithium salts	12
1.3. Flammability evaluation methods for electrolytes.....	15
1.4. Structure of this thesis.....	21
Chapter 2. Experimental approaches.....	23
2.1. Experimental Setup.....	23
2.2. Experimental Designing.....	27
2.2.1. Wick-LOC tests for single and mixed solvents	27
2.2.2. Experimental design of flame stability study with OPC additions.....	28

2.2.3. Experimental design of lithium salts involved combustion tests	29
2.3. Basic Experimental Procedures	30
Chapter 3. Validations and applications of wick-LOC method.....	31
3.1. Wick-LOC with experimental condition variations	31
3.1.1. Axial flow velocity effect	31
3.1.2. Exposed wick length effect.....	33
3.1.3. The effect of elapsed time after ignition.....	34
3.2. Correlations to other flammability properties.....	36
3.3. Applications in binary solvent mixtures	40
3.4. Flame-retardant effectiveness of OPC additives.....	43
3.5. Concluding remarks	48
Chapter 4. OPC effects on the wick flame stability	50
4.1. Two flame modes on a candle-like configuration	50
4.1.1. Introduction of full and wake flame stability	50
4.1.2. Determination of stability limits of the full and wake flames	51
4.2. Flame extinction processes	53
4.2. Flame stability limits of electrolyte solvents with OPC addition	56
4.3. Flame extinction mechanisms.....	61
4.4. Concluding remarks	67
Chapter 5. Lithium salts effects on electrolytes combustion characteristics.....	69
5.1. Flame behaviors at constant oxygen level	69
5.2. Comparison of flame extinction limits	72

5.3. Flame spectrum analyses	74
5.4. Combustion residues analyses	79
5.5. Concluding remarks	82
Chapter 6. Summary and future work.....	83
6.1. Significance of this work	83
6.2. Summary of conclusions.....	84
6.3. Recommendations for future work	86
References	88
Appendix	103
Achievements	105

List of Figures

Fig. 1.1. Various applications of LIBs from small scale to large scale.	1
Fig. 1.2. Schematic of the LIB work mechanism.	2
Fig. 1.3. The structure of 18650 cell LIB [8].	3
Fig. 1.4. Schematic of potential causes of LIB fire accidents [5].	4
Fig. 1.5. Approaches to improve the electrolyte safety.	6
Fig. 1.6. Experimental apparatuses of common flammability tests [42,74–76].	15
Fig. 1.7. Examples of SET methods [29,42,78–80].	16
Fig. 1.8. Examples of oxygen-related methods, (a) premixed-LOC, (b) counterflow-LOC, (c) LOI for a cup burner, (d) LOI using [74,78,86,88,89],	18
Fig. 1.9. Structure of this thesis.	21
Fig. 2.1. Schematic of the wick combustion system.	24
Fig. 2.2. Real images of the wick combustion system.	25
Fig. 2.3. Schematic of the temperature measurement by R-type thermocouple.	25
Fig. 2.4. Optical fiber probe setting for flame spectrum measurement.	26
Fig. 3.1. The wick-LOC of pure DMC and EMC solvents under different axial flow velocities.	32
Fig. 3.2. The wick-LOC of DMC with the change of exposed wick length at a constant axial flow.	33
Fig. 3.3. Wick-LOC dependence of elapsed time after ignition.	35
Fig. 3.4. Correlations of wick-LOC with other flammability properties.	38
Fig. 3.5. Wick-LOC of mixture of linear and cyclic carbonates in different mixing ratios.	

.....	41
Fig. 3.6. Wick-LOC of mixtures of carbonates and ether-based solvents in different mixing ratios.	42
Fig. 3.7. Wick-LOC change with addition of OPC in DMC-based solvents.	44
Fig. 3.8. Wick-LOC change with different OPC additions in EMC-based solvents.....	45
Fig. 3.9. Measured temperature distribution along the centerline of flames given by pure EMC and EMC+TMP 10 wt%.	46
Fig. 4.1. Photographs of flame extinction process under continuous O ₂ decrease. (a) pure DMC, extinction with transition from full to wake flame; (b) DMC+10%TMP, full flame direct extinction (blow-off); (c) DMC+10%TMP, wake flame extinction.....	54
Fig. 4.2. Averaged flame height changes for full flame and wake flame in the cases of pure DMC and DMC+10wt.% TMP with oxygen change rate of 10cm/s in external flow	55
Fig. 4.3. Flammability map given by flame stability limits of DMC-based electrolyte as a function of TMP addition	56
Fig. 4.4. Flame stability limits of DMC-based electrolytes as a function of OPC addition: (a) DMC+TEP; (b) DMC+DMMP.	59
Fig. 4.5. Flame stability limits with the addition of TMP to other linear alkyl carbonates: (a) EMC and (b) DEC.....	60
Fig. 4.6. Schematic description of stabilization of wake (left) and full flame (right) over wick configuration.....	62
Fig. 4.7. Images of stabilized flames of DMC/TMP mixture near stability limits (LOC +	

0.2%).....	63
Fig. 4.8. Normalized flame volume of near-limit stabilized flames as a function of OPC addition in DMC	66
Fig. 5.1. Flame colors and burning behaviors of different DMC-based mixtures: (a) pure DMC, (b) DMC+1wt% TMP, (c) DMC+10wt% TMP, (d) DMC+1M LiPF ₆ , (e) DMC+1M LiBF ₄ , (f) DMC+1M LiTFSI.....	70
Fig. 5.2. Wick-LOC of DMC-based solvents and electrolytes.	72
Fig. 5.3. Measured flame spectrum from different fuels: pure DMC, DMC+10 wt% TMP and DMC+1M LiPF ₆	74
Fig. 5.4. Measured flame spectrum of DMC+1M LiBF ₄ in different stages of combustion: red flame, transition and green flame.	76
Fig. 5.5. Measured flame spectrum of DMC+1M LiTFSI in different stages of combustion: initial state and 30s after ignition.	77
Fig. 5.6. Direct and SEM images of combustion residues on the cotton wick (a) original cotton wick, (b) LiPF ₆ , (c) LiTFSI.....	79
Fig. 5.7. XRD patterns of combustion residues of electrolytes adding LiBF ₄ (green line) and LiPF ₆ (orange line).....	80
Fig. 5.8. Possible path of LiPF ₆ involving in the DMC wick flame.	81

List of Tables

Main body

Table 1.1. Properties of organic solvents from MSDS and [39,40] (a) linear carbonates, (b) cyclic carbonates, (c) ether-based solvents; (d) common solvents.	8
Table 1.2. Properties of OPCs used in this research from MSDS and [39,40].	12
Table 1.3. Properties of lithium salts used in this research from MSDS and [39,40].	14
Table 2.1. Specimens and experimental designing of wick-LOC test for single and mixed solvents.	27
Table 2.2. Carbonates and OPCs mixtures for the determination of flame stability limits.	28
Table 2.3. DMC-based solutions with/without salts for experiments.	29

Appendix

Table A. 1 Specification of combustion chamber	103
Table A. 2 Specification of temperature measurement devices	103
Table A. 3 Specification of flame spectrometer	103
Table A. 4 Specification of temperature measurement devices	104

Chapter 1. Introduction

1.1. Background of Lithium-ion battery fire safety

1.1.1. Overview of lithium-ion batteries

Facing the increasing demand for high power and energy storage sources, the rechargeable lithium battery technologies have been developed for several decades. Since the lithium-ion batteries (LIBs) were first commercialized by Sony in 1991, LIBs have become a part of our daily lives [1]. Due to their high energy density, good performance, no memory effect, and portability, LIBs are widely utilized in many fields like portable electronic devices, uninterrupted power supply (UPS) and electric vehicles (EVs) [2,3]. Applications at larger scales are expected as well, such as for the storage of the excess electricity produced by power plants during off-peak periods of electric grids [4,5]. Some applications of LIBs in different scales were presented in Fig. 1.1 below.



Fig. 1.1. Various applications of LIBs from small scale to large scale.

Since the first practical battery, namely, Volta cell (also called Galvanic cell), was invented 2 centuries ago, the batteries have been developed in various types based principally on the same working mechanism [6]. A typical LIB cell is comprised of four main components, cathode, anode, electrolyte and separator. As shown in Fig. 1.2, the lithium ions move from the cathode to the anode through the electrolyte in a charging state, and the lithium ions move back to the cathode during discharging to apply the current for devices [7].

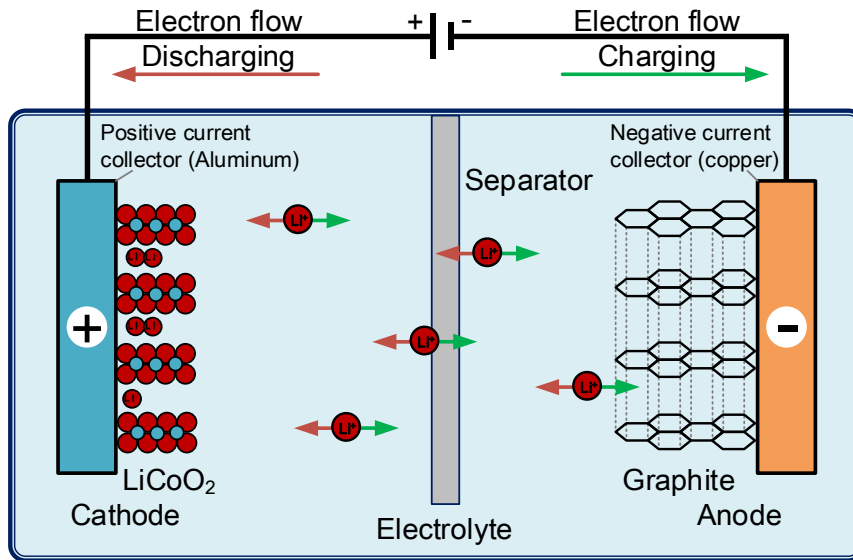


Fig. 1.2. Schematic of the LIB work mechanism.

In recent decades, the materials and shape of the LIB cell have been developed for higher electrochemical performance, more portable size, and safer utilization. The shapes and components of LIB cell differ in various LIB configurations (cylindrical, coin and prismatic cell), and the new structure like plastic Li-ion or Li-ion polymer batteries were developed [2]. In the cylindrical and prismatic cells, the anode, separator and cathode materials were stacked together with the electrolyte and entangled to form a multilayered structure. As one of the most

commonly used cells in commercial electronic devices, the structure of the 18650 cell was shown in Fig. 1.3 from Ref. [8].

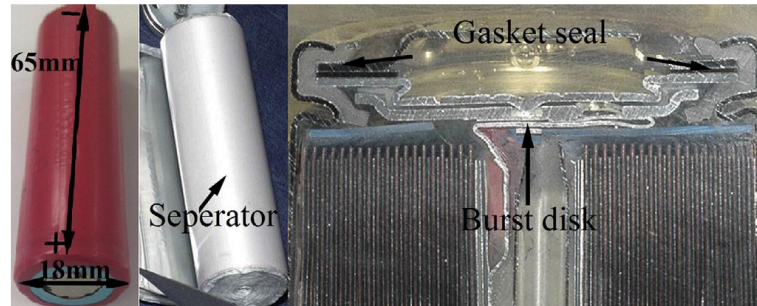


Fig. 1.3. The structure of 18650 cell LIB [8].

1.1.2. LIB fire safety

With the explosive growth of LIB usage, some serious fire and explosion accidents associated with LIBs have been frequently reported in recent years. Since the severe fire broke out at of SONY manufacturing site in November 1995, the safety of LIB has started to be noticed. In the last decade, the battery fire accidents in the laptops have been frequently reported, which led to the battery recall of Dell in 2006 and Panasonic's in 2015. After the explosions of Samsung Note7, the fire safety issues of LIB have attracted attention all over the world. According to the statistics, 582 LIB failure incidents have reported in the five years until fiscal 2017 in Japan, and 70 percent of them involved with fires [9]. According to the Federal Aviation Administration (FAA), 258 air/airport incidents involving LIB failures have been recorded from 1991 to 2019 [10]. Now, with the explosive growth of the market share of electric vehicles like Tesla, EV fires have threatened public safety. From 2011 to 2015, 31 EV fire incidents have been recorded in China, it faced many difficulties in fire prevention and suppression.

Wang and co-workers have summarized the potential causes of LIB fire accidents [5], as shown in Fig. 1.4. The direct cause of LIB fire is the thermal runaway from the internal components' reactions. Under misuse or abuse conditions, like crushing, overcharging, short-circuit, overheating and so on, the internal short circuit is triggered as a common cause of thermal runaway. With the heat accumulating inside the sealed battery cell, the internal pressure increases dramatically until the explosion occurs. The venting aerosol and gas are generally flammable and toxic including electrolytes and some byproducts. Based on the fire triangle, the utilization of flammable electrolytes brought the main fuel to the LIB fire and explosion. In the case of internal thermal decomposition of the cathode, or the venting cases to the external air, oxygen can be supplied continuously. With the presence of internal exothermic reaction or external heat source, electrolytes can be ignited leading to the flaming even larger propagation incidents.

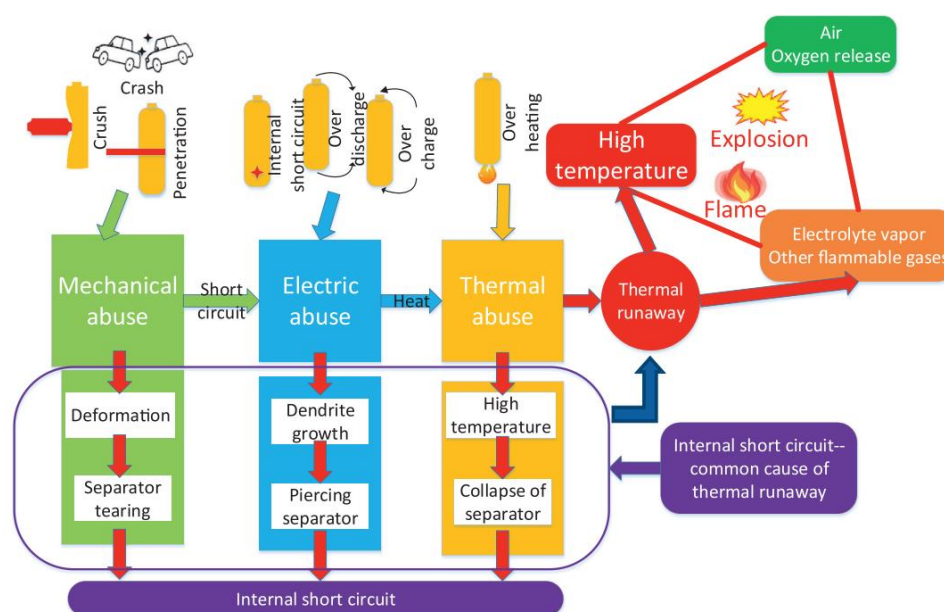


Fig. 1.4. Schematic of potential causes of LIB fire accidents [5].

To prevent the LIB fire and control the damage, a series of researches in different scales and levels have been done, both from the communities of LIB and fire safety. From the perspective of LIB products managers or firefighters, detecting and suppressing the LIB fire are the main tasks. However, from the perspective of manufacturers and researchers, the safety issues of LIB cells and components are considered with the balance of safety, performance, and cost. For the safety on a system or a battery cell level, the safety devices are incorporated into the LIB including safety vents, current interrupt device, positive temperature coefficient device, shutdown separator, and battery management system [5,11]. For the inherent safety of the LIB on a component level, screening safer materials are necessary, including the modifications of cathode and anode materials [5,12], adding functional additives like flame retardant (FR) additive [13–15], and other types of safer/nonflammable electrolytes [16–18]. As the fuel in the battery, the electrolyte components are directly linked to the fire hazard of LIB cell and systems. The main objective of this thesis is finding a scientific way to screen safer material of electrolyte components.

1.2. Safety issues of LIB electrolyte components

Even the most of LIB fire accidents are directly caused by the thermal runaway reactions under the various failure modes, the main contribution of the LIB fire can be traced back to the combustion of electrolytes [12]. As the organic solvents (carbonates or ethers) are used in commercial battery electrolytes, their flammability can bring larger combustion energy than the electrochemical energy of the battery cell [19]. To mitigate the fire hazard of electrolytes, the flammability and thermal instability studies are always required including different organic solvents and multi-component electrolytes with lithium salts or some functional additives.

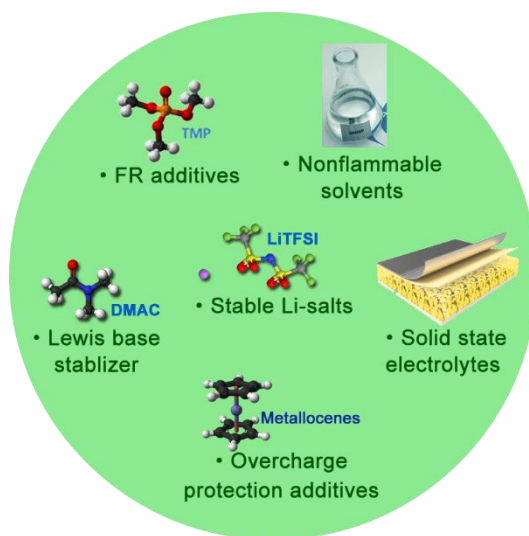


Fig. 1.5. Approaches to improve the electrolyte safety.

There are several approaches to enhance electrolyte safety in the LIB industry [1,12,20–22], as shown in Fig. 1.5. Considering the instability of lithium salts, replacing the traditional lithium salt (LiPF_6) to more stable salts [23–26] or adding Lewis base stabilizer [27,28] in the commercial LIB could be the effective methods to improve the safety of LIB. To reduce the

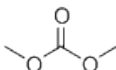
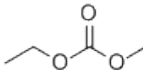
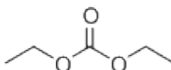
flammability of electrolyte solvents, series of studies on FR additives [14,29–31], new nonflammable solvents [16,18,32] and solid-state electrolytes [2,33] have been conducted and still under development. Besides the above approaches, adding overcharge protection additives like redox shuttle [34,35] or electrochemical polymerization additives [36,37] could be an effective way to consume excess current or release the voltage under overcharge condition. For a deeper understanding of the other functional additives, ionic liquid or solid-state electrolyte from the perspective of material science, the review paper by Wang [12], Xu [1,22], and Liu [38] could be helpful. While, in this thesis, the potential contributions to the electrolyte flammability were considered to be three main components, organic electrolyte solvents, flame retardant additives, and lithium salts.

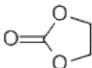
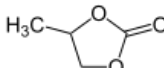
1.2.1. Organic electrolyte solvents

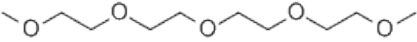
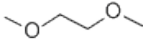
In the LIB industry, an ideal electrolyte solvent should fulfill at least four requirements [22]: (1) Enough dissolubility of lithium salts for a high dielectric constant; (2) unreactive to the charged surface of electrode during cell operation; (3) Wide operation range in both low and high temperature; (4) Non-flammable, non-toxic and eco-friendly. However, the reality is far from perfect.

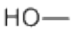

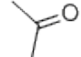
At present, most of the commercial LIB cells utilize organic solvents to dissolve the lithium salts, particularly, 1 mole/L LiPF_6 dissolved in the mixture of linear carbonates (DMC, EMC, and DEC), cyclic carbonate (EC and PC) or ethers (DME and TEGDME). Some properties of the organic electrolyte solvents and some common solvents mentioned in this thesis were shown in Table 1.1.

Table 1.1. Properties of organic solvents from MSDS and [39,40] (a) linear carbonates, (b) cyclic carbonates, (c) ether-based solvents; (d) common solvents.

(a) Linear carbonates solvents:	Dimethyl carbonate	Ethyl methyl carbonate	Diethyl carbonate
Abbreviations	DMC	EMC	DEC
Structure			
Formula	C ₃ H ₆ O ₃	C ₄ H ₈ O ₃	C ₅ H ₁₀ O ₃
MW	90.08	104.1	118.13
ρ (g/mL)	1.07	1.015	0.9751
MP (°C)	2~4	-55	-43
BP (°C)	90	109	126
FP (°C)	18	23	33
AIT (°C)	458	446	445
VP (Pa)	5300	3600	1100
ΔH _c (kJ/g)	14.45	18.12	21.06

(b) Cyclic carbonates solvents:	Ethylene carbonate	Propylene carbonate
Abbreviations	EC	PC
Structure		
Formula	C ₃ H ₄ O ₃	C ₄ H ₆ O ₃
MW	88.06	102.09
ρ (g/mL)	1.321	1.206
MP (°C)	36.4	-49
BP (°C)	248	242
FP (°C)	160	132
AIT (°C)	465	455
VP (Pa)	1.31	6
ΔH _c (kJ/g)	12.84	17.81

(c) Ether-based solvents:	Tetraethylene glycol dimethyl ether	1,2-dimethoxyethane
Abbreviations	TEGDME	DME
Structure		
Formula	$C_{10}H_{22}O_5$	$C_4H_{10}O_2$
MW	222.28	90.12
ρ (g/mL)	1.01	0.868
MP ($^{\circ}C$)	-30	-58
BP ($^{\circ}C$)	276	84
FP ($^{\circ}C$)	140	-2
AIT ($^{\circ}C$)	265.56	202
VP (Pa)	<1.33	6400
ΔH_c (kJ/g)	27.86	26.59

(d) Common solvents:	Methanol	Ethanol	Acetone
Structure			
Formula	CH_3OH	C_2H_5OH	CH_3COCH_3
MW	32.04	46.069	58.08
ρ (g/mL)	0.791	0.7893	0.791
MP ($^{\circ}C$)	-98	-114.14	-94
BP ($^{\circ}C$)	64.7	78.28	56.05
FP ($^{\circ}C$)	12	14	-18
AIT ($^{\circ}C$)	470	363	561
VP (Pa)	13020	5950	30600
ΔH_c (kJ/g)	19.94	26.64	31.36

Most compositions of LIB electrolytes are based on two or more solvents for a balance performance. The combinations of electrolyte solvents should follow the electrochemical

performance and interaction of anode, cathode and separator materials, which were intensively explained by Jow and Xu [1,21,22]. Simultaneously, safety-related properties should be concerned from many perspectives. For a wider operation temperature range, a lower melting point (MP) and a higher boiling point (BP) of electrolyte solvents are required, like PC and TEGDME. A lower vapor pressure (VP) can reduce the risk of battery bursting. Flash point (FP) and auto ignition temperature are intuitive indicators to rank the ignitability of solvents. By comparing with the common solvents, we can have a basic understanding of the electrolyte solvents related to the safety concern. However, with the complexity of fire phenomena, scientific and quantitative flammability evaluations are expected to be improved.

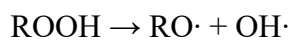
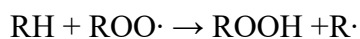
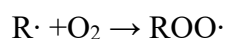
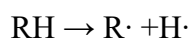
1.2.2. Flame retardant (FR) additives

In the current stage, using FR additives to inhibit the electrolyte flammability is an effective strategy without changing the structure of the LIB cell [41,42]. The FR additives generally have a physical or chemical effect to reduce the flammability of electrolytes. The physical FR effects basically can be classified as cooling and isolation effects which are limited by using FR additives alone. Thus, the chemical flame inhibition is the main approach to reduce the flammability of electrolyte by capturing the free radical during combustion. At present, the FR additives in LIB industry can be divided into four categories [12]: organophosphorus compounds (OPC) additives, Halogen additives (e.g. fluoride), ionic liquid additives and composite retardant additives.

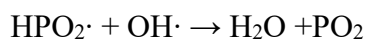
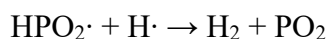
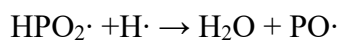
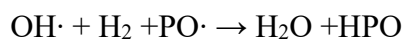
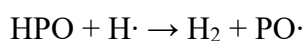
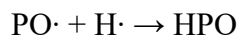
Among the FR additives, the organophosphorus compounds (OPCs) are promising candidates with low environmental impact [13,18,30,43] and excellent flame-retardant effectiveness [44,45] in comparison with halogenated flame retardants. Their suitable physical

characteristics, good compatibility, and low cost attracted a widespread attention [46]. The chemical flame inhibition effects of OPCs are widely studied to clarify the reaction mechanisms in the flames [45,47–55]. The intermediate products (radicals like PO, PO₂, HPO, and HPO₂) from the phosphorus source involved in the catalytic reactions with OH and H radicals generate in the electrolyte solvents combustion. The radical formation reactions of electrolyte combustion (R1) and radical capturing mechanisms (R2) can be summarized as below [52,56,57]:

- Electrolyte combustion reactions: (R1)



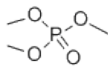
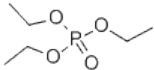
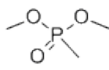
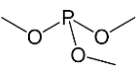
- Flame retardant reactions: (R2)



The OPC additives reduce the flammability of LIB effectively, but most of them degrade the battery performance in terms of electrochemical cycling stability, capacitance and/or lifetime [14,58]. Therefore, improvements are being sought which requires higher flame

retardancy with less OPC addition. To meet such balance, the flammability of electrolyte mixtures should be quantified, and the flame-retardant effectiveness of OPC additives should be evaluated as well. Table 1.2 shows some properties of typical OPCs mentioned in this thesis.

Table 1.2. Properties of OPCs used in this research from MSDS and [39,40].

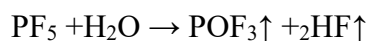
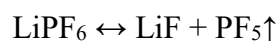
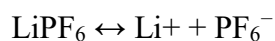
OPCs:	Trimethyl Phosphate	Triethyl Phosphate	Dimethyl Methyl Phosphonate	Trimethyl Phosphite
Abbreviations	TMP	TEP	DMMP	TMP(i)
Structure				
Formula	C ₃ H ₉ O ₄ P	C ₆ H ₁₅ O ₄ P	C ₃ H ₉ O ₃ P	C ₃ H ₉ O ₃ P
MW	140.08	182.15	124.08	124.08
ρ (g/mL)	1.217	1.07	1.16	1.054
MP (°C)	-70	-56	-50	-78
BP (°C)	180-195	216	181	110
FP (°C)	107	111	69	28
AIT (°C)	391	454	unavailable	250
VP (Pa)	113	52	128	3200
ΔH _c (kJ/g)	15.71	21.13	unavailable	unavailable

1.2.3. Lithium salts

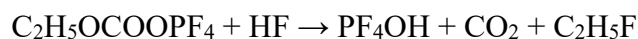
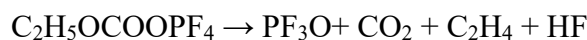
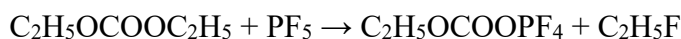
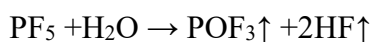
The instability of lithium salts plays an important role in LIB fire safety, especially in the thermal runaway reactions. On the other hand, thermal stabilities of lithium salts and their based electrolytes have been widely investigated at elevated temperature (usually up to 350°C) [26,59–62]. The onset of thermal decomposition and endo-/exothermic processes of salts are always of interest to these studies.

Lithium hexafluorophosphate (LiPF₆), even as the most popular salt in the commercial LIBs, has unsatisfying thermal stability and easily hydrolyzes [63–65]. Lu and co-workers [66] have found that LiPF₆ showed the worst thermal stability among six kinds of lithium salts. The onset of LiPF₆ decomposition was found at 255 °C in DEC and 235-240°C in DMC [23]. Replacements of LiPF₆ with a better thermal and moisture stabilities are expected [63,64,66–72]. The hydrolyzation (R3) and thermal decomposition reactions (R4) of LiPF₆ have been reported by Kawamura and co-workers [23,73], as shown below:

- Hydrolyzation reactions: (R3)



- Thermal decomposition reactions in DEC solvent: (R4)

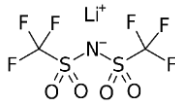


From the reactions above, besides the heat release from the reactions, the toxic gases (HF, POF₃) and other byproducts are also threatening the LIB cell and environmental safety. However, LiPF₆ has good advantages in ion conductivity, solubility, and low cost. Moreover,

the decomposition of LiPF_6 can form AlF_3 to provide a protective passivation film on the aluminum current collector. These facts make people love and hate LiPF_6 .

In this thesis, two other lithium salts, lithium tetrafluoroborate (LiBF_4) and lithium bis(trifluoromethanesulfonyl)imide [LiTFSI , $\text{LiN}(\text{CF}_3\text{SO}_2)_2$] were utilized to comparing with the LiPF_6 . Even LiBF_4 is a kind of traditional lithium salts used in past decades, its improved cell cycling performance at low/high temperature brought it back into recent research favor [1,22]. LiTFSI is a new promising lithium salt researched in recent years. All of these salts showed better thermal stabilities attempting to replace the LiPF_6 in the battery cell [22,66,70]. Some basic information of three lithium salts used in this research were shown in Table 1.3.

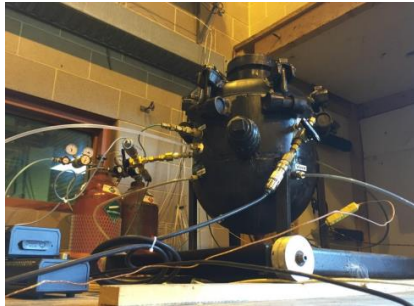
Table 1.3. Properties of lithium salts used in this research from MSDS and [39,40].

Lithium salts:	Lithium hexafluorophosphate	Lithium tetrafluoroborate	Lithium bis(trifluoromethanesulfonyl)imide
Structure	$\text{Li}^+ \left[\begin{array}{c} \text{F} \\ \\ \text{F}-\text{P}-\text{F} \\ \\ \text{F} \end{array} \right]^-$	$\text{Li}^+ \left[\begin{array}{c} \text{F} \\ \\ \text{F}-\text{B}-\text{F} \\ \\ \text{F} \end{array} \right]^-$	
Formula	LiPF_6	LiBF_4	$\text{LiTFSI} / \text{LiN}(\text{CF}_3\text{SO}_2)_2$
MW	151.905	93.746	287.075
ρ (g/mL)	1.5	0.852	1.33
MP ($^\circ\text{C}$)	200	310	234

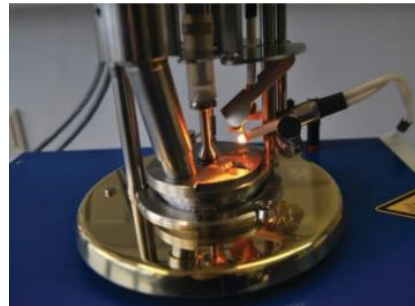
The thermal stability focuses more on the prevention of electrolytes ignition and thermal runaway; however, it might be inadequate to reflect the role of lithium salts on burning cases of electrolytes. Suitable flammability studies should be conducted to make a better understanding of the role of lithium salts on electrolytes combustion.

1.3. Flammability evaluation methods for electrolytes

Take a glance at literature, that various methods have been used for the flammability evaluation of electrolytes at a component level. For the preliminary screening of single component used for electrolyte solvent, several flammability characteristics are referred including upper or lower flammable limits (UFL/LFL), flash points (FP), the auto-ignition temperature (AIT), the heat of combustion (ΔH_c) and so on [22,42,74], as shown in Fig. 1.6. These methods could provide exact information of a single component from the perspectives of fuel and heat in fire triangle. However, the electrolyte formulation in LIB always comprises several chemical components (solvents, additives, and lithium salts) with a specific ratio, which make it difficult to characterize the mixed electrolytes by above properties only. Simpler method for evaluate the flammability of the full electrolyte formulation are expected.



(a) UFL/LFL measurement [74]



(b) FP measurement (closed cup) [42]



(c) AIT apparatus [75]



(d) Bomb calorimeter [76]

Fig. 1.6. Experimental apparatuses of common flammability tests [42,74–76].

Therefore, a convenient indicator in terms of burning behavior, self-extinguishing time (SET), is frequently used for electrolyte mixtures. SET describes the duration or the rate of burning for an ignited electrolyte sample, but the test method varies in different publications, as shown in Fig. 1.7. Most of the SET tests use open flame method to ignite the solvent directly [42] or through a porous media soaking with electrolyte [1,22,29,77–80]. in which the results are strongly affected by the ignition source and the liquid volatilization, especially the evaporation rate of highly volatile solvent.

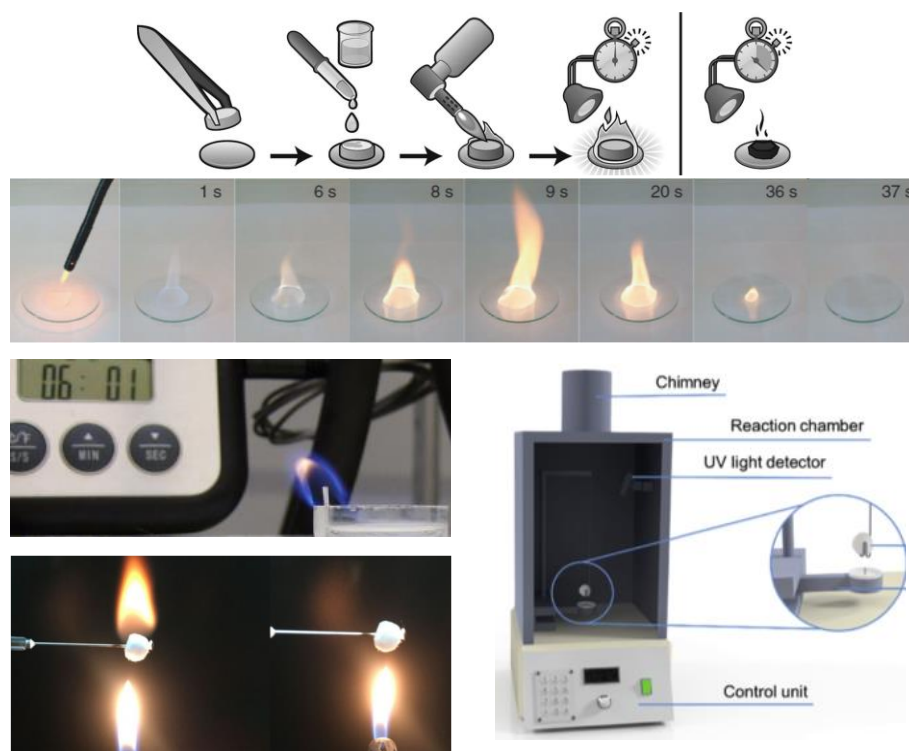


Fig. 1.7. Examples of SET methods [29,42,78–80].

Besides the SET tests, two common methods were also reported, the linear flame propagation tests [78,80] modified from ASTM D5306 [81] and the test of flame extinction probability [31,82,83]. However, due to the considerable errors caused by the uncertain

experimental conditions, SET and the other two methods often give qualitative classifications of flammability (“flammable”, “flame-retarded” and “non-flammable”).

The methods above can hardly quantify of the improvement in flame retardancy following the modification of the electrolyte formulations, especially by changing the type or quantity of co-solvents and fire-retardant additives. Along with the breakthroughs of safer electrolytes in LIB research [12], the improvements of flammability evaluation method for electrolytes is also expected, which requires quantitative indicators and scientific understandings of electrolyte combustion.

For the quantitative material screening, the limiting concentrations of oxidizers for ignition or flame extinction are widely used for evaluating the flammability of gaseous fuels, volatile solvents and solid materials [84]. Comparing with the flash point, the flammable limits in terms of oxidizer are more related to the chemical properties in the combustion reaction of fuels. If the oxygen can be controlled below such limits, the burning of the fuels can be prevented. The limiting oxygen concentration (LOC) of the premixed combustion is a typical indicator to evaluate the flammability of gases and vapors like LFL and UFL, as shown in Fig. 1.8(a). Utilizing a spherical premixed chamber, Zabetakis has measured the premixed-LOC of many volatile liquid fuels [85]. Osterberg also tested nine organic solvents in the pharmaceutical industry to prevent explosion hazard [86]. However, the electrolytes in commercial LIB always use low vapor pressure components like propylene carbonate or ethylene carbonate mixing with other solvents, additives, and lithium salts. It is difficult to vaporize such mixed electrolytes for the premixed combustion tests. Thus, some researchers [74,87] preferred to use premixed combustion test for the flammability evaluation of vent gases from the LIB cell during thermal

runaway rather than original mixed electrolytes in LIB.

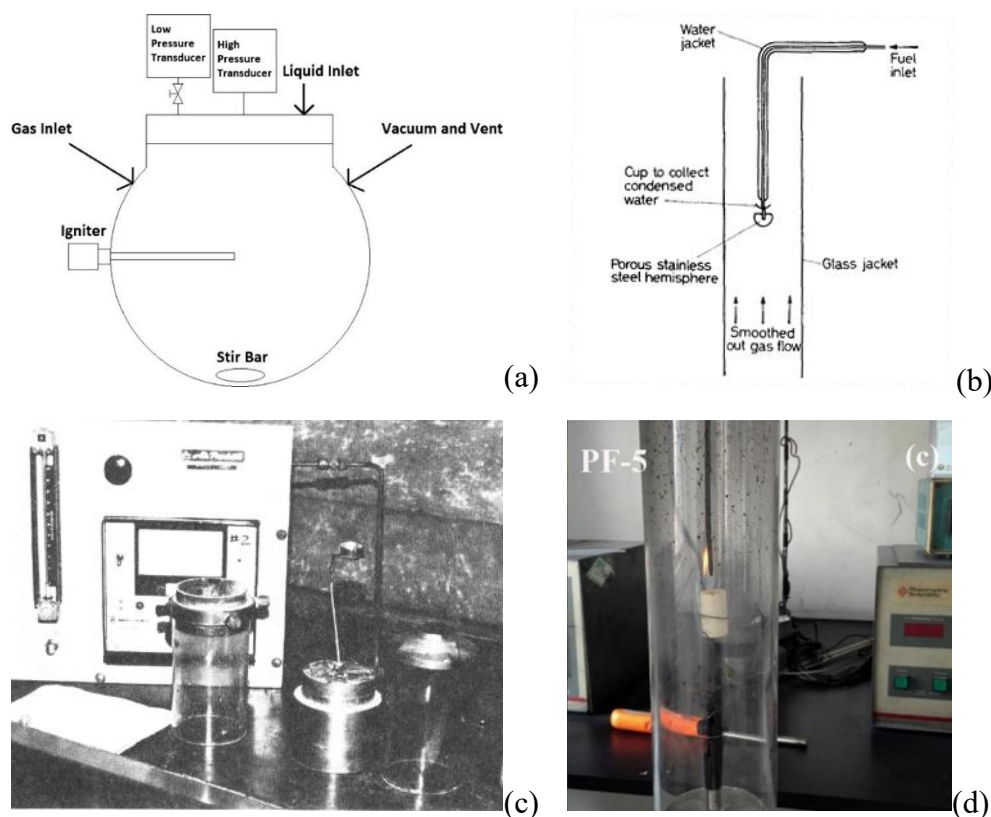


Fig. 1.8. Examples of oxygen-related methods, (a) premixed-LOC, (b) counterflow-LOC, (c) LOI for a cup burner, (d) LOI using [74,78,86,88,89],

Therefore, a simpler diffusion flame configuration might be more suitable for electrolyte combustion involving evaporation and decomposition of multi-component fuel. The LOCs for counterflow diffusion flames of liquid fuels have been reported by Simmons [90], which can quantify the flammability of gas and liquid mixtures effectively, as shown in Fig. 1.8(b). However, igniting the liquids with high boiling points made the LOC determination more difficult and less accurate. The applications of counterflow-LOC for liquid electrolytes may have more difficulties when dealing with viscous solvents and additives.

Besides counterflow-LOC, the limiting oxygen index (LOI) in a candle-like diffusion flame has been widely accepted as an index of the fire-retardant characteristics of solid materials in ISO 4589-2 [91]. LOI is the oxygen concentration at extinction in a defined axial flow velocity under specific test conditions. The terms of limiting oxygen index (LOI) or limiting oxygen concentration (LOC) of a wire, rod, and wick flame have been widely reported in the combustion and fire researches [92–100]. Some modifications for electrolyte solutions are reported using a small cup burner [78,101,102], as shown in Fig. 1.8 (c-d). When the electrolyte burned in such small cup (typically a pool fire configuration), the concentration of high boiling point component can be increased by distillation effect, which may overrate the flame-retardant effectiveness.

The flammability evaluation methods reviewed above can provide two types of properties of materials: ignition-related and propagation-/extinction-related properties. The ignition-related properties like FP and AIT are important to prevent a fire or a flaming incident. Besides, the flame propagation-/extinction-related properties are equally important to the material flammability, especially for fire suppression and damage control; however, sometimes they are not consistent with each other [89]. When we want to evaluate the effects of lithium salts on an electrolyte fire, each stage of fire should be considered including heating, ignition, growth and fire extinction. The ideal thermal stability of lithium salts is required to be comparable to that of other electrolyte components without exceeding the operative temperature of LIBs [33]; while in a fire case of much higher temperature, the salts can play a distinct role which may affect the fire suppression and toxicity [8,103]. To understand how the addition of salts affecting the fire growth and extinction fundamentally, the combustion analyses are expected. The pool

fire of electrolytes with 1M LiPF₆ addition has been investigated using a cone calorimeter by Fu and co-workers [104], while heat release rate and flame geometry results can hardly reflect the effect of salts explicitly. Eshetu and co-workers have used Tewarson calorimeter to study the lithium salts effect on fire behaviors under an oxygen-rich environment. Their results showed that the heat release rate profiles and toxic gas products differed in electrolytes of LiPF₆ and LiFSI [105]. Variations of limiting oxygen index (LOI) tests were also applied in screening safer electrolyte formulations [16,78,88,101,102], however, the insights into salts effect on electrolytes combustion are still in development.

In this thesis, a unique wick combustion system will be introduced to measure the limiting oxygen concentration of the wick flame (called wick-LOC) for electrolyte mixtures and try to solve the drawback of above existing test methods. The combustion experiments using the wick-LOC method have covered different fuel cases including single solvents, mixed solvents, OPC-added solvents, and salt-added electrolytes. During the experimental studies, some limitations of the wick-LOC method would be found in OPC- and salt- added mixtures. Then, the specific procedures for LOC determinations will be defined to minimize the potential disturbances, more in-depth findings for OPC- and salt- added cases will be discussed as well.

1.4. Structure of this thesis

In this thesis, a unique wick combustion system was developed in conjunction with limiting oxygen concentration (LOC) of candle-like flame, named wick-LOC method. Using the wick-LOC method, the flammability study of electrolyte components in LIB were conducted. The structure of this thesis is shown in Fig. 1.9.

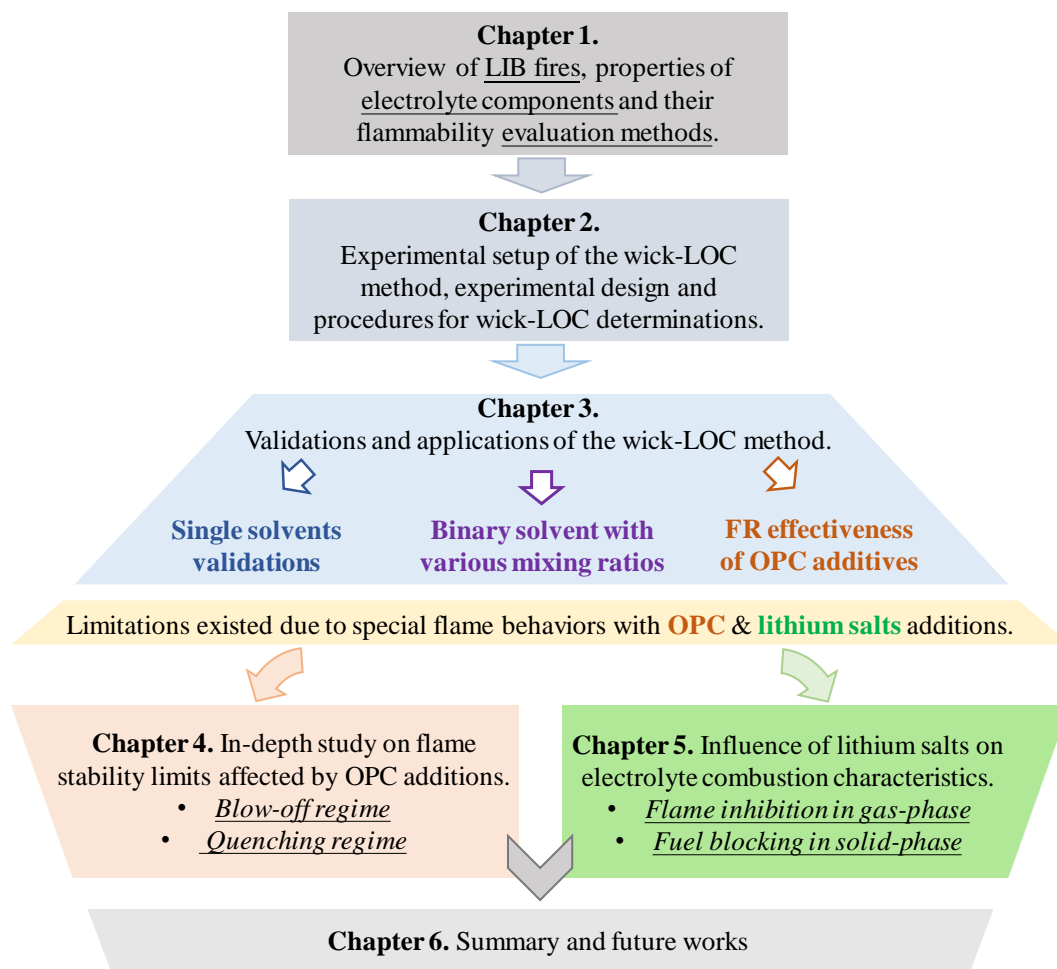


Fig. 1.9. Structure of this thesis.

After introducing the scientific background and the experimental approaches, this thesis first validated the reproducibility and reliability of the wick-LOC method. Then the wick-LOCs

of single solvents, binary solvents, and solvents with OPC additives were quantified and discussed. Due to the special flame behaviors found in the OPC- and Li-salts-added cases, the limitations of the wick-LOC method were considered, and the specific experimental procedures for the OPC- and Li-salts-added cases were redefined. To make an in-depth understanding of the effect of OPC additives in terms of wick flame extinction, the flame stability limits (the full and wake flames) were then studied. The blow-off regime and quenching regime were found in the flammability maps when OPC added. Finally, the influences of three typical lithium salts (LiPF_6 , LiBF_4 , and LiTFSI) on electrolyte combustion and wick flame extinction were investigated. The gas-phase flame inhibition of LiPF_6 addition can be found by the wick-LOC method. Furthermore, the solid-phase reactions due to the salt decomposition provided some inspirations in suppressing the electrolyte fire. In the final section, the significance of the research was explained, conclusions were summarized, and the future work was recommended for deeper and wider development.

Chapter 2. Experimental approaches

This chapter describes the experimental setup of the wick-LOC method. A series of flammability tests for different electrolyte solutions were designed and the basic experimental procedures to determine the wick-LOCs were elaborated.

2.1. Experimental Setup

A series of combustion experiments on electrolytes were carried out by the means of the wick-LOC method which was modified from the LOI method. The limiting oxygen concentration (LOC) to sustain the flame can be determined by precise adjustment of oxygen. The schematic of the experimental setup used to determine the wick-LOC value is shown in Fig. 2.1. The wick combustion system comprises three main parts: the fuel supply system (left) to provide a continuous supply of electrolytes; the gas control system (right) to supply the well-mixed gas of N_2/O_2 ; and the combustion chamber (middle) to generate a wick-stabilized flame under a constant external flow velocity.

Along the centerline of the combustion chamber, the wick complying with the quality standards specified in ASTM D1322 [106] was supported by a stainless alloy tube (inner diameter: 6mm, outer diameter: 7mm) in the glass chamber. The wick height was set at 7 mm above the top end of the stainless tube. The capillarity effect helped to feed a liquid fuel (a mixed solvent) from the wick bottom to the wick tip.

The fuel supply system is shown on the right side of the schematic. It can keep a constant liquid level ensuring a stable and sufficient fuel supply rate during combustion. To avoid the

wick self-trimming (baking wick fabric) due to the weak capillary effect, the liquid level of fuel was stabilized at 10 mm lower than the top end of the stainless tube in each test of this research.

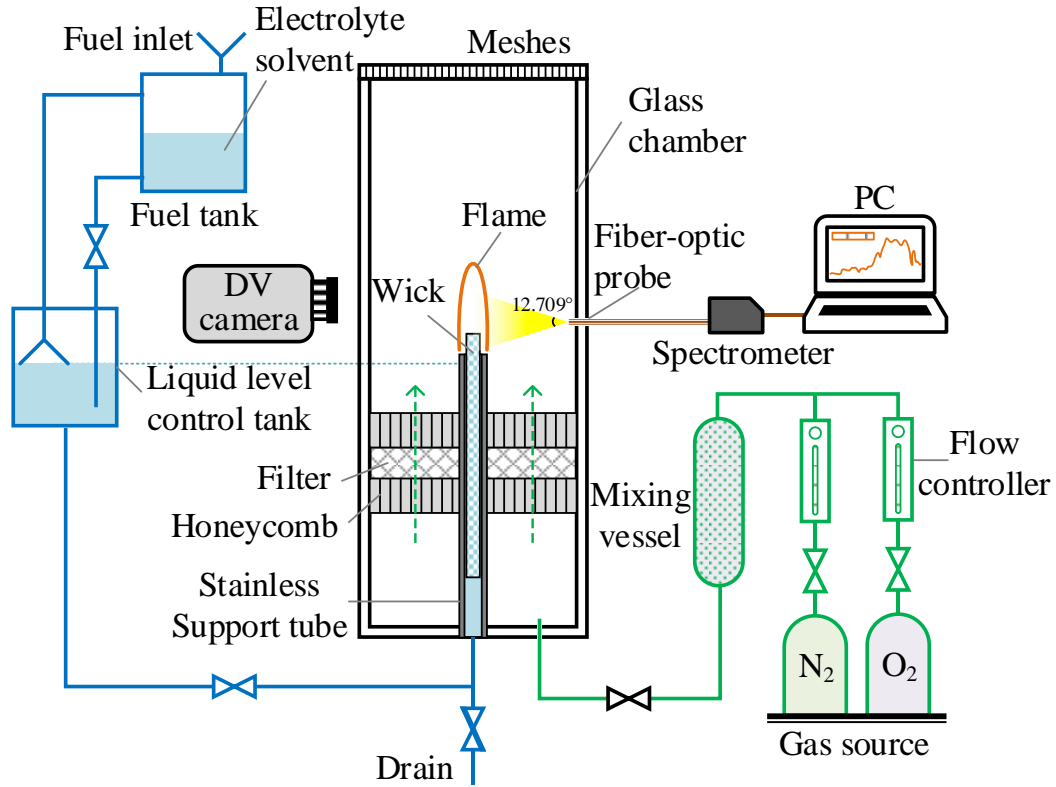


Fig. 2.1. Schematic of the wick combustion system.

The gas supply system is illustrated on the left side of the schematic. The supplied gas was comprised of nitrogen and oxygen. The nitrogen and oxygen were well mixed before feeding to the combustion chamber. The oxygen concentration of external gas was set in the range of 0 to 25 vol% with a small increment of 0.1 vol%. The mixed gas was uniformly supplied by a honeycomb flow straightener to the wick combustion region. The axial flow velocity, an average value of total flow flux divided by the cross-sectional area of the chamber, could be varied from 4 cm/s to 18 cm/s. The real images were shown as Fig. 2.2.



(a) Overview



(b) Wick combustion chamber

Fig. 2.2. Real images of the wick combustion system.

Under a specific experimental condition, the liquid fuel vapor burned at the tip of the wick and the diffusion flame was recorded by a digital video camera (Panasonic HDC-TM70). When a stable flame formed, an R-type thermocouple of 0.3 mm in diameter was placed on an X-Y motion stage to measure the flame temperature of each position. The thermocouple wire was shaped to minimize the thermal conduction from touching the flame, as shown in Fig. 2.3.

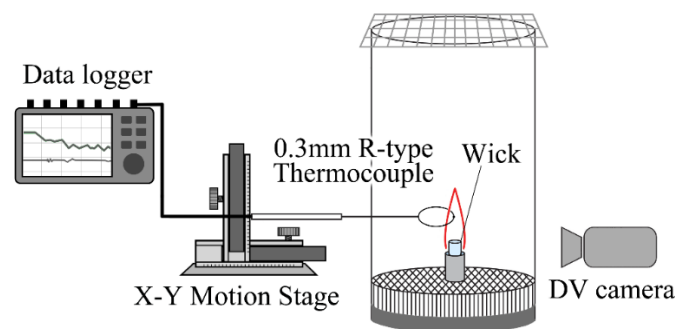


Fig. 2.3. Schematic of the temperature measurement by R-type thermocouple.

The fiber-optic spectrometer was utilized to measure the light emission intensities of the

flames given by the electrolytes. The detailed setting as shown in Fig. 2.4 to minimize the disturbance of inserted probe on the flow field. The measurable wavelength range of the spectrometer is 200~800 nm, which has been commonly applied in combustion research [107,108]. For each trial of flame spectrum measurement, the dark mode was recalibrated to avoid the effect from external light.

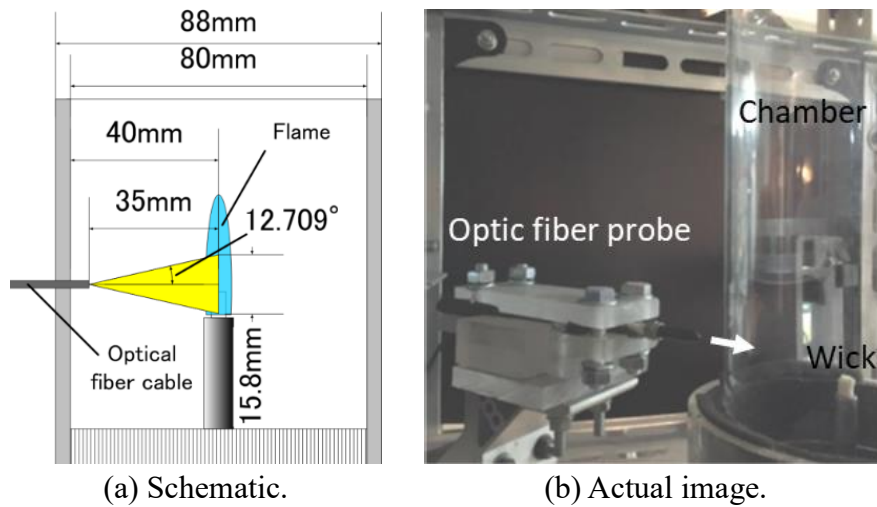


Fig. 2.4. Optical fiber probe setting for flame spectrum measurement.

The combustion residues from burned wick were characterized utilizing scanning electron microscopy (SEM) and X-ray diffraction (XRD) from Material Analysis and Structure Analysis Open Unit (MASAOU) in Hokkaido University. The specifications of the combustion chamber, DV camera, spectrometer, and thermocouple can be found in the appendix.

2.2. Experimental Designing

2.2.1. Wick-LOC tests for single and mixed solvents

For the validation and application of the wick-LOC method, seven kinds of typical solvents used in LIB electrolyte, three referred solvents and four kinds of OPC additives were used and tested by wick-LOC method. To clarify wick-LOC of single, binary and OPC added solvent, the specimen was prepared, and experiments were designed, as shown in Table 2.1. The wick-LOC of mixed solvents were evaluated depending on the mixing ratio of carbonate or ether solvents and the addition of OPCs, respectively. The experimental results and related discussions will be presented in Chapter 3.

Table 2.1. Specimens and experimental designing of wick-LOC test for single and mixed solvents.

(a) Single solvents tests (4 types solvents)							
•	Linear carbonates:	DMC		EMC		DEC	
•	Cyclic carbonates:	EC		PC			
•	Ether-based solvents:	DME		TEGDME			
•	Referred common solvents:	Methanol		Ethanol		Acetone	
(c) Binary solvents tests (varying mixing ratios)							
•	EC / EMC:	0 / 1	1 / 4	1 / 2	1 / 1	2 / 1	
•	PC / EMC:	0 / 1	1 / 4	1 / 2	1 / 1	2 / 1	4 / 1 1 / 0
•	PC / TEGDME:	0 / 1	1 / 4	1 / 2	1 / 1	2 / 1	4 / 1 1 / 0
•	PC / DME:	0 / 1	1 / 4	1 / 2	1 / 1	2 / 1	4 / 1 1 / 0
•	DMC / DME:	0 / 1	1 / 4	1 / 2	1 / 1	2 / 1	4 / 1 1 / 0

(c) Solvents with OPCs [varying OPC additions (wt%)]					
• DMC + TMP:	0	1	2	5	10
• DMC + TEP:	0	1	2	5	10
• EMC + TMP:	0	--	--	5	10
• EMC + TEP:	0	--	--	5	10
• EMC + DMMP:	0	--	--	5	10
• EMC +TMP(i):	0	--	--	5	10

2.2.2. Experimental design of flame stability study with OPC additions

In the study of wick flame stability limits with OPC additions, three linear alkyl carbonates, namely, DMC, EMC, and DEC, were tested; and three types of typical OPC addition, namely, TMP, TEP and DMMP, were examined. The experiments were designed as Table 2.2. The selected solvents have a similar structure with different numbers of ethyl group. The OPC additives have different molar numbers of phosphorus per unit mass.

Table 2.2. Carbonates and OPCs mixtures for the determination of flame stability limits.

Solvents with OPCs [varying OPC additions (wt%)]					
• DMC + TMP:	0	1	2	5	10
• DMC + TEP:	0	1	2	5	10
• DMC + DMMP:	0	1	2	5	10
• EMC + TMP:	0	1	2	5	10
• DEC + TMP:	0	1	2	5	10

2.2.3. Experimental design of lithium salts involved combustion tests

In the combustion experiments involving lithium salts, DMC was selected as the only solvent to unify the solvent effect. As the simplest linear carbonate commonly used in LIB electrolytes, DMC can simplify the electrolyte formulation in this comparative study and highlight the role of lithium salts. Three kinds of typical lithium salts, (LiPF₆, LiBF₄, and LiTFSI) were selected as 1 mole/L (1M) addition in DMC. As the control groups, pure DMC, DMC with 1 and 10 wt% TMP additions were compared as well, to show closer flame extinction limits (LOC) to the salt-added cases. The DMC solvent (purity > 99.5%) and salts (purity > 99.5%) were obtained from Kanto Chemical Co., Inc.; the TMP (purity > 98%) was obtained from TCI Co., Ltd. Six DMC-based solutions/solvent were prepared as shown in Table 2.3.

Table 2.3. DMC-based solutions with/without salts for experiments.

Designation	Solvent	Flame retardant addition	Lithium salts addition
(a)	DMC	--	--
(b)	DMC	1 wt% TMP	--
(c)	DMC	10 wt% TMP	--
(d)	DMC	--	1M LiPF ₆
(e)	DMC	--	1M LiBF ₄
(f)	DMC	--	1M LiTFSI

2.3. Basic Experimental Procedures

Based on the traditional LOI tests [109], the experimental procedure of wick-LOC method was specified. At the beginning of the experiment for a new solvent, the wick tip was ignited to generate a stabilized flame at a higher oxygen concentration (above 20 vol%). The oxygen was then reduced step by step under the constant flow velocity until flame extinction, where the approximate value of LOC can be found in this preliminary test. Subsequently, repeated tests (at least four times) were conducted for a precise and reliable wick-LOC by averaging the repeated results. The minimum decrement of oxygen concentration was 0.1 vol%. According to the replacement time (less than 20s) of the new gas mixture in the gas supply system, the test duration at a given condition was at least one minute. If the flame kept burning more than 1 min, it was judged as “sustained combustion” state which required further oxygen decrease. Otherwise, it was judged as “extinction” state when the flame was extinguished within one minute. The wick-LOC value was determined between the closest two states above. In the experiment, each wick was only used in the same solvent or solution. The wick was refreshed by cutting the used head in each test to avoid the aging effect of the wick.

Chapter 3. Validations and applications of wick-LOC method

This chapter presents the experimental results using the wick-LOC method. Firstly, to specify a proper experimental condition, the sensitivity of the LOC results to different experimental conditions were investigated. Then, the reliability of the wick-LOC results was validated and discussed by correlating with other flammability properties. Applications of the wick-LOC method followed to quantify the flammability of binary solvents with different mixing ratios. Finally, the wick-LOCs of solvents with OPC additions were measured to distinguish the FR efficiency of OPCs in different additive amounts and types.

3.1. Wick-LOC with experimental condition variations

To analyze the effects of experimental conditions on the wick-LOC results, three aspects were considered: the axial flow velocity, the exposed wick length and the elapsed time after ignition. The experimental conditions specified in the previous section were validated and applied to the flammability comparison of single-component solvent and mixtures.

3.1.1. Axial flow velocity effect

The flow velocity is one of the environmental variables that may affect the material flammability and fire dynamics in an opposed flow diffusion flame configuration [93,110]. According to the blow-off mechanism of a wire or candle-like flame [111,112], the increased axial flow velocity can shorten the fluidic residence time and lead to an earlier extinction (corresponding to a higher LOC). The axial flow velocity of the wick-LOC method should also be specified properly for the flammability comparison of solvents. The wick-LOC results of

pure DMC and pure EMC in different axial flow velocities were measured experimentally, shown in Fig. 3.1. The plot indicates the relation between wick-LOC values and axial flow velocities from 4 cm/s to 18 cm/s. The flame images show the stabilized flames near flame extinction (LOC+0.2 vol%). Overall, the LOC of each solvent climbed gradually with the increase of axial flow velocity, and the DMC was less flammable than EMC with around 1 vol% difference of LOC. The velocity dependence of LOC could be explained as the change of residence time in Damköhler under the blow-off mechanism as mentioned above. While in a low external flow from 4 cm/s and 18 cm/s, the wick-LOC seemed to be not sensitive to the axial flow velocity. Referring to some researches [113,114], the 10 cm/s was selected as a standard value of the axial flow velocity in the following tests.

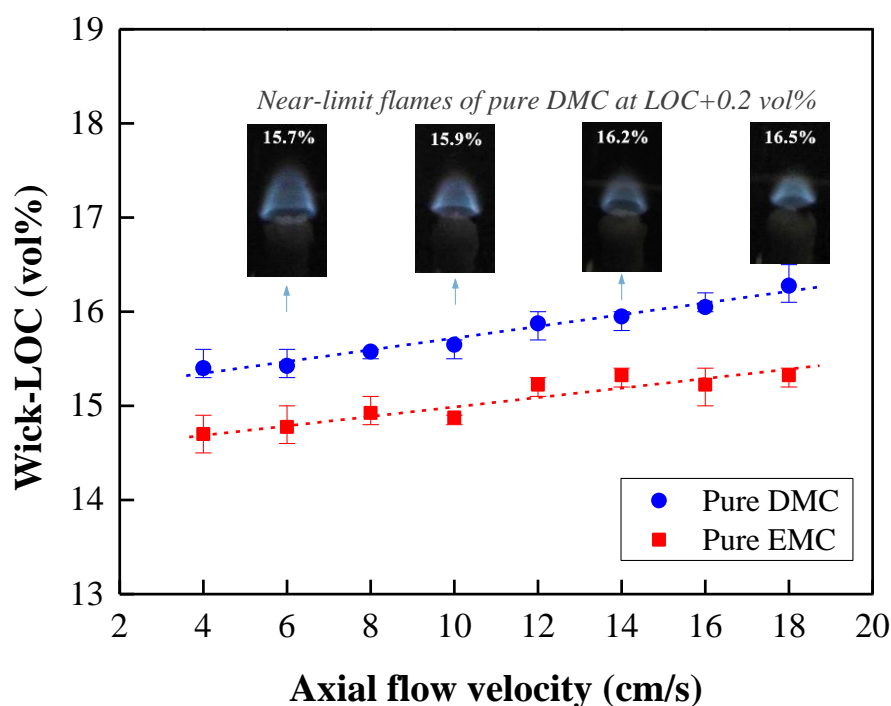


Fig. 3.1. The wick-LOC of pure DMC and EMC solvents under different axial flow velocities.

3.1.2. Exposed wick length effect

The wick length exposed out of the stainless tube should be proper to supply sufficient fuel to the wick tip and provide reproducible LOC results. As the geometry of exposed wick may affect the capillary action of the liquid fuel [115] and the wick flame shapes [98], a fixed exposed wick length should be specified for reliable flammability comparison in this work. Thus, the wick-LOC change of pure DMC flame under the 10cm/s axial flow velocity were measured experimentally by varying exposed wick length from 2mm to 15mm, as shown in Fig. 3.2.

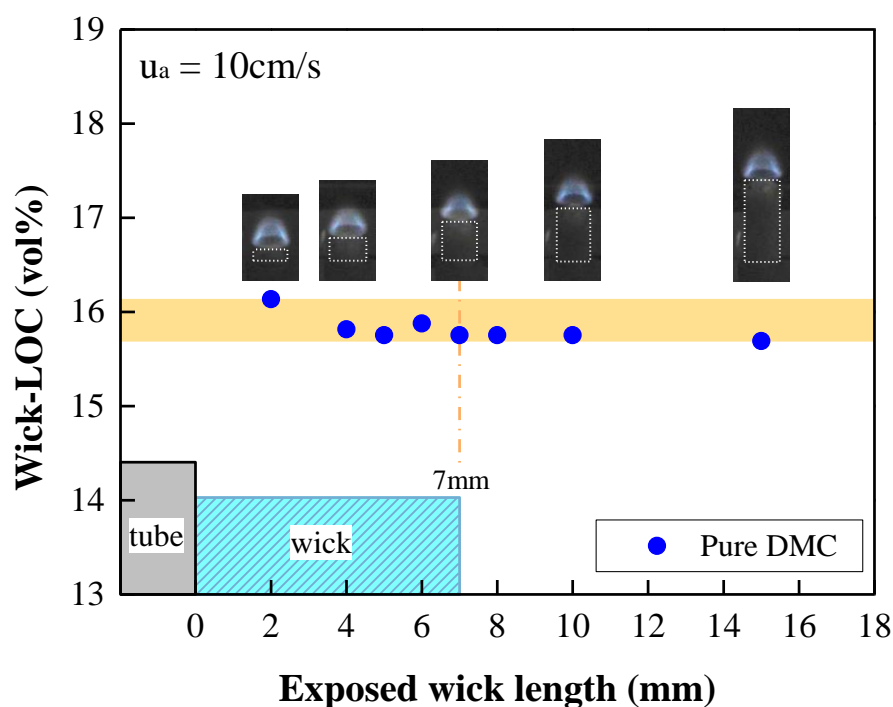


Fig. 3.2. The wick-LOC of DMC with the change of exposed wick length at a constant axial flow.

The flame images indicate the near limit stabilized flames (LOC+0.2 vol%). As the local flow velocity around the boundary layer decreases along with the downstream, the LOC of

15mm exposed wick length showed lower (flame is more stable) than that of 2 mm. However, it shows that the exposed length of wick in the range of 4 to 10 mm had limited effects on the wick-LOC results. In this paper, the exposed wick length of 7mm was chosen as a standard value because of ease of wick handling.

3.1.3. The effect of elapsed time after ignition

To quantify the flame-retardant effectiveness of OPC-added solution, one of the concerns is the effect of distillation (solution composition might change during combustion due to the boiling point difference). For example, the boiling points of DMC, TMP, and TEP are 90 °C, 197 °C, and 216 °C, respectively, as shown in Table 2.1. If in a pool fire configuration of DMC with addition OPC, the OPC concentration may increase during continuous burning, which would overrate the flame-retardant efficiency of OPC addition. To clarify such potential effect on wick-LOC results, the elapsed time after the ignition was varied from 0 to 30 mins, and the wick-LOCs of DMC with 10 wt% addition of TMP and TEP were measured, as shown in Fig. 3.3.

The elapsed time in the experiments was the burning time at the axial flow velocity (u_a) of 10 cm/s and the oxygen concentration of 20%. The wick-LOC results had a small fluctuation range (within 0.4%) which was close to error range of a single experiment. It indicated that the wick-LOC was almost independent of the elapsed time after ignition. Due to the continuous fresh fuel supplement from the tank to the wick, the OPC organic solvents can be supplied to the flame zone simultaneously with negligible distillation effect.

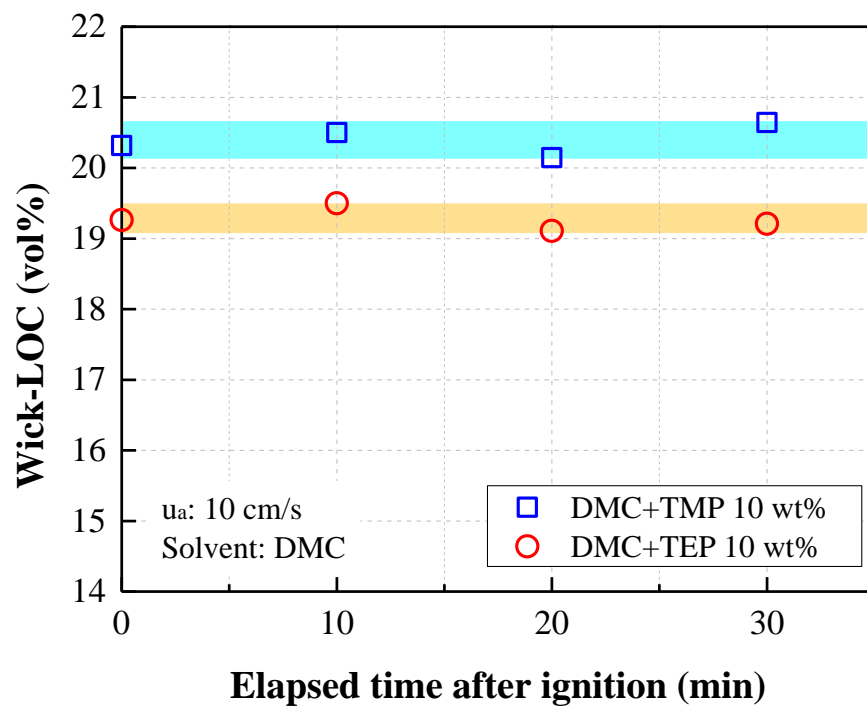
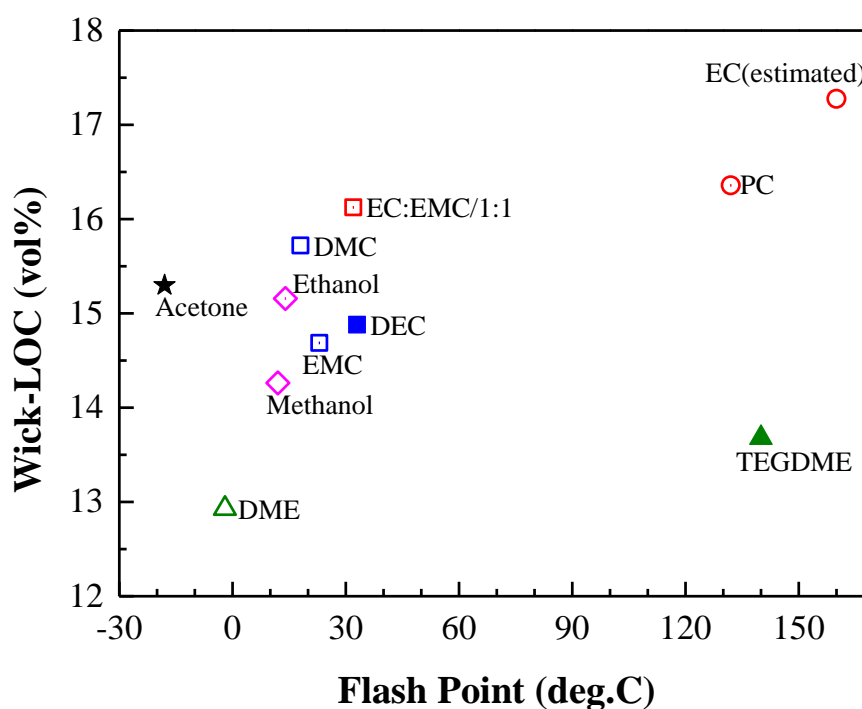


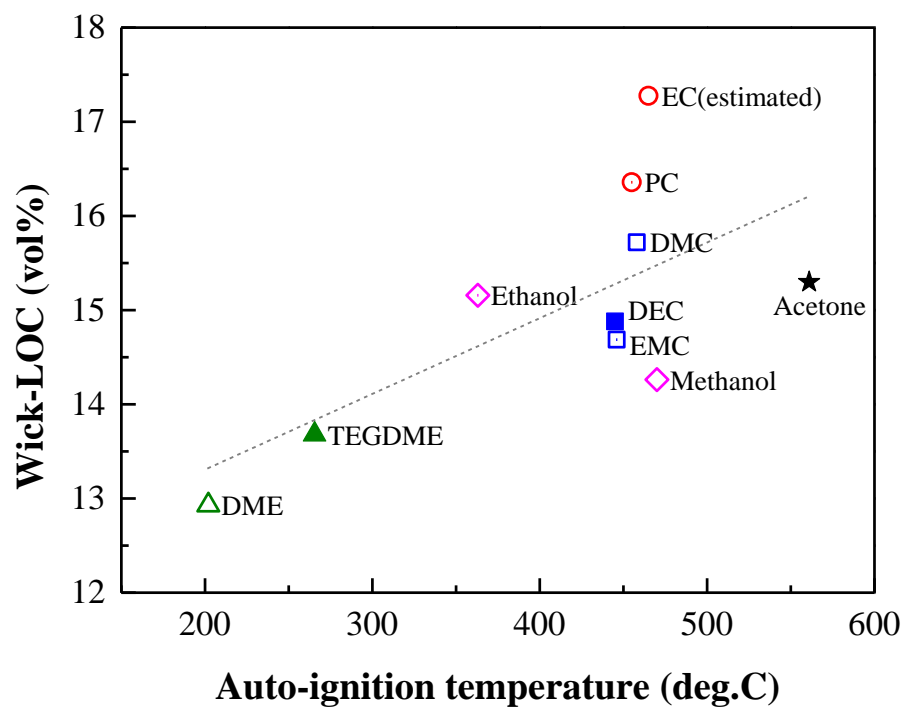
Fig. 3.3. Wick-LOC dependence of elapsed time after ignition.

3.2. Correlations to other flammability properties

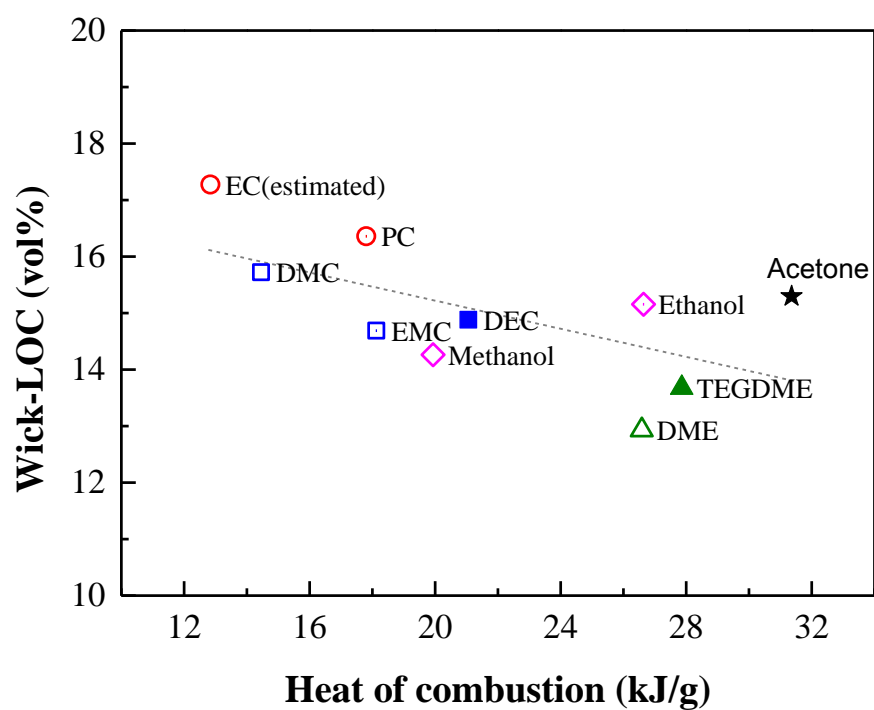
As modified from the LOI method, the wick-LOC reflects the extinction limit of a candle-like diffusion flame, where the lower wick-LOC obtained means more flammable the solvent is. To validate the wick-LOC method for the flammability evaluation of LIB electrolyte solvents, the correlation study of wick-LOC with other flammability properties was conducted, as shown in Fig. 3.4. The wick-LOCs of typical electrolyte solvents and reference solvents in Table 1.1 were tested and compared with their flash points, auto-ignition temperatures, the heats of combustion and other types of LOC available. The flash point of EC:EMC/1:1 is referred from Hess [42]; the heat of combustion values were referred from databases [39,40]; and the wick-LOC of pure EC was estimated in Fig. 3.5 in next section.



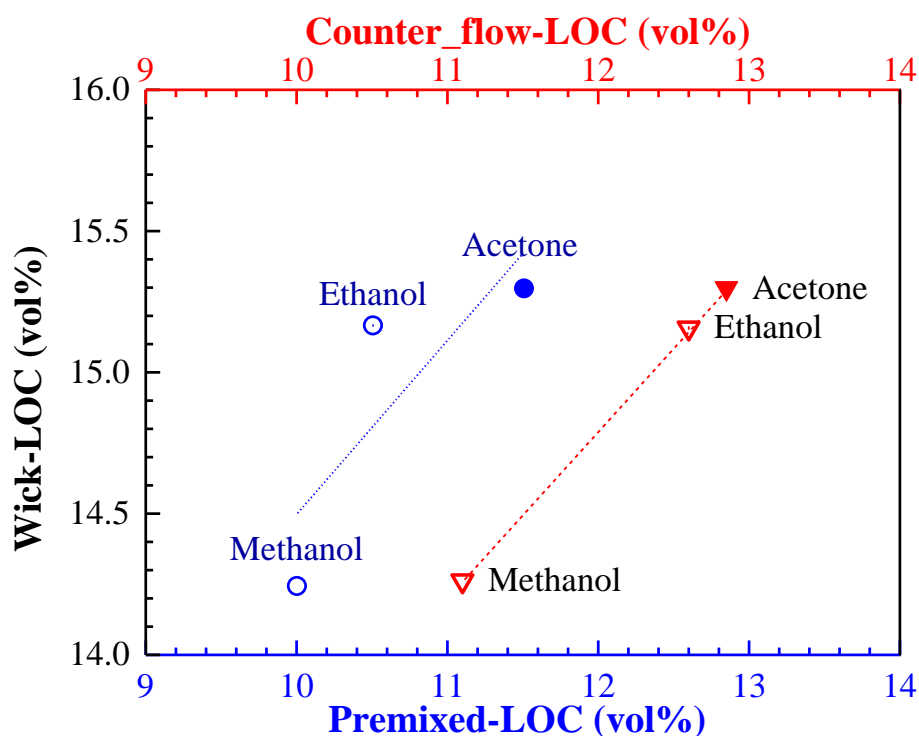
(a) Flash point



(b) Auto-ignition temperature



(c) Heat of combustion



(d) Premixed- and counterflow-LOC

Fig. 3.4. Correlations of wick-LOC with other flammability properties.

In Fig. 3.4 (a), the wick-LOCs showed a rough positive correlation to the flash points of most solvents but excluding Acetone and TEGDME. The wick-LOC would be controlled by the burning velocity of the fuel-air mixture due to insufficient oxygen for combustion; while the flash point is more related to the evaporation process to generate flammable mixture. Therefore, Acetone gave the lowest flash point but medium LOC value; while TEGDME was very flammable in low oxygen level even with a high flash point.

The wick-LOC had broad correlations to auto-ignition temperature and heat of combustion corresponding to Fig. 3.4 (b) and (c). Since the AIT and ΔH_c are related to the activation energy and enthalpy of formation, respectively, they can reflect the chemical aspects of combustion. Technically, the wick-LOC is considered to be dominated by the Damköhler number (the ratio of flow residence time to chemical time). Transport properties and chemical parameters like

activation energy and pre-exponential factor can affect the LOC result simultaneously. The scientific expression of the LOC is expected to use several intrinsic properties of the material for discovering the essential meaning.

In comparison with other recognized LOC methods in Fig. 3.4 (d), the wick-LOC of reference solvents showed a good consistency with LOCs for premixed flame [85] and counterflow diffusion flame [90], respectively. Being different from premixed-LOC and counterflow-LOC focusing on the gaseous fuel or volatile liquid, wick-LOC method involves processes of liquid-phase transport in the wick, phase change and gas-phased combustion, which is applicable for both high- and low-volatile solvents. Based on the above comparisons, the wick-LOC method is competent to quantify the flammability of liquid solvents for LIB electrolyte.

3.3. Applications in binary solvent mixtures

Most electrolytes are combined with different types of solvents such as cyclic carbonates, linear carbonates or ethers to balance the pros and cons of each solvent in practical applications [22]. Cyclic carbonates like EC and PC have both high dielectric constant and viscosity. However, the poor cycling efficiency of PC and the high melting point of EC make them difficult to be used alone. Linear alkyl carbonates and some ethers have low melting points and viscosities; they can provide higher ionic conductivity and better low-temperature performance when mixing with cyclic carbonates. For a balanced electrolyte formulation in both performance and safety aspects, not only electrochemical performances but also flammability of such mixed solvents should also be quantified.

As shown in Fig. 3.5, the wick-LOCs of the mixed solvents of linear and cyclic carbonates with different ratios were plotted. The LOC values were determined at an axial flow velocity (u_a) of 10 cm/s. The horizontal axis shows the mass fraction of EC or PC in the mixtures. The wick-LOC of pure EMC was measured around 14.85 vol%. The LOC increased linearly with the additions of both EC and PC, but the growth gradient of LOC is higher with EC addition. The mass fraction of EC was varied from 0 to 66 wt% due to the EC solubility limit in EMC [116]. The pure EC is a crystalline solid in the room temperature, so its LOC was estimated as 17.3 vol% by extrapolating the linear fitting (solid circle point in Fig. 3.5). Comparatively, the pure PC (liquid in the room temperature) with a measured LOC of 16.3% was more flammable.

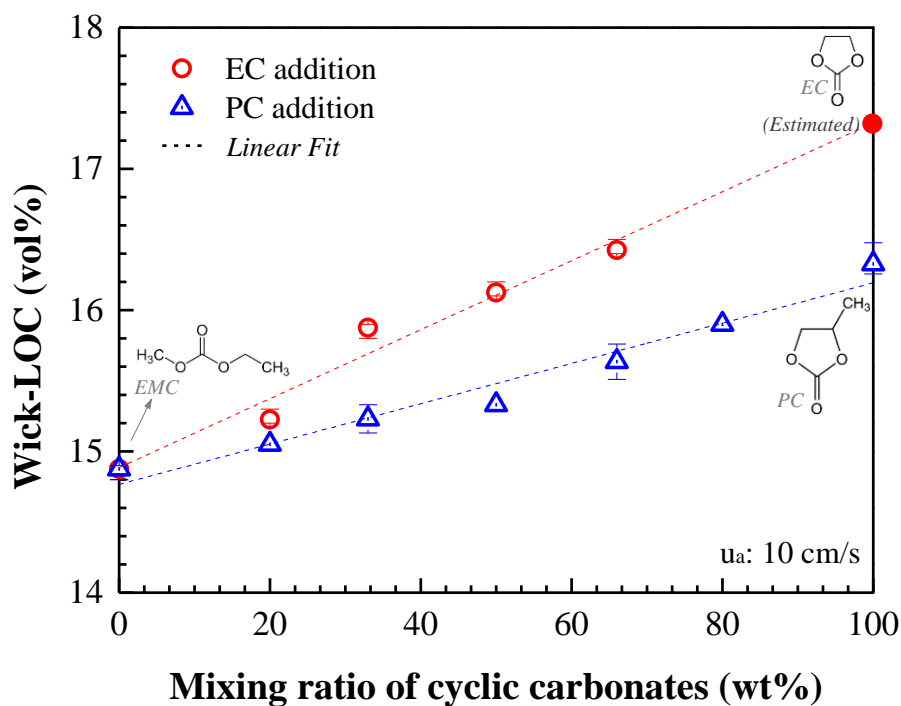


Fig. 3.5. Wick-LOC of mixture of linear and cyclic carbonates in different mixing ratios.

Being different from the binary carbonates, carbonate-ether mixed solvents had non-linear changes of LOC with ratio variation, as shown in Fig. 3.6. The DME and TEGDME with LOC of 12.9 vol% and 13.45 vol%, respectively were more flammable than the carbonates tested. The nonlinear change of LOC in Fig. 3.6 showed that a small amount of ether addition in carbonates can decrease the LOC significantly. The LOC values of carbonate-ether solutions with equal ratio were always lower than the mean LOC values of two pure solvents.

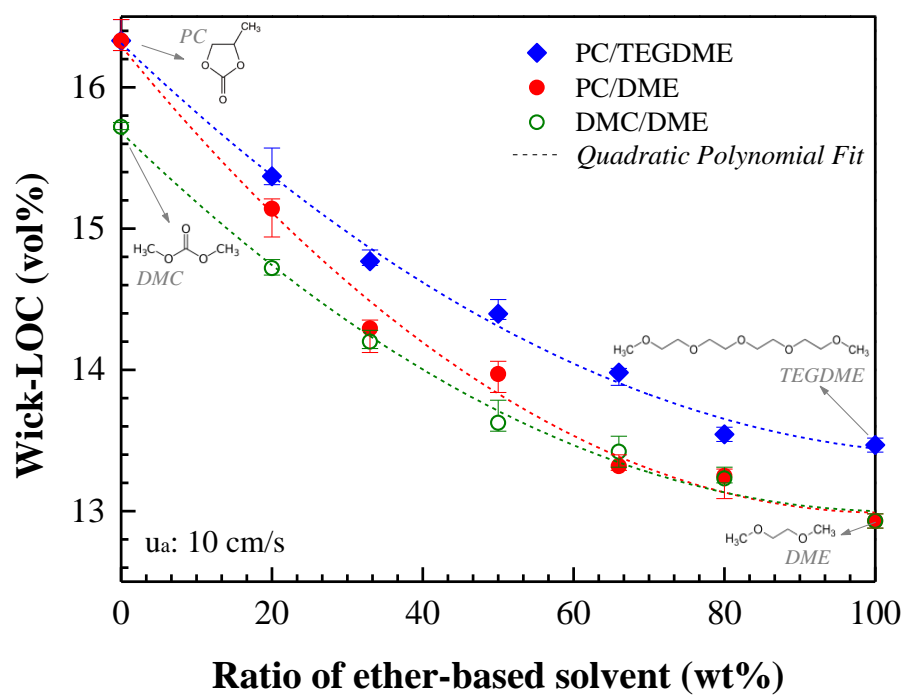


Fig. 3.6. Wick-LOC of mixtures of carbonates and ether-based solvents in different mixing ratios.

3.4. Flame-retardant effectiveness of OPC additives

As mentioned in Section 1.2.2, OPCs are effective flame-retardant additives used in electrolytes of Li-ion batteries. To quantify the flame-retardant effectiveness of OPC additives in electrolyte solvents, the wick-LOCs of different OPC-added solvents were measured in this section.

The effect of different OPC additions on the flammability of DMC-based solvent was shown in Fig. 3.7. In this figure, the vertical axis is the wick-LOC (in vol%) and the horizontal axis is the amount of OPC (TMP or TEP) added (in wt%). The flame images in the figure are stabilized flames of DMC with different TMP addition near extinction conditions (0.2 vol% above LOC). Small amounts of added OPC had a significant impact on the LOC of DMC solvent, and the LOC growth rate was quite large within 2 wt% OPC addition. However, the gradient of LOC increase became smaller as the amount of OPC continuously added. In the comparison of two OPCs, TMP showed better flame-retardant effectiveness than TEP with the same addition into DMC, but both had diminished effectiveness in a higher OPC addition. Such marginal effect on flammability was also found in cup-burner tests by Bouvet and Babushok using DMMP as a fire suppressant [11,41]. It was explained as the fuel effect of OPC and the loss of active phosphorus compound. As shown in Fig. 3.7, the size and luminance of the near-limit flames increased with the addition of TMP, the fact of increased particle formation (condensation of active phosphorus compound) was consistent with such explanations.

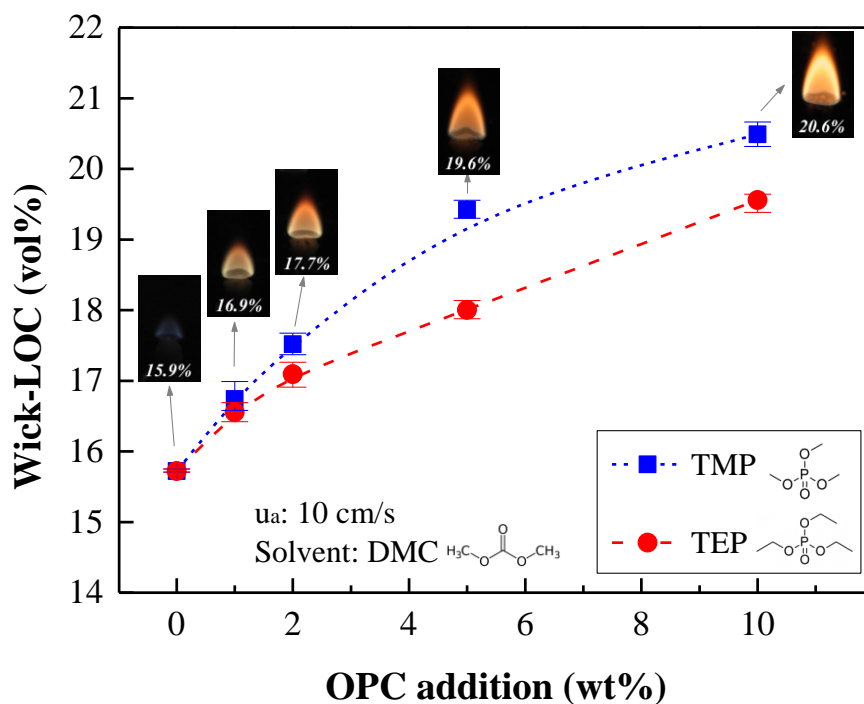


Fig. 3.7. Wick-LOC change with addition of OPC in DMC-based solvents.

Similarly, the flame-retardant effectiveness of different OPC in EMC-based solvents was compared in Fig. 3.8. Four kinds of typical OPC additives, TMP, TEP, DMMP and TMP(i), were tested with 0, 5 and 10 wt% additions. The wick-LOC increased significantly with additions of all types of OPCs, but the growth rate decreased slightly. The flame-retardant effectiveness of TEP was the lowest among the four OPC, while DMMP showed the best performance. The effect of OPC addition on flammability was explained as the radical capture in the combustion of carbonate solvents. The effective phosphorus compounds capture H and OH radicals to form H₂O without being consumed [117]. The combustion reaction rate can be decreased by the reduction of chain carriers. Since the intensity of this inhibition mechanism is dominated by the number of phosphorus atoms added to the system, the different flame-

retardant effectiveness of the four OPCs (in Fig. 3.8) can be explained as the different amount phosphorus atoms in the same weight of OPCs.

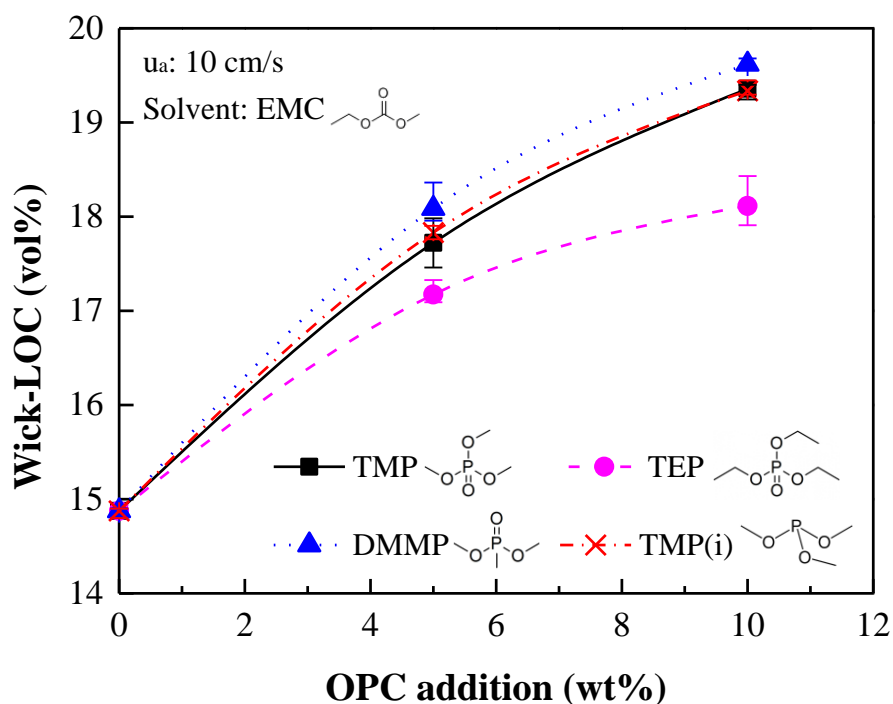


Fig. 3.8. Wick-LOC change with different OPC additions in EMC-based solvents.

Besides the flame inhibition of OPC in the gas-phase chemical reaction, the potential physical effect of OPC addition should be concerned as well. As reported by Korobeinichev in his chemical calculations [54], OPCs have promotion effect leading to a temperature rise of hydrogen flames. Here, to check such double-edged effect experimentally, the wick diffusion flame temperatures were measured with and without adding OPC. The temperature profiles of the stable flames at 20% oxygen given by pure EMC and EMC + 10 wt% TMP were shown in Fig. 3.9. The vertical axis shows the axial flame temperature along the centerline of the flame, and the horizontal axis is the distance from the top of the wick. The curves were the averaged

values under at least 3 times measurements, and the shaded areas represented the ranges of error.

The R-type thermocouple with 0.3mm thickness was shaped and utilized for the temperature measurement. Even without the compensation of radiation effect on the temperature, the potential temperature discrepancy can be controlled up to 40K under 1400K.

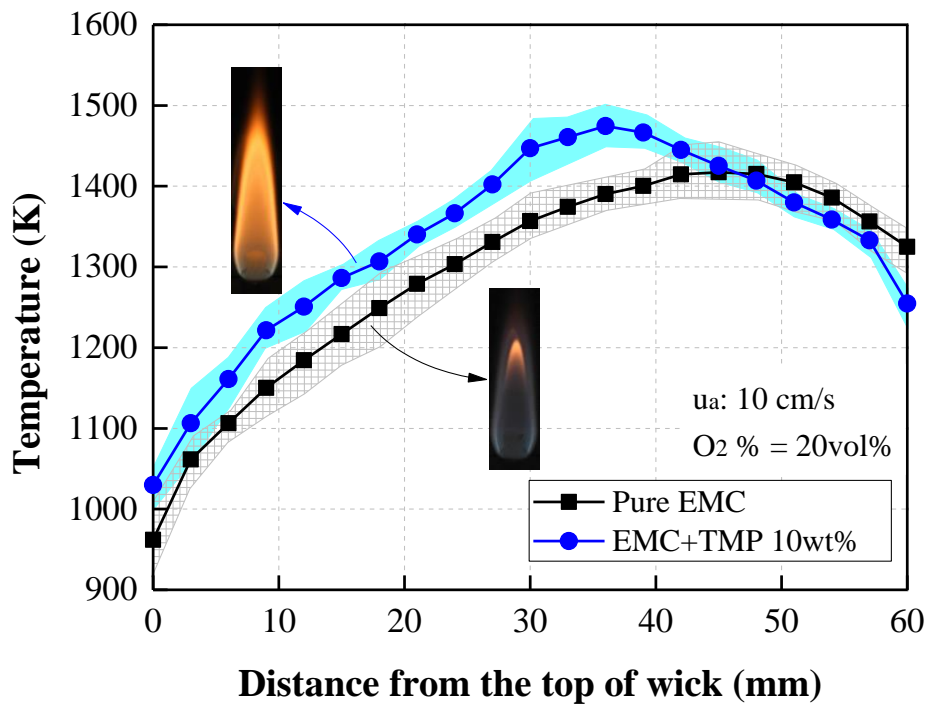


Fig. 3.9. Measured temperature distribution along the centerline of flames given by pure EMC and EMC+TMP 10 wt%.

The addition of OPC to EMC (EMC + TMP 10 wt%) produced a higher temperature distribution in the flame. Because of the exothermic radical-capture reaction by phosphorus compound, temperature increases in the main body of the flame (0 ~ 45 mm) with OPC addition. While the high luminosity due to the particle formation of EMC + TMP 10wt% flame causes a large amount of radiant heat loss in the tail of the flame (≥ 45 mm), which leads to a lower

temperature distribution in the downstream than the case of pure EMC. The difference in flame luminosity and temperature accounts for different heat feedback from the flame to the wick. Such additional heat feedback could accelerate the evaporation of the fuel, which led to a larger flame size near extinction, as shown in Fig. 3.7. It could be a potential explanation for the marginal effect of high OPC additions on the LOC increase.

3.5. Concluding remarks

The flammability limits of electrolyte solvents in lithium-ion batteries were studied experimentally using the wick-LOC method, a wick combustion system in conjunction with the limiting oxygen concentration method under a candle-like burning configuration. The results were summarized as follows:

(1) The wick-LOC of electrolyte solvents were determined under well specified the experimental conditions. The effect of various experimental conditions like the axial flow velocity, the exposed wick length and the elapsed time after ignition on wick-LOC were investigated to provide reproducible results.

(2) The correlations of wick-LOC to other flammability properties (flash points, auto-ignition temperatures, the heat of combustion and other types of LOC) were analyzed among several solvents. According to the correlations, the quantification of solvents flammability can be provided by the wick-LOC method with reliable results.

(3) With the application for binary solvent mixtures, the effects of different mixing ratios on wick-LOC were studied. The linear change of LOC in binary carbonates solvents and non-linear change of LOC in carbonate-ether mixed solvents were found experimentally.

(4) The flame-retardant effectiveness of different types and amounts of OPC additions in carbonates solvents were quantified. The wick-LOC results showed that small amounts of OPCs had significant flame-retardant effects, but the efficiency decreased with the higher OPC additions. The effectiveness of four OPCs were rated as DMMP > TMP(i) \approx TMP > TEP. Besides the flame inhibition, the potential promotion effect of OPC addition was discussed using flame temperature measurements.

By using the wick-LOC method, not only the flammability of single solvents, but also the role of mixing and OPC additions on solvents combustion can be quantified. However, with the addition of OPCs or lithium salts, the special flame behaviors can be observed (in following chapters), which implied the limitations of the basic experimental procedure of the wick-LOC method. Thus, in the following chapters, the specific procedure to determine LOC will be introduced, the in-depth studies on the roles of OPC and Li-salt additions in electrolyte combustion will be investigated as well.

Chapter 4. OPC effects on the wick flame stability

In the previous chapter, the LOC results were determined standardly under the same mode of stabilized flame before extinction, that is, the flame stabilized in the wake region of the wick (wake flame). However, in addition to the wake flame, another mode in which a side-stabilized flame enveloped the entire wick (full flame) was observed during experiments. With increasing OPC addition (up to 10 wt.%) into the electrolyte solvents, the flame could be extinguished directly from the full flame, and the corresponding LOC was lower than the LOC for extinction from the wake flame, which showed that full flame is more stable in the high OPC addition case. Thus, the original experimental procedure to determine the wick-LOC might be improved considering the different flame modes to find the minimum LOC. In this chapter, the full and wake flame stability limits on a candle wick configuration were determined with different OPC addition in the carbonate solvents. The extinction mechanisms of the wick-stabilized flame were discussed considering the OPC effects.

4.1. Two flame modes on a candle-like configuration

4.1.1. Introduction of full and wake flame stability

The wake flame and the full flame modes were already discovered in the flame downward spread and extinction of solid material based on the LOI test method [112,118,119], and they have always been called wake-stabilized flame and side-stabilized flame for a candle-like solid slab/rod sample, respectively. By reducing the oxygen concentration of the external flow in the traditional LOI test, the flame extinction process has always been reported as follows. The base of the side-stabilized flame is pushed by external flow toward the downstream until the wake

region with a shortening flame height; then, the flame proceeds to extinction. Extensive researches focusing on the change in extinction limits at different flow velocities, sample widths/thicknesses, and gravity [109,112,120,121] conditions have been conducted, and in these researches, the wake flame was always more stable as a consequence of the side-stabilized flame (or full flame). This phenomenon is commonly ascribed to the higher residence time of the wake flame compared to the side-stabilized flame according to the Damköhler number, which is widely used to explain the blow-off mechanism of the side-stabilized flame [122–125].

The flame in the wick-LOC method shows a configuration similar to that of downward flame propagation on a candle-like solid material during extinction. However, with increasing OPC addition, the flames are separated into two extinction processes given by the full and the wake flames near extinction. Moreover, the different extinction processes behave in a manner opposite to the common understanding mentioned in previous paragraph, according to which the full flame becomes more stable with increasing OPC addition, and its LOC decreases to be lower than that of the wake flame. To clarify the influence of OPC addition to electrolyte solvent on the wick flame extinction in the wick-LOC method, the flame stability limits of two modes of stabilized flame (full flame and wake flame) were determined depending on OPC addition in the present work. Then, the extinction mechanism of each flame mode considering electrolyte solvent added OPC was discussed.

4.1.2. Determination of stability limits of the full and wake flames

During the wick-LOC determination, two types of candle-wick flame can be found, namely, full flame and wake flame, which have different stability limits in terms of low oxygen. Similar to the basic procedure, both the full and the wake flame stability limits were obtained during

oxygen decrease in steps of 0.2% when approaching the limits. When adjusting the oxygen, the time for new gas flow to replace the entire flow path was conservatively estimated as 10 sec. To avoid the hysteresis of flow and confirm the stable flow, the waiting time after each step change of oxygen was set to more than 1 min. Each flame stability limit was determined as the average value of at least four repeated tests under an external flow of 10 cm/s, and deviations from the average value were recorded in the form of error bars.

After several preliminary tests, the flame stability limits could be estimated approximately. The wick was ignited at a higher O₂ concentration to generate a full flame; then, O₂ was reduced in steps until an unstable flame base led to direct extinction or transition to wake flame; finally, the minimum O₂ concentration to sustain a stable full flame was considered as the full flame stability limit. The approach to determining the wake flame stability limit depends on whether the full flame can transition to wake flame under decreasing O₂. With a successful transition, the wake flame limit can be obtained by further decreasing O₂ until flame extinction. Otherwise, the full flame is extinguished directly. In this case, a stable wake flame should be re-established through ignition above the tip of the wick with a proper oxygen fraction. By reducing the oxygen carefully, the wake flame stability limit can be found at the minimum O₂ concentration at which the wake flame oscillates and shrinks to extinction.

4.2. Flame extinction processes

During the flame stability limits measurement of each pure electrolyte solvent and its mixtures with different proportions of OPCs, the extinction processes of each stabilized flame were observed by reducing oxygen in the external flow. Typical examples of pure DMC and DMC with TMP addition are shown in Fig. 4.1. During the extinction process of pure DMC flame in Fig. 4.1 (a), the full flame is stable at a higher oxygen concentration; then, with decreasing oxygen concentration, the full flame becomes unstable and it turns into the wake flame, followed by extinction with further decrease in oxygen concentration. During the transition from full to wake flame, flame oscillation can be observed, which is a common behavior in candle flames [96,126]. The flames of the other pure electrolyte solvents (EMC and DEC) showed similar behaviors as that of the pure DMC flame in the extinction test.

However, when more OPC was added to the electrolyte, two distinct branches of the extinction process were observed. In the case of DMC with 10%TMP addition, once the stabilized full flame was obtained, it extinguished directly (blow-off) without transition to the wake flame, as shown in Fig. 4.1 (b). When a stable wake flame was obtained by ignition at the tip face of the wick, the flame proceeds to extinction through oscillating motion, without transitioning to the full flame when the oxygen decreased, as shown in Fig. 4.1 (c). These two branches of the extinction process can be found in the other high-OPC-addition cases as well.

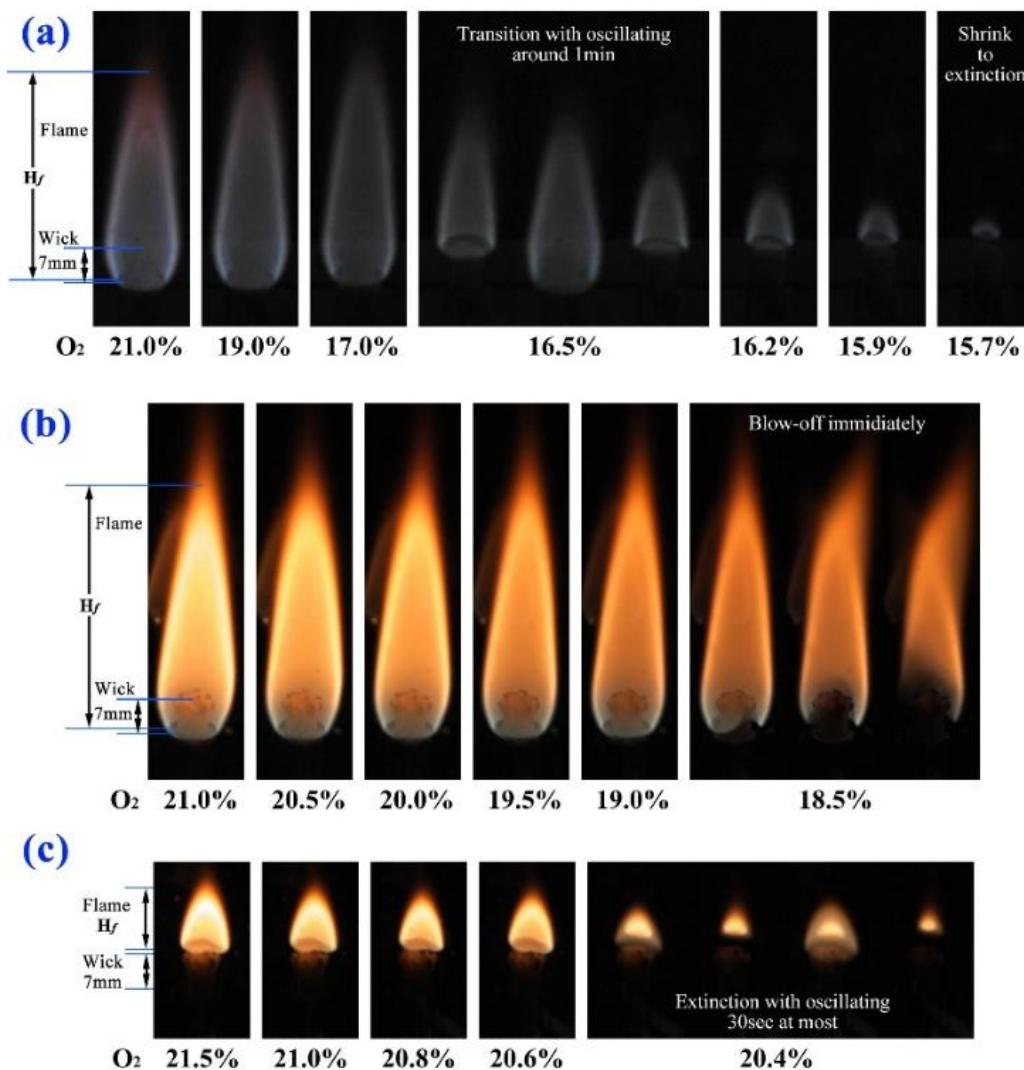


Fig. 4.1. Photographs of flame extinction process under continuous O_2 decrease. (a) pure DMC, extinction with transition from full to wake flame; (b) DMC+10%TMP, full flame direct extinction (blow-off); (c) DMC+10%TMP, wake flame extinction

The flame height was measured as the length from the visible flame base to the flame tip, as marked in Fig. 4.1. To clearly illustrate the different extinction phenomena of the wick flame in the case of pure DMC and DMC+10%TMP mixture, the changes in averaged luminous flame height during O_2 concentration decrease were recorded and plotted, as in Fig. 4.2. The solid lines with left-pointing arrows represent the change in flame height under decreasing oxygen

concentration; the dashed lines with right-pointing arrows reflect flame growth from wake to full flame under increasing oxygen concentration. The barriers show the range of existence of each flame mode. The changes in the pure DMC wick flame indicate a common mutual transformation between the full and the wake flames. These findings are consistent with the numerical results obtained for a thick solid slab by using LOI method [112], where the hysteresis phenomenon was observed in the transition region. By contrast, the flame of DMC+10%TMP showed only unidirectional change from wake flame to full flame with increasing oxygen concentration; the stability limit of the full flame was lower than that of the wake flame.

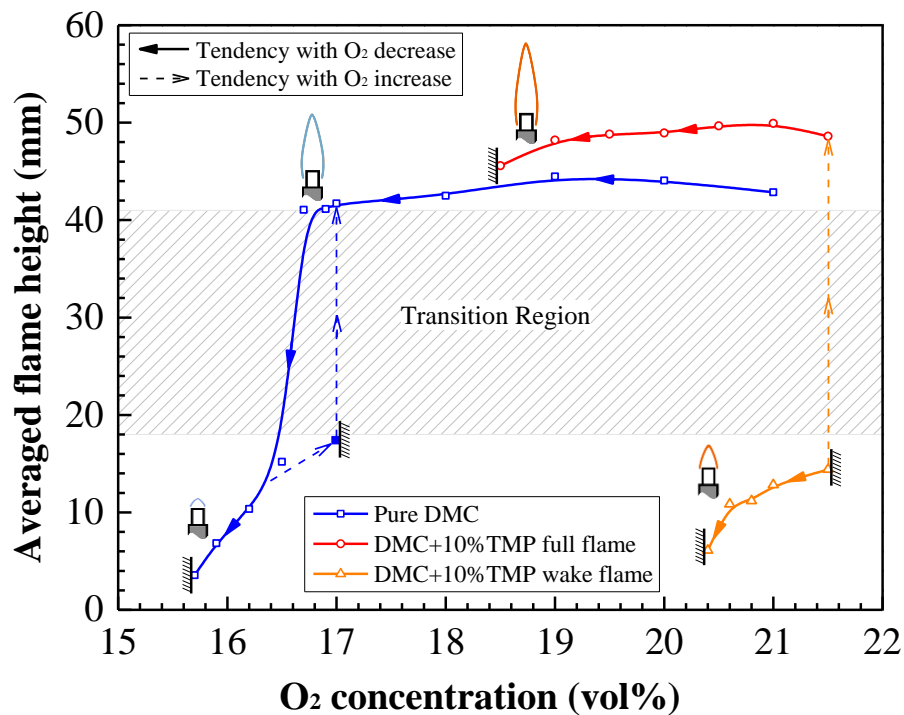


Fig. 4.2. Averaged flame height changes for full flame and wake flame in the cases of pure DMC and DMC+10wt.% TMP with oxygen change rate of 10cm/s in external flow

4.2. Flame stability limits of electrolyte solvents with OPC addition

The definition of flame stability limit in this paper is the lowest oxygen concentration required to stabilize each flame mode (wake or full flame). This means there are two stability limits for a specific fuel corresponding to the two flame modes.

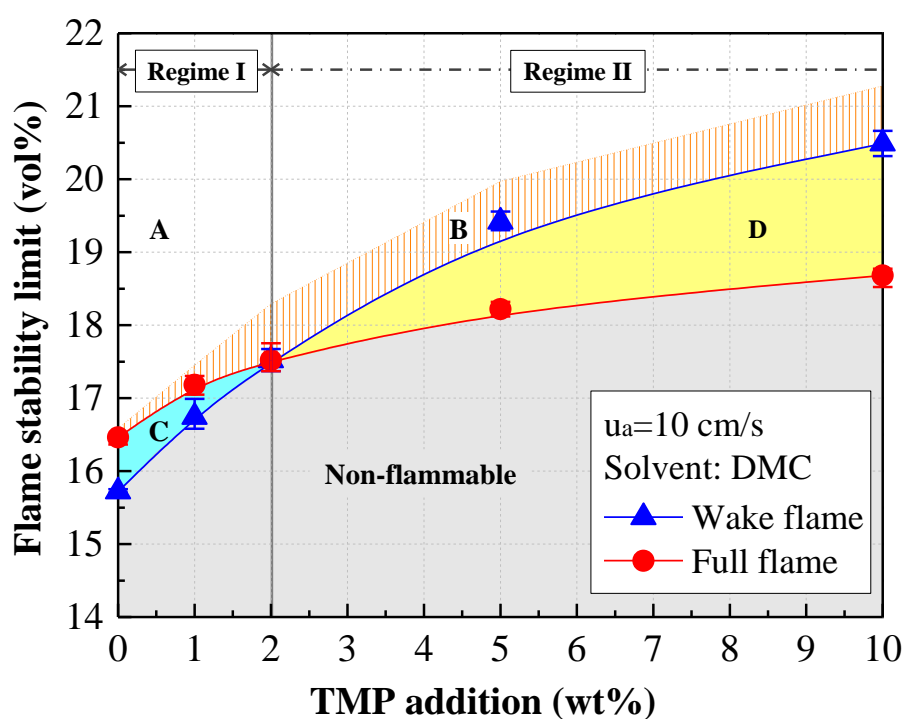


Fig. 4.3. Flammability map given by flame stability limits of DMC-based electrolyte as a function of TMP addition

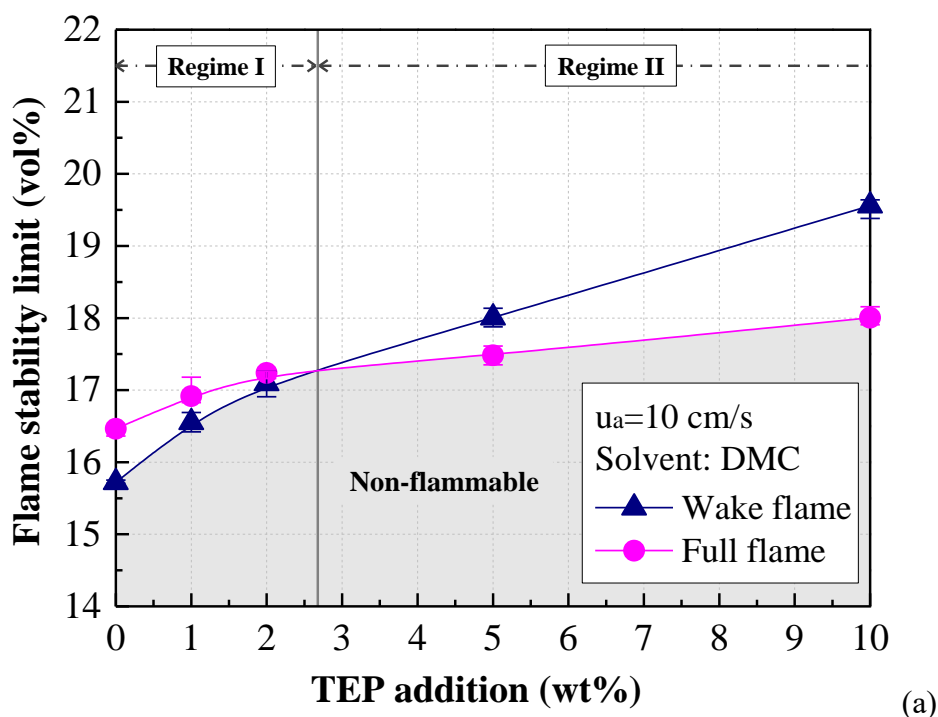
The flame stability limits of DMC with added TMP (as a typical case) were first plotted, and a flammability map with five parts, as in Fig. 4.3, was obtained. Both flame limits increased with TMP addition, but the growth rate of flame limits declined, reflecting the marginal

effectiveness of fire-retardation ability. The rise in wake flame limits of DMC with TMP addition showed strong sensitivity to TMP addition, which is consistent with the LOC results reported in Section 3.4 [127]. However, the ascent of the full flame limits with the addition of TMP was less sensitive to the amount of TMP added. This comparison between the wake flame and the full flame showed that the wake flame was always more stable with no or low TMP addition, until the amount of added TMP exceeded the critical amount of around 2wt.%. After the addition of this critical amount of TMP, the full flame becomes more stable, as evidenced by the lower limiting oxygen concentration than that of wake flame, and with the increased TMP addition, the discrepancy between the limits of the full and the wake flames increases. As a result, the point of intersection of the full and the wake flame limit curves divides the figure into two regimes, Regimes I and II.

Combined with the stabilized flame modes at various oxygen levels, a flammability map with TMP addition can be formed in five parts, as in Fig. 4.3. The flammable zone is composed of parts A–D, while the bottom part is the non-flammable zone. The full flame exists solely in a higher oxygen levels in part A; and the zone of coexistence of the full and the wake flame is marked as B; only wake flames at lower oxygen levels occupy part C; part D indicates that only full flame can exist in this lower-oxygen region. The wake flame has a very limited range of existence according to areas of parts B and C. The fact that there is only one zone each in which the wake and the full flames exist under the lower oxygen condition is attributed to the dominant mechanisms in Regimes I and II, respectively.

To compare the influence of the type of added OPCs on the flame stability limits, TEP and DMMP were added separately to DMC for additional investigation. The flame stability limits

of the DMC-based electrolyte with TEP and DMMP are plotted as a function of OPC addition in Fig. 4.4 (a) and (b), respectively. The increase in flame stability limits due to the addition of TEP and DMMP in DMC show trends similar to those in the case of TMP addition, albeit their respective effectiveness levels differ. Compared with the effect of TMP addition on the flammability of DMC, TEP not only shows a weaker fire-retardant effect on DMC but also has a later switch point between the two regimes (around 2.6% TEP addition compared to 2% TMP addition), and the discrepancy between the full and the wake flame limits under the addition of large amounts of TEP is smaller than that in the case of TMP addition. By contrast, DMMP is more effective than TMP in terms of flame retardation, and the switch to the second regime occurs with a lower amount added DMMP addition (1.2wt.%) than that in the case of TMP addition.



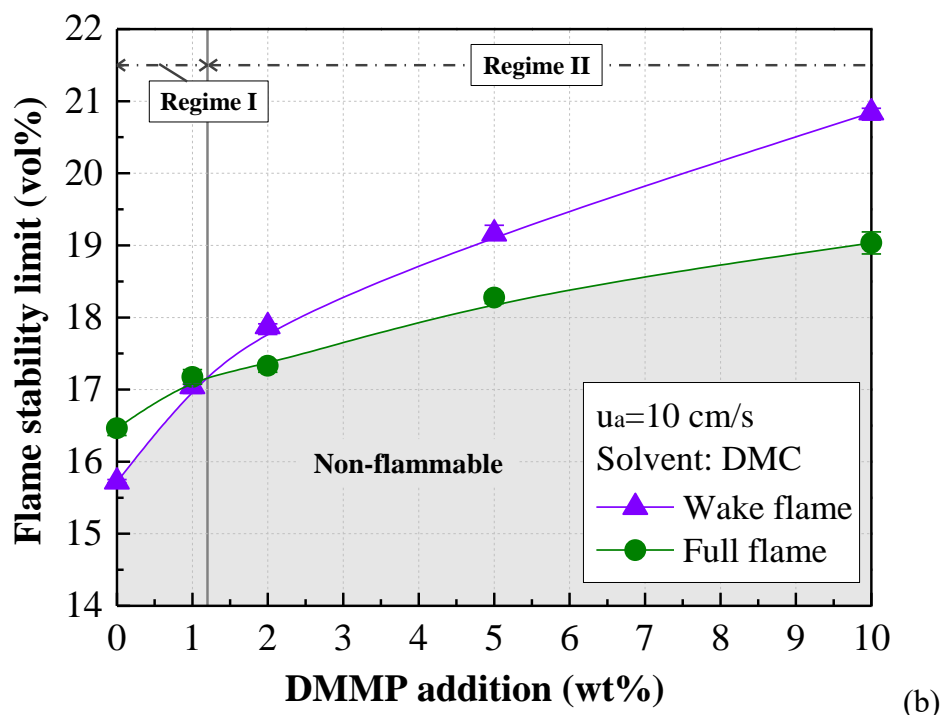


Fig. 4.4. Flame stability limits of DMC-based electrolytes as a function of OPC addition:

(a) DMC+TEP; (b) DMC+DMMP.

A comparison of flammability among the different electrolytes under the same level of OPC addition was made as well. EMC and DEC were selected as the same series of linear alkyl carbonates for comparison with DMC, and these three compounds have two, one, and zero ethyl groups, respectively. The flame stability limits of EMC and DEC with TMP are shown in Fig. 4.5 (a) and (b) for comparison with the DMC-based electrolyte solution. Although similar trends of the full and the wake flame limit curves is obtained, the absolute values of flame stability limits and the switch points of the two regimes are different. From these three tested electrolytes, the full flame limit shows sensitivity similar to that achieved with the TMP addition (around 2vol.% increase by adding 10wt.% TMP), whereas the wake flame becomes less sensitive than that in the DMC case, especially with the addition of DEC. Even though pure DEC has a slightly higher LOC than EMC, the fire-retardation effect of high TMP addition on DEC is weaker than

that on the other electrolytes owing to the insensitivity of DEC to the TMP addition.

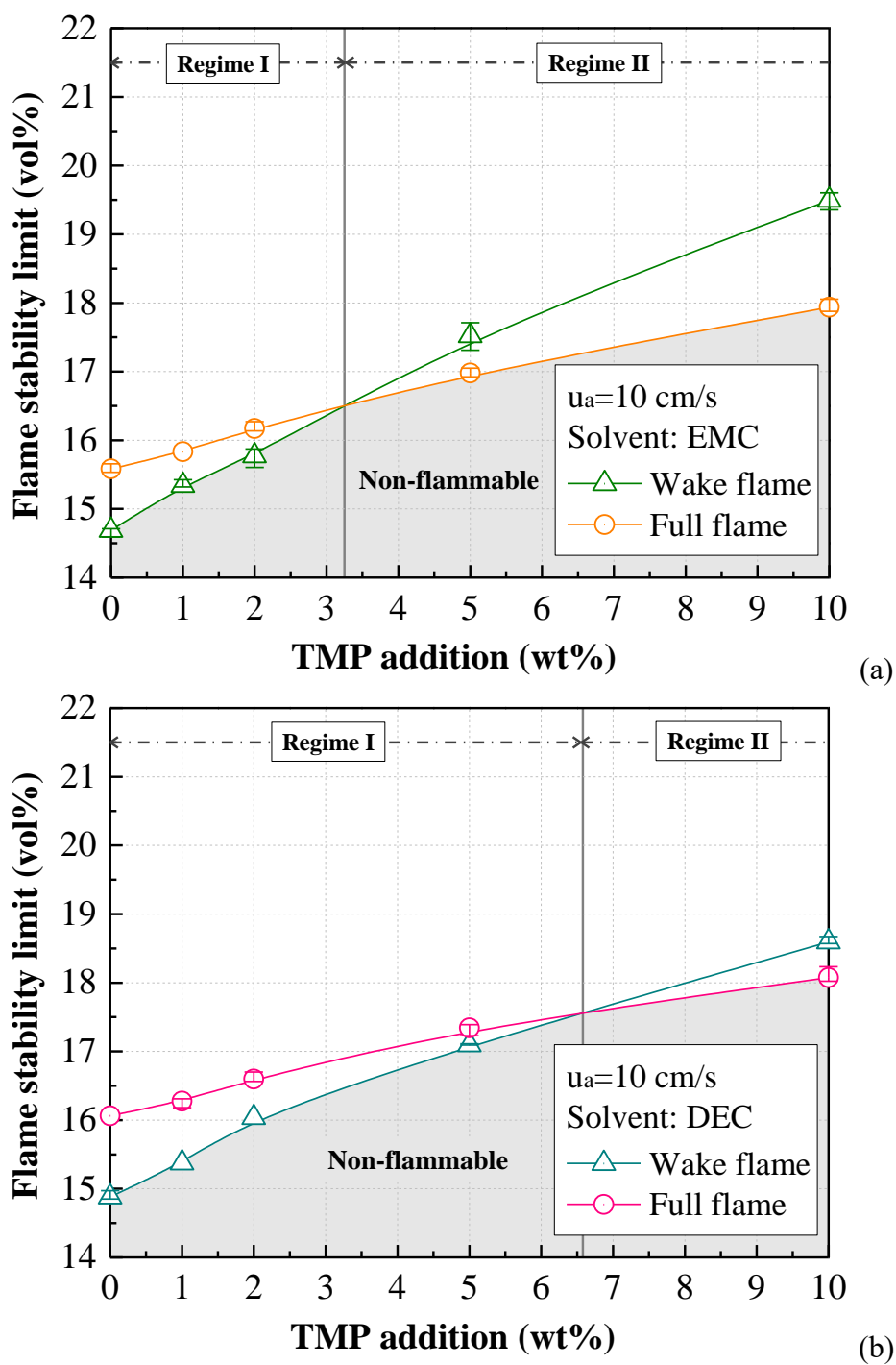


Fig. 4.5. Flame stability limits with the addition of TMP to other linear alkyl carbonates:

(a) EMC and (b) DEC.

4.3. Flame extinction mechanisms

In the previous section, two extinction limit branches corresponding to different flame modes (full flame and wake flame) were presented as a function of OPC addition. With addition of OPC, not only does the fire-retardant effect decrease, but also the most stable flame switches from the wake flame to the full flame. This is contrary to the case (and ordinary experience) without any retardant in a candle-like flame configuration. High OPC addition was found to be marginally effective in terms of the retardation of gas-phase flames based on the condensation of phosphorus-containing intermediates and the fuel effect of OPC, which was found in extinguishment tests on a cup burner flame by using OPC-containing extinguish agents [45,49,128]. However, the aforementioned works did not consider reversal of the flame stability limits of the full and the wake flames. In the following section, the mechanisms of the reversal of the order of extinction limits in the two different regimes is discussed.

It is known that there exist two branches of the extinction limit for a candle-like flame (under LOI method configuration) [125,129]. The first branch is blow-off and the second branch is quenching extinction.

At the base of the near limit wick-stabilized flame, it has an edge flame structure under an opposed flow condition (see Fig. 4.6). From the viewpoint of fluid dynamics, the flame leading edge (base of the wick flame) was stabilized under the balance of the flame downward propagation and opposed upward local flow [111,130] If the flame propagation speed is comparable to the local flow velocity required, the flame base position can be maintained; otherwise, blow-off extinction occurs.

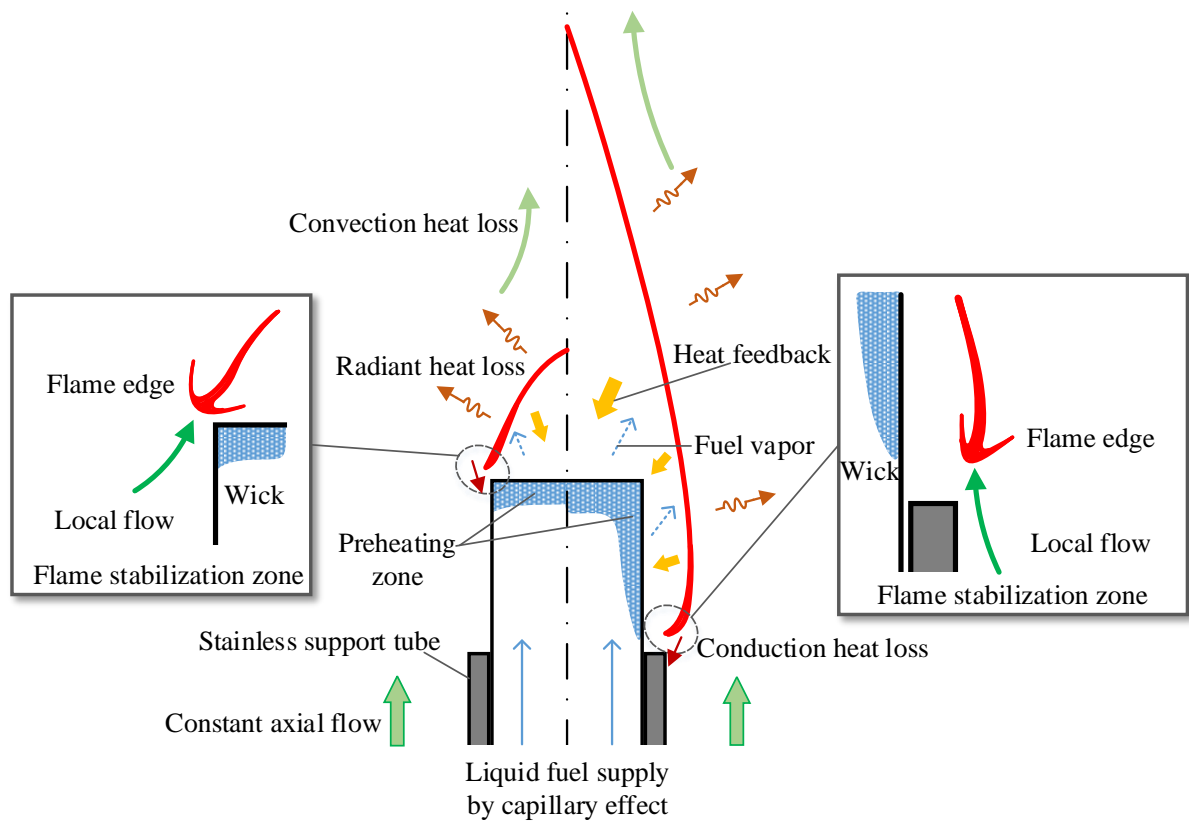


Fig. 4.6. Schematic description of stabilization of wake (left) and full flame (right) over wick configuration

Generally, the local flow velocity of the wake flame at the flame base is less than that for the full flame because of small flame size and the resulting weak buoyancy-induced flow. Furthermore, if the flame is stabilized behind the top end of the wick, local flow velocity should be much less in the wake of the wick. Therefore, if we explain the extinction limit based solely on this blow-off mechanism, the extinction limit with the wake flame should be always lower (in other words, more stable) than that of the full flame because the local flow velocity near the flame base is lower with the wake flame, as explained above. The order of the stability limits in the low-OPC-addition range is consistent with this understanding (in Regime I), and this is also true in the case of the solid material flammability limit obtained using the LOI method

based on ISO4589-2 [109,112,118,119,131]. By contrast, it cannot be explained by the order of flame stability is switched in the high-OPC-addition case, also called Regime II, according to the above understanding. In this case, the quenching mechanism could potentially be the key to understanding the switching mechanism.

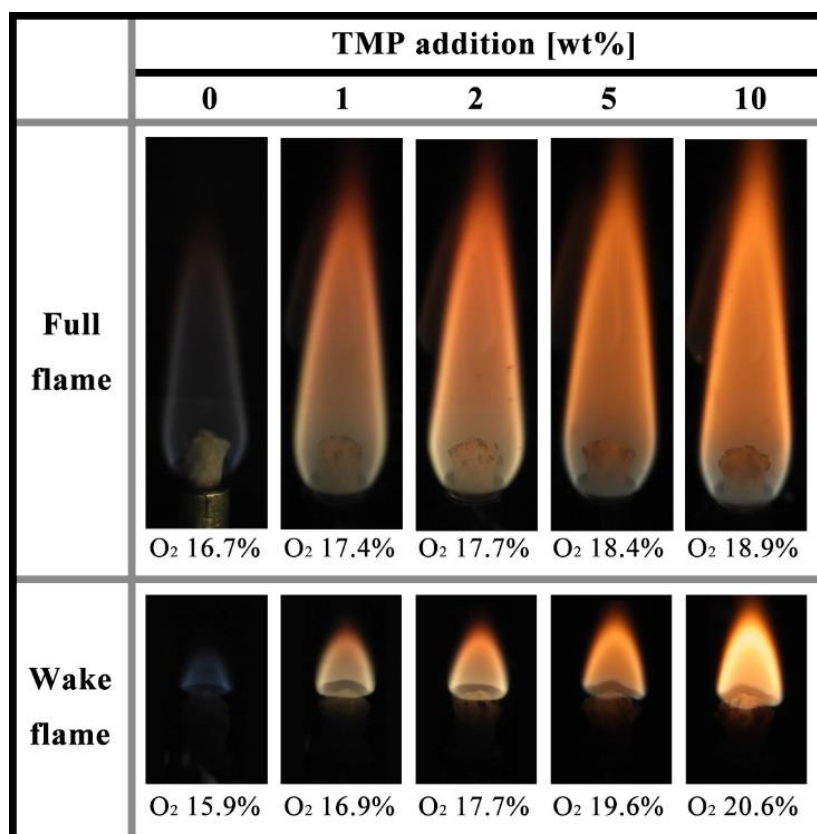


Fig. 4.7. Images of stabilized flames of DMC/TMP mixture near stability limits (LOC + 0.2%)

An example of the stabilized flames of DMC with various amounts of TMP addition near the extinction limits (LOC + 0.2%) is shown in Fig. 4.7. A blue translucent flame is generated from pure DMC, whereas a more luminous and yellow flame is generated with increasing TMP addition in the case of the full flame and the wake flame. The presence of the luminous flame

is mainly attributed to the increased formation of phosphorus-containing particles from the added OPC [45,128]. In addition, we previously reported that the flame temperature increases with OPC addition at the same O₂ concentration in Section 3.4 [127], which could be explained by enhanced transitions from radical species (such as OH and H radicals) to stable species (typically H₂O) with aid of phosphorus compounds in gas-phase combustion. Similar facts have been reported by Korobeinichev [53,54] as the promotion effect on flame temperature of OPC, in addition to its chemical inhibition effect. Owing to such increases in temperature, OPC addition should lead to an increase in total heat loss from the flame to the surroundings, with an increased temperature gradient.

Generally, it is understood that in combustion phenomena, the heat generated by a flame is a function of the flame volume, whereas the heat conduction from the reacting zone to the environment is proportional to the flame surface area. In the typical stabilized diffusion flame, the larger flame volume or size corresponds to the larger fuel consumption to the reaction zone. The total heat release of the flame is generally proportional to the fuel consumption rate and reflected by the flame volume. While, the quenching mechanism of flame extinction always caused by the excessive heat conduction from the flame reacting zone to the outside leading to the temperature drop, especially for a small-scale flame[112,120]. Thus, the ratio of heat loss to heat generation is dominated by the surface volume ratio (S/V) of the flame.

The unique feature of the wake flame can be ascribed to its smaller size than that of the full flame, which results in a large S/V ratio. Therefore, the impact of OPC addition on the wake flame in terms of the temperature drop from the adiabatic flame temperature is quite significant in comparison to that in the full flame case. As a result, OPC addition degrades the stability of

the wake flame to a greater extent than that of the full flame owing to the larger temperature drop in the former case. In this scenario, the flame extinction limit in the case of the wake flame should be higher (more unstable) than that in the case of the full flame.

As discussed above, flames are divided into two regimes based on the critical amount of OPC addition, as follows: Regime I represents the scenario in which the local flow velocity dominates the extinction limit of the two types of stabilized flame, and it is called the "blow-off regime." By contrast, regime II represents the scenario in which the smaller flame is at a disadvantage owing to excessive heat loss, and it is called the "quenching regime."

As already discussed, the wake flame has a higher ratio of heat loss to heat generation than that of the full flame owing to its smaller size. Assuming there exists a critical heat loss ratio at which the flame is maintained, flame volume should increase with increasing flame temperature. As the flame temperature increases with increasing OPC addition [53,54,127], we can expect the flame volume to increase with increasing OPC addition to sustain combustion, even near the extinction limit. Fig. 4.8 shows the change in normalized flame volume near the extinction limit as a function of OPC addition for the wake flame and the full flame. As can be seen in the figure (straight-line-fitting of TMP case), the rate of increase in flame volume is considerably larger in the case of wake flame, implying that quenching is the dominant mechanism governing extinction of the wake flame.

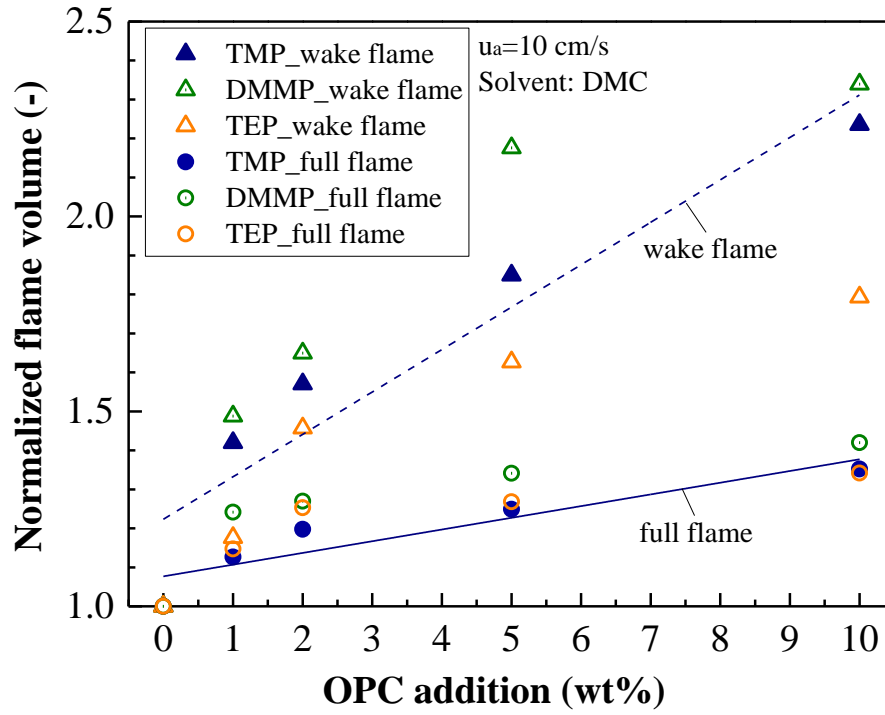


Fig. 4.8. Normalized flame volume of near-limit stabilized flames as a function of OPC

addition in DMC

Because quenching dominates extinction of the wake flame in regime II, the extinction limit in terms of oxygen concentration is higher than that of the full flame because with increasing flame temperature, the smaller flame size is not favorable from the viewpoint of the flame stability.

4.4. Concluding remarks

In this study, the low oxygen limits of typical electrolytes mixed with different types and amounts of OPC retardants were investigated using the wick-LOC method. Two modes of the wick-stabilized flame were found near extinction, namely, wake flame and full flame (side-stabilized enveloping flame). It was discovered that the wake flame can be less flammable than the full flame when the OPC addition exceeds a critical value, which is contrary to the case without OPC. The major findings are as follows:

(1) Flame extinction processes were observed under decreasing oxygen concentration. In case of the blue flame of pure DMC, the full flame successfully transitioned to the wake flame and, finally, extinguished with decreasing oxygen concentration. By contrast, in the 10% TMP addition case, no transition was found; instead, the extinction limit of the full flame was lower than that of the wake flame.

(2) Flame stability limits were determined to compare the two stabilized flames with OPC addition. The reversal points of the two flame stability limits were found at 2wt.% TMP addition in DMC solvent, which divided the flammability map into two regimes with different regions of existence of the two stabilized flames near extinction.

(3) Comparison experiments were conducted to show the effects of the type of OPCs and electrolyte solvents on flame stability limits. TEP showed weaker fire retardation and a higher regime switching point (2.6wt.%) than TMP, while the effect of DMMP addition in DMC was the strongest, with the regime switching point occurring at 1.2wt.%. Lower sensitivities of the wake flame to TMP addition to EMC and DEC were found, as manifested in the higher regime switching points (3.2wt.% to EMC and 6.6wt.% in DEC).

(4) The flame extinction mechanisms were discussed to clarify the reversal of the flame stability limits of the full and the wake flames. In addition to blow-off mechanism, heat loss in the flame was emphasized based on the flame volume near the extinction limit. The flammability map is divided by the critical amount of OPC addition into two regimes: “blow-off regime” and “quenching regime,” which can explain the influence of OPC addition on the flame stability in each flame modes.

For the flammability test in the wick-LOC method, the addition of OPC flame retardant can change the contribution ratio of chemical reaction, kinetics, and thermal balance in terms of the flame extinction mechanism. Thus, the flammability map combining the full and wake flame limits is suitable for assessing the fire hazard. If we want to neglect the thermal promotion effect of OPC for a fair comparison, the wake flame limits could be better indicator. To some degree, the added heat feedback from wake flame to the wick may compensate the heat loss of wake flame body.

Chapter 5. Lithium salts effects on electrolytes combustion characteristics

In this Chapter, the wick-LOC method was utilized to investigate the combustion characteristics and flammability of salt-added electrolytes. Three typical lithium salts, LiPF_6 , LiBF_4 and LiTFSI , were dissolved in DMC as 1M addition to compare the influence of salts on combustion characteristics of DMC-based electrolytes. Because of the special flame behaviors given by salt-added electrolytes, the experimental procedure of the wick-LOC was improved to eliminate the disturbance of solid phase reaction. Thus, the extinction limits were determined, and the combustion residues were investigated. The potential hazards were discussed referring to the pure DMC combustion and TMP-added cases as well.

5.1. Flame behaviors at constant oxygen level

To compare the flame behaviors, the preliminary experiments for different DMC-based mixtures were conducted at 21 vol% oxygen concentration with the external flow velocity of 10 cm/s. The flame behaviors of different solvents or electrolytes were shown in Fig. 5.1. The stable flames of pure DMC, DMC with 1 wt% and 10 wt% addition of TMP were shown in Fig. 5.1 (a), (b) and (c), respectively. In contrast, the flames of electrolytes with lithium salts addition (LiPF_6 , LiBF_4 and LiTFSI) can hardly sustain the steady state and finally went to self-extinguishing, as indicated in Fig. 5.1 (d), (e) and (f) correspondingly. The solid residue of each salt-added case was recorded as the last image of each row.

Comparing with the blue flame of pure DMC, luminous yellow/orange flames of DMC with 1 wt% and 10 wt% TMP addition can be found. The luminous flame reflected the formation

of phosphorus-containing particles in the flame due to the addition of organophosphorus compound as flame retardant [45]. With more addition of TMP, the luminosity and height of the flame slightly increased. The cotton wicks in all salt-free solvents flames showed no trimming or charring during the combustion.

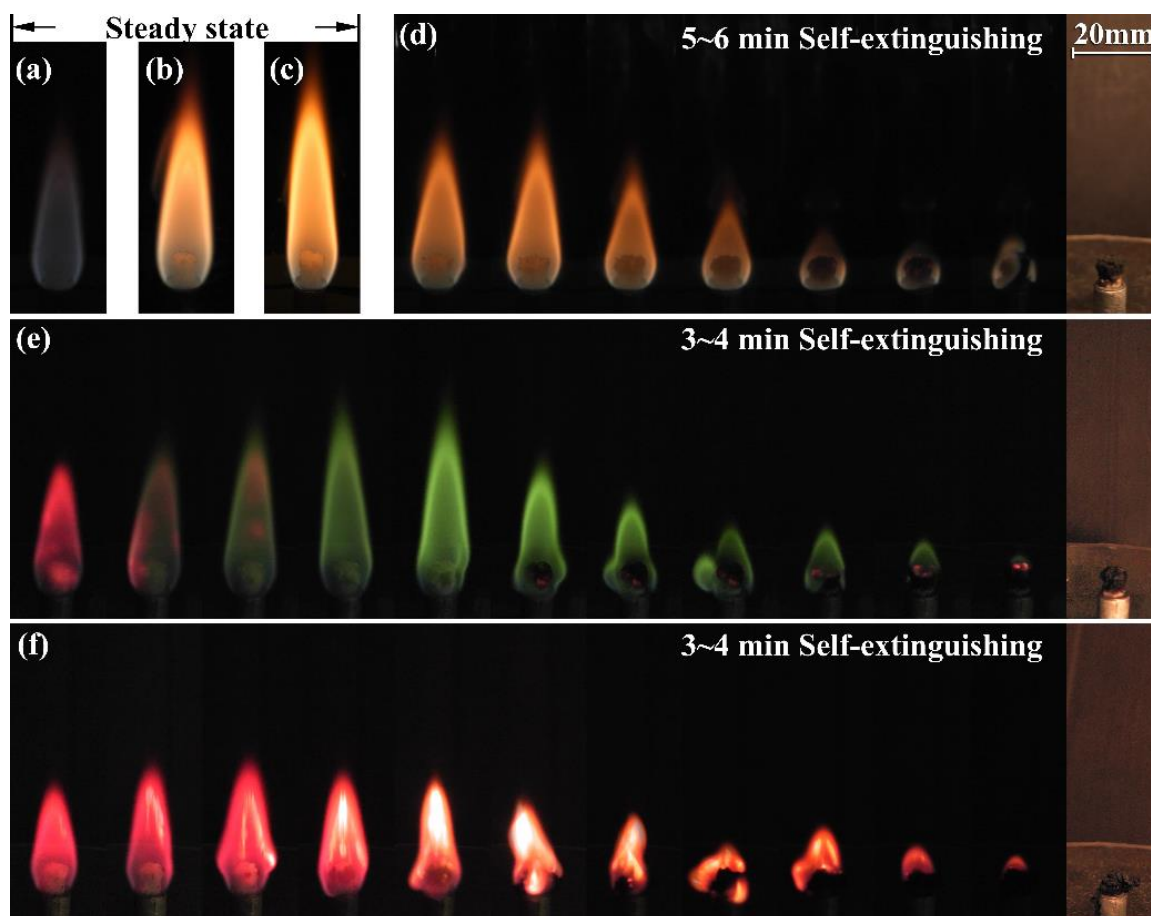


Fig. 5.1. Flame colors and burning behaviors of different DMC-based mixtures: (a) pure DMC, (b) DMC+1wt% TMP, (c) DMC+10wt% TMP, (d) DMC+1M LiPF₆, (e) DMC+1M LiBF₄, (f) DMC+1M LiTFSI.

Similarly, the electrolyte of DMC+1M LiPF₆ initially gave a yellow/orange flame, but the flame height and luminosity are lower than that of TMP-added cases. As some white solid

products formed and accumulated on the surface of the wick, the flame shrunk gradually due to insufficient fuel vapor release. Finally, the wick was charred, and the flame went to extinction. The main solid product was inferred to be lithium fluoride (LiF) as a thermal decomposition product from LiPF_6 [70]. Further residue analyses were conducted to confirm it.

The flame of DMC+1M LiBF_4 showed a unique color change during combustion. A red flame was obtained right after igniting, then it gradually changed to a green flame within 1 min, the flame height slightly increased as well. After the transition of flame color, a similar flame self-extinguishing process was observed due to the accumulation of solid products.

For the flame behavior of DMC+1M LiTFSI , the red flame can be seen throughout the burning process. Then, some bright yellow parts of the flame were generated and expanded, accompanied by the erosion and charring of the wick. Different from LiPF_6 and LiBF_4 , no accumulation of white solid products can be observed with the presence of LiTFSI , while the black viscous (char- and tar-like) residue took place because of cotton wick pyrolysis. Finally, the flame went to self-extinguishing by serious charring and insufficient fuel vapor release.

5.2. Comparison of flame extinction limits

According to the preliminary experiments in the previous section, the solid products from lithium salts decomposition would damage the surface of the wick in a continuous burning. As the fuel vapor release can be blocked by the surface accumulation of the solid products, the wick-LOC values would be overestimated when the burning time was long. Therefore, a specific procedure to determine the extinction limit with shorter burning time was required until the surface effect can be neglected. First-step was finding the approximate range of LOC by adjusting the O₂% for ignition to check whether the flame can be ignited. In the second-step, the wick soaked with electrolytes was ignited from the near-LOC conditions to generate a small flame stabilized on the top of the wick; followed by a quickly O₂ decrease with small decrement until flame extinction. Before each new ignition, the exposed wick should be cut and refreshed.

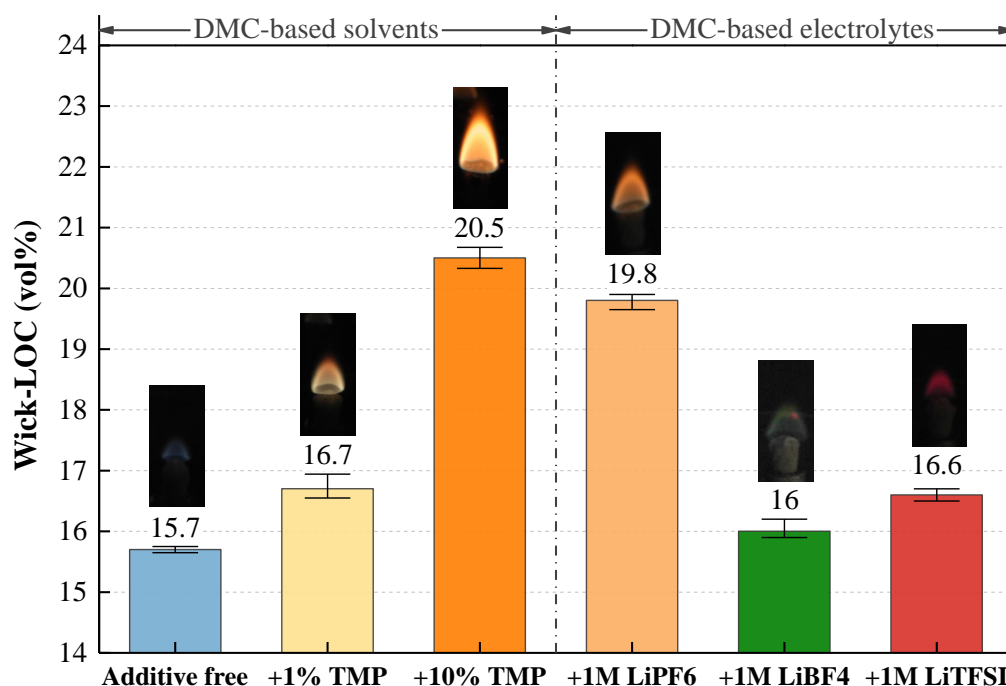


Fig. 5.2. Wick-LOC of DMC-based solvents and electrolytes.

As a result, the wick-LOC of DMC-based solvents or electrolytes were summarized in Fig. 5.2, and the images of stabilized flame near extinction limit (at LOC+0.2 vol%) were recorded correspondingly. The wick-LOC results were determined as the average value of at least four repeated tests.

With the addition of TMP as a flame-retardant additive, the wick-LOC of DMC-based solvents increased obviously. In comparison, a higher extinction limit of DMC+1M LiPF₆ showed a similar flame-retardant effect possibly due to the presence of phosphorus-containing compound in the flame. However, the wick-LOC results of DMC+1M LiBF₄ indicated the negligible effect of LiBF₄ on electrolyte flammability, even fluorine existed in the salt. The addition of 1M LiTFSI to DMC also gave a limited effect on the flame extinction, with about 1 vol% LOC increase.

5.3. Flame spectrum analyses

According to the different burning behaviors and flame extinction limits of electrolytes with three lithium salts additions, the flame spectrum analysis was conducted to clarify the salts effects on combustion, especially in flame. The light emission intensities of flames given by DMC-based solvents and different salt-added electrolytes were indicated from Fig. 5.3 to Fig. 5.5. Some radicals can be identified depending on the spectral bands at some specific wavelengths. The light emission intensity of each radical is not only related to its concentration but also to the flame temperature.

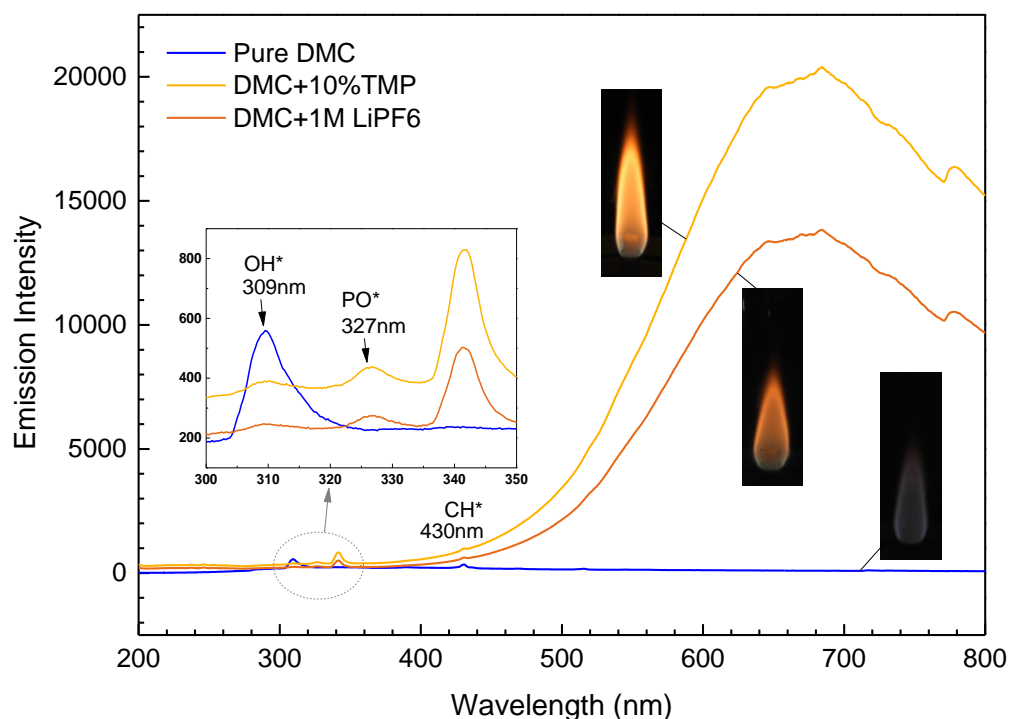


Fig. 5.3. Measured flame spectrum from different fuels: pure DMC, DMC+10 wt% TMP and DMC+1M LiPF₆.

In Fig. 5.3, the flame spectrum of pure DMC as a baseline only had two small peaks at 309nm and 430nm corresponding to the OH and CH radicals, respectively [132–134]. The flame spectrum profiles of DMC+10 wt% TMP and DMC+1M LiPF₆ were quite similar, both showed weakened emission intensities of OH and strong continuous emission of visible light. With the presence of phosphorus compounds like HPO₂, PO, PO₂ and HPO in the flame, the radicals OH and H can be captured to suppress the gas-phase combustion [47,52,57]. The small PO emission around 327 nm [135,136] and PO₂ involved in visible continua [137] suggested the a similar role of LiPF₆ and TMP in gas-phase combustion. Such behaviors were also consistent to the flame inhibition and particle formation in cup burner flame when the phosphorus containing compounds added into the oxidizers [45].

As the radical recombination were catalyzed by phosphorus oxides and acids in the flame, the effective amount of phosphorus atoms from the phosphorus element sources (LiPF₆ and TMP) dominate the effectiveness of flame inhibition. Generally, the molar fraction of phosphorus atoms is higher in DMC+1M LiPF₆ than that in DMC+10 wt% TMP, which is 1 mol/L and 0.846 mol/L, respectively. However, the flame spectrum intensities and extinction limits gave reserved results. The potential reason is that the major part of the P atoms was lost as a noneffective compound (gaseous PF₅) during the thermal decomposition of LiPF₆. Although LiPF₆ contains lithium, there was no light emission from Li radicals in the flame at 670.4 nm [108]. Most of the lithium was considered to form the most stable solid product, lithium fluoride (LiF), on the wick surface with no transport into the flame region. Therefore, the LiPF₆ addition gave two effects one the electrolyte combustion: one is the extinction limit of DMC flame due to the phosphorus from the anion; the other is the solid products formation

from the lithium. The solid residues will be clarified under following analyses.

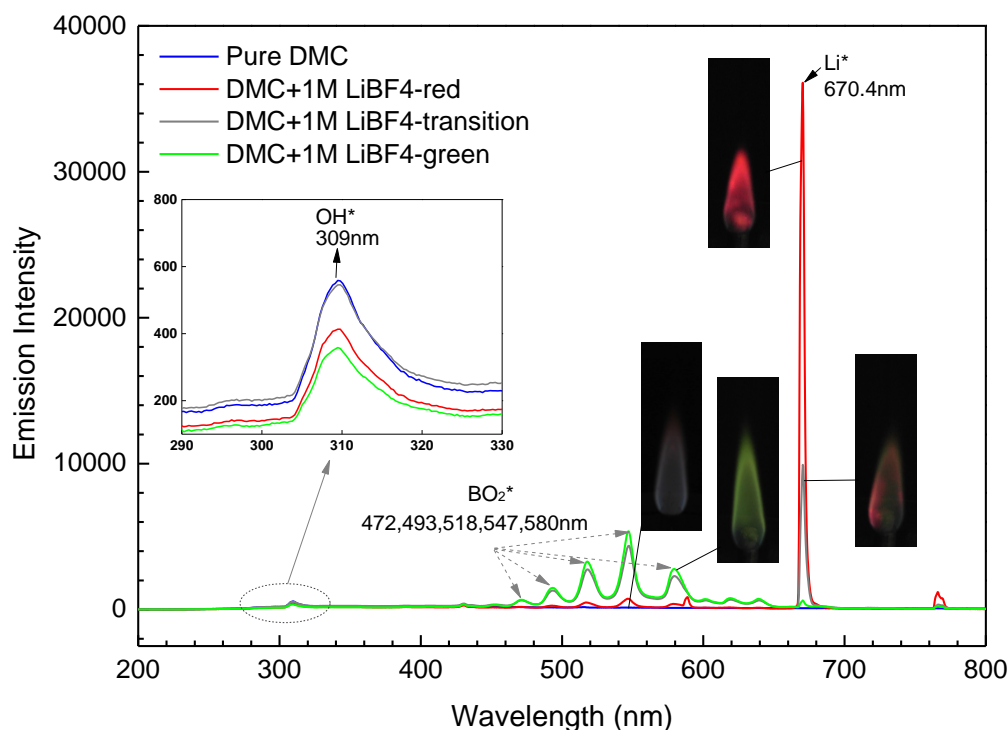


Fig. 5.4. Measured flame spectrum of DMC+1M LiBF₄ in different stages of combustion:
red flame, transition and green flame.

Comparing with pure DMC, the flame spectrum of DMC+1M LiBF₄ in different states (red flame at initiation, transition state from red to green flame, and green flame after transition) were presented in Fig. 5.4. Initially, the red flame had a strong emission intensity on 670.4 nm corresponding to Li radicals but very small intensities on the other wavelengths. During the transition of flame color, the emission intensity at 670.4 nm dropped dramatically, and some peaks from 472~580 nm becomes stronger reflecting the boron component (BO₂) release [138]. While after the transition, the clear green flame occurred because of BO₂ release. Most of the lithium were captured on the surface of the wick to form solid products (LiF), and it finally

affected the self-extinguishing of the wick flame. As shown in enlarged spectrum of OH, small difference of OH intensity can be found for pure DMC and LiBF₄ added electrolyte. Therefore, the LiBF₄ addition, especially boron atoms, had a negligible effect on the flammability of electrolyte in the gas-phased combustion.

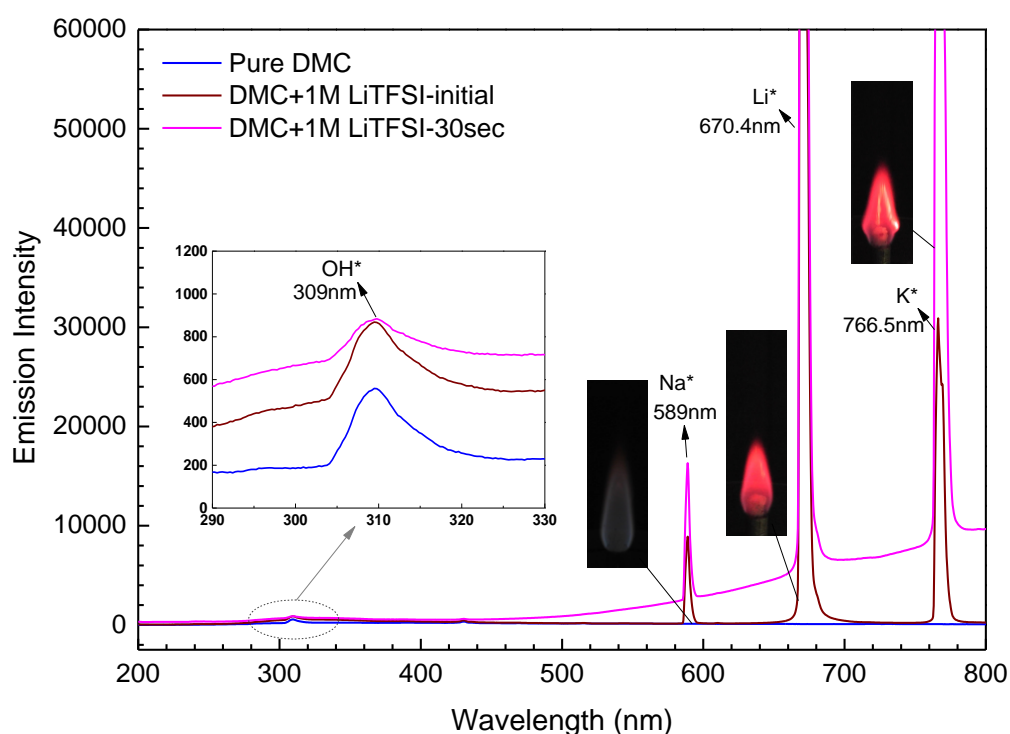


Fig. 5.5. Measured flame spectrum of DMC+1M LiTFSI in different stages of combustion: initial state and 30s after ignition.

In Fig. 5.5, as the red color existed throughout the burning of DMC+1M LiTFSI, strong intensities (exceed the boundary) at 670.4 nm showed the continuous emission of Li radicals to the flame region. After 30sec combustion, the emission intensity peaks at 589 nm and 766.5 nm wavelength increased significantly, along with the occurrences of bright yellow part in the flame and charring of the wick. These two peaks were related to the light emissions of Sodium (Na)

and Potassium (K) radicals, respectively [108], which were attributed to the pyrolysis (charring) of cotton wick [139]. The intensities of OH radical implied that the local flame temperature increases with LiTFSI addition, but the reaction rate decreased slightly when wick charring. As it has been reported that the decomposition of LiTFSI was exothermic [66,70], such heat release might cause charring of the wick. Concerning the layered structure of a LIB cell, the separator made by nonwoven fibers or polymer films could be affected by such exothermic reaction in combustion. A potential hazard is that the other solid combustibles in cell could involve into the overall combustion and make larger damage. On the other hand, the charring could be regarded as a flame-retardant effect in solid phase to prevent the heat and oxidizers. Yet the mechanism has not been fully understood, further investigations are expected.

5.4. Combustion residues analyses

The self-extinguishing of the wick flame has been found in the three salt-added cases at 21 % oxygen. Due to the solid phase behaviors on the wick surface: solid products accumulation in LiPF_6 and LiBF_4 cases, and charring in LiTFSI case, the flammable vapor was blocked from reacting with the oxidizer. To characterize the combustion residues, the SEM images were taken in comparison with the original cotton wick, as shown in Fig. 5.6.

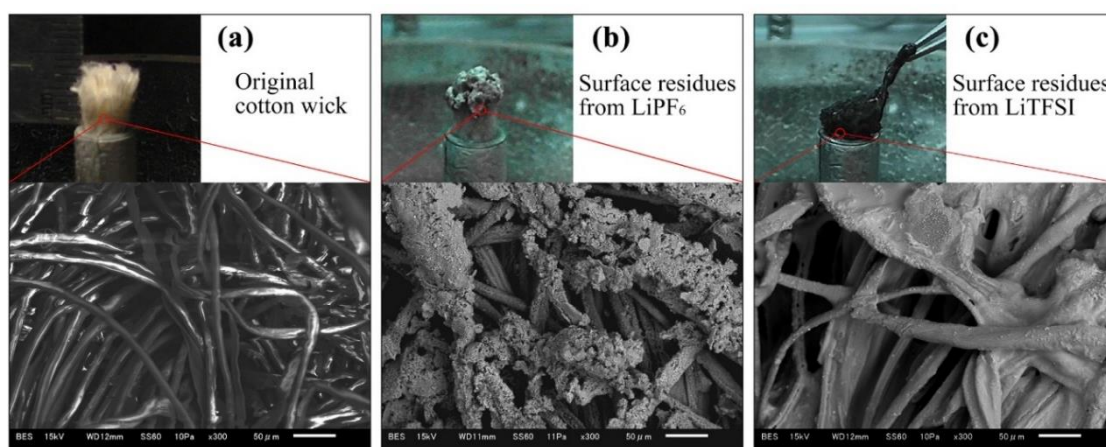


Fig. 5.6. Direct and SEM images of combustion residues on the cotton wick (a) original cotton wick, (b) LiPF_6 , (c) LiTFSI .

The SEM image of the original cotton wick [Fig. 5.6 (a)] showed a clear fibrous structure, the pores can provide the outlets to the fuel and vapor. During the combustion of LiPF_6 - and LiBF_4 -added electrolytes, the grayish-white solid products were formed on the surface of the wick. The SEM image (b) showed the solid product accumulating through the wick fibers and gradually covering the pores on the surface. In the cases of LiPF_6 and LiBF_4 addition, the wick as a porous media seemed not to react with the solid products, but it was just baked before flame

self-extinguishing. The wick for LiTFSI-added electrolyte combustion, by contrast, was charred seriously with some tar-like products formed, as can be seen in Fig. 5.6 (c). In the SEM image, the tar-like residues melt and finally covered the pores on the wick surface as well. Combining with the existed results, LiTFSI gave more complicated behaviors during the electrolyte combustion: reactive with solid combustible (cotton wick) leading to a larger damage and heat release; charring effect to suppress the flame in the later period. Due to the complexity of the combustion residues of LiTFSI-added electrolyte, more investigation on the intermediate products from LiTFSI in flame are expected in the future.

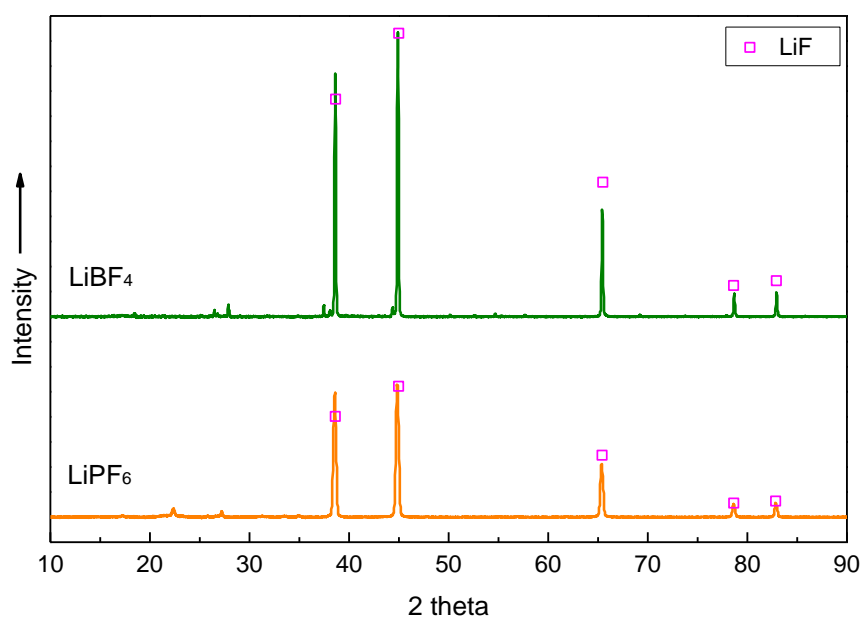


Fig. 5.7. XRD patterns of combustion residues of electrolytes adding LiBF_4 (green line) and LiPF_6 (orange line).

To identify the combustion residues of LiPF_6 - and LiBF_4 -added electrolytes, the accumulated solid residues were collected for the further XRD analysis, as shown in Fig. 5.7. Referring to the XRD pattern of lithium fluoride (LiF) [140], the crystalline material of

combustion residues in both cases are mainly composed of LiF. The XRD results confirmed the decomposition products of LiPF₆- and LiBF₄-added electrolytes even in combustion scenarios. According to the overall thermal decomposition reactions reported by Kawamura [73] and Hong [70] below, the forward reactions are promoted during combustion.



Along with the crystalline LiF accumulated on the surface, the gas products PF₅ or BF₃ released to the flame region, and some complex intermediate reactions with O₂, H₂O and DMC followed. Inferring from the flame spectrum results, the intermediate compounds like phosphorus oxides and acids can further affect the combustion chain reactions of DMC. The possible path of LiPF₆ can be suggested as Fig. 5.8.

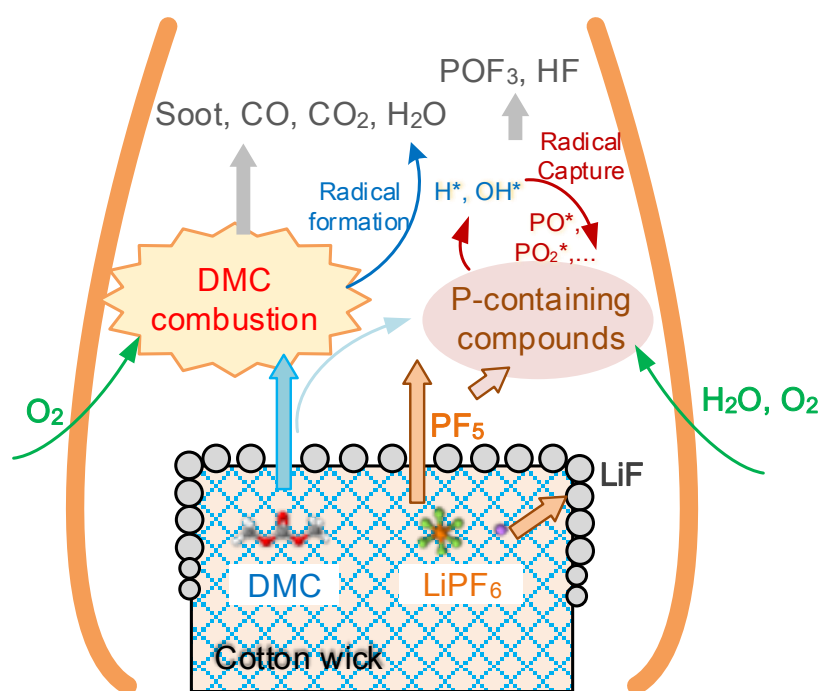


Fig. 5.8. Possible path of LiPF₆ involving in the DMC wick flame.

5.5. Concluding remarks

The combustion characteristics of DMC with lithium salts addition (LiPF_6 , LiBF_4 and LiTFSI) were investigated using the wick-LOC method, the main results are summarized below.

(1) The flame behaviors of DMC-based solvents/electrolytes at 21% oxygen were observed. Differing from the stable flame of pure DMC and TMP added solvent, the flames with salts addition always showed unsteady nature leading to self-extinguishing. The unique behaviors including different flame shapes, colors and the changes of wick surface were found as well.

(2) The flammability of electrolytes with lithium salts were successfully quantified by the wick-LOC method. It showed that the electrolyte with LiPF_6 addition has a considerable flame-retardant effect; while both LiBF_4 and LiTFSI addition has limited effect on flame extinction.

(3) With flame spectrum analysis, the unique flame behaviors of three electrolytes can be explained by the light emission of radicals. Combined with the LOC results, the anions of three lithium salts played different roles on the electrolyte combustion. The PF_6 anion in the solution had a quite similar role to the TMP additive in terms of the flame inhibition, but lower efficiency.

(4) The combustion residues were analyzed by SEM and XRD to clarify the solid behaviors in combustion. The solid products of LiF from LiPF_6 - and LiBF_4 -added electrolytes combustion confirmed the decomposition reaction proceeded in combustion scenarios. However, in the case of LiTFSI addition, the combustion complexity like serious charring brought more concern about the potential hazard of LiTFSI .

Chapter 6. Summary and future work

6.1. Significance of this work

The flammability studies on electrolyte components in LIB have been conducted utilizing a wick combustion method. The wick-LOC method was developed for the quantitative flammability evaluation of single and binary-mixed electrolyte solvents, as well as the OPC-added and salt-added electrolyte solutions. The significance of this work can be divided into three points below:

- (1) Development of the flammability test method for safer electrolyte formulations.

As mention in the introduction, the traditional flammability tests for screening safety materials in the LIB industry are expected to be improved for scientific, quantitative, and comprehensive evaluations. The proposal of the wick-LOC method was to quantify the flammability of electrolyte components from the perspective of combustion science. The results provided the wick-LOC, an extinction-related fire property in low oxygen, to fill the inadequate understanding of the electrolyte flammability. The well-specified experimental conditions ensured the reliability and reproducibility of LOC results. In addition, the limitations of the wick-LOC method on OPC- and salt-added cases were discussed to make a further development of the methodology.

- (2) Better understanding of the candle-like flame extinction mechanisms.

The study on flame stability limits of the full and wake flames revealed the unique impact of OPC additives on the candle-like flame extinctions. The two regimes found with OPC addition variations showed that adding OPC flame-retardant can change the flame extinction

from a blow-off control mechanism to a quenching control mechanism. These findings can be useful information for developing LOI-related methods when testing FR materials. It can be evidence of physical promotion effects of OPC in the condensed fuel combustion. Such effects would be concerned in the flame-retardant industry and fire suppression. For example, in the higher OPC addition cases, cooling and blowing can suppress the flame more effectively.

(3) New findings on the role of lithium salts in electrolyte combustion.

By using the simple electrolyte formulation with DMC and lithium salts, the wick flame showed unique behaviors depending on the salt additions. LiPF_6 , the most commonly used salt, shown FR effect reflected by the LOC increase, which can be a new point for the salt selection from the perspective of fire suppression. The flame spectrum and combustions residue analyses result suggested the path of LiPF_6 contributing to the electrolyte combustion. LIB fire suppression and protection research can pay more attention on the role of lithium salts.

6.2. Summary of conclusions

The wick-LOC method has been utilized to quantify the flammability limits of organic electrolyte solvents used in lithium-ion batteries. By controlling the oxygen-nitrogen ratio of external flow of the wick diffusion flame, the flammability limits (LOC) of electrolyte solvents have been determined experimentally.

In Chapter 3, validations and applications of the wick-LOC method have been conducted. The effects of axial flow velocity, exposed wick length and elapsed time after ignition on the wick-LOCs have been studied. The 10 cm/s of axis flow and 7 mm of wick length have been specified for reproducible experimental comparison. Then, the correlation analyses have shown the reliability of wick-LOC on flammability evaluation. The wick-LOC method was then

applied to quantify the flammability of binary solvent mixtures. The linear changes of wick-LOC with mixing ratios were found in the mixture of linear and cyclic carbonates, while the non-linear trends were found in carbonate-ether mixed solvents. By the flame retardancy evaluations of OPC additives, small amounts of OPCs showed significant FR effects, but the efficiency decreased with the higher OPC additions. The effectiveness of four OPCs was distinguished as DMMP > TMP(i) ~ TMP > TEP.

In Chapter 4, In-depth studies on the candle-wick flame extinction affected by OPC additions have been conducted considering the wake and full flame modes. Due to the presence of two flame modes, the determination approach of flame stability limits was improved based on the basic experimental procedure. In the case of OPC addition, the full and wake flame stability limits have been measured. The wake flame was shown to be consistently more stable at low levels of OPC addition. However, once the OPC addition exceeded a critical amount, the full flame shows higher stability with a lower LOC than the wake flame. In the most stable flame mode, the regime switched from the wake flame to the full flame with increasing OPC addition, and they were defined correspondingly as “blow-off regime” and “quenching regime”.

In Chapter 5, the DMC-based electrolytes with 1M addition of different lithium salts (LiPF₆, LiBF₄, and LiTFSI) have been studied comparing with pure DMC and TMP-added solvents. The three lithium salts gave unique and distinct flame behaviors including flame shapes, colors and the changes of wick surface until self-extinguishing. Thus, the experimental procedure was improved to obtain reliable wick-LOCs for salt-added flames. The wick-LOC results indicated a FR effect of LiPF₆ addition, while other salts have minor effects on the flame extinction. The flame spectrum and combustion residue analyses revealed the roles of salts

during combustion. The PF_6 anion played a similar role with the TMP additive in the gas phase flame inhibition. In the cases of LiPF_6 and LiBF_4 , the solid products (LiF) accumulation blocked the fuel supply from the wick to the flame region. The combustion complexity of LiTFSI on the cotton wick charring and heat release were considered as a potential hazard on solid combustible in the real fire cases.

6.3. Recommendations for future work

According to the results of the present work, the following are recommendations to pursue the studies on electrolyte flammability and candle-wick combustion method:

(1) The wick-LOC method has been used to quantify several typical electrolyte solvents used in commercial LIBs. However, more candidates of electrolyte solvent are being concerned, like triglyme, ethylene sulfite, ethyl acetate, vinylene carbonate and so on. Wider tests with clear classifications of these solvents would be useful to establish the database for the LIB electrolyte design. and the law of flammability change with different types of solvents could be summarized.

(2) The wick-LOC method was based on the candle-like diffusion flame in opposed flow configuration. Typically, such candle-like flame is extinguished due to the small Damköhler number. With this understanding, near-limit stabilized flame is under the balance of downward flame propagation speed and upward local flow velocity. As the flame base has a triple-flame structure, its propagation speed is proportional to the laminar burning velocity. Therefore, the LOC can make a correlation with the limiting laminar burning velocity under a specified local flow, which implies the strong relationship between the experimental LOC and combustion reaction rate coefficient. More fundamental studies are expected using theoretical and

numerical methods to clarify such relations for a further practical application.

(3) The OPC effects on the stability limits of the full and wake flame on the candle-wick configuration have been investigated experimentally. During the experimental work, more interesting phenomena were found, like near-limit flame oscillation and different size and luminosity of near-limit stabilized flame. More fundamental studies are expected to clarify the mechanism of such flame behaviors with OPC addition effect.

(4) For the well-formulated solution of an electrolyte, the flammability can be hardly quantified by traditional methods. Besides the wick-LOC method in present work, the ignition-related properties of electrolyte could be developed as well. With consideration of heating of LIB, oxygen generation from the cathode, and venting gases from the LIB, the ignition-related the properties are expected to give a more comprehensive evaluation of flammability.

(5) The lithium salts showed a unique impact on the combustion of electrolytes using the wick LOC method. The on-line gas chromatography could be used to draw a clearer image of a gas phased effect of lithium salts. The solid phased effects (LiF accumulation and cotton charring) can be considered as a double-edged sword for the flammability. The self-extinguishing of flame on the porous wick pointed an inspiration for the future LIB fire protection method.

References

- [1] T.R. Jow, K. Xu, O. Borodin, M. Ue, *Electrolytes for Lithium and Lithium-Ion Batteries*, Springer New York, New York, NY, 2014. doi:10.1007/978-1-4939-0302-3.
- [2] J.-M. Tarascon, M. Armand, Issues and challenges facing rechargeable lithium batteries, *Nature*. 414 (2001) 359–367. doi:10.1038/35104644.
- [3] J.B. Goodenough, Y. Kim, Challenges for Rechargeable Li Batteries †, *Chem. Mater.* 22 (2010) 587–603. doi:10.1021/cm901452z.
- [4] M. Dubarry, A. Devie, Battery durability and reliability under electric utility grid operations: Representative usage aging and calendar aging, *J. Energy Storage*. 18 (2018) 185–195. doi:10.1016/j.est.2018.04.004.
- [5] Q. Wang, B. Mao, S.I. Stoliarov, J. Sun, A review of lithium ion battery failure mechanisms and fire prevention strategies, *Prog. Energy Combust. Sci.* 73 (2019) 95–131. doi:10.1016/j.pecs.2019.03.002.
- [6] K. Matsuki, K. Ozawa, General Concepts, in: *Lithium Ion Recharg. Batter.*, Wiley-VCH Verlag GmbH & Co. KGaA, Weinheim, Germany, 2008: pp. 1–9. doi:10.1002/9783527629022.ch1.
- [7] A. Brunning, Periodic graphics: Why Li-ion batteries catch fire, *C&EN Glob. Enterp.* 94 (2016) 33–33. doi:https://doi.org/doi:10.7282/T38P62PJ.
- [8] Y. Fu, S. Lu, K. Li, C. Liu, X. Cheng, H. Zhang, An experimental study on burning behaviors of 18650 lithium ion batteries using a cone calorimeter, *J. Power Sources*. 273 (2015) 216–222. doi:10.1016/j.jpowsour.2014.09.039.
- [9] JJI, Incidents of fires and extreme heat from lithium-ion batteries on the rise in Japan, *The Japan Times*. (2019).
<https://www.japantimes.co.jp/news/2019/01/25/national/incidents-fires-extreme-heat-lithium-ion-batteries-rise-japan/#.XKC-1y-ZNhE>.
- [10] FAA HMSP Battery Incident Chart: 1991 to present, (2018).
https://www.faa.gov/hazmat/resources/lithium_batteries/media/Battery_incident_chart.pdf.
- [11] P.G. Balakrishnan, R. Ramesh, T. Prem Kumar, Safety mechanisms in lithium-ion

- batteries, *J. Power Sources*. 155 (2006) 401–414. doi:10.1016/j.jpowsour.2005.12.002.
- [12] Q. Wang, L. Jiang, Y. Yu, J. Sun, Progress of enhancing the safety of lithium ion battery from the electrolyte aspect, *Nano Energy*. 55 (2019) 93–114. doi:10.1016/j.nanoen.2018.10.035.
- [13] X. Wang, E. Yasukawa, S. Kasuya, Nonflammable Trimethyl Phosphate Solvent-Containing Electrolytes for Lithium-Ion Batteries: II. The Use of an Amorphous Carbon Anode, *J. Electrochem. Soc.* 148 (2001) A1066. doi:10.1149/1.1397774.
- [14] H.F. Xiang, H.Y. Xu, Z.Z. Wang, C.H. Chen, Dimethyl methylphosphonate (DMMP) as an efficient flame retardant additive for the lithium-ion battery electrolytes, *J. Power Sources*. 173 (2007) 562–564. doi:10.1016/j.jpowsour.2007.05.001.
- [15] P.-H. Huang, S.-J. Chang, C.-C. Li, Encapsulation of flame retardants for application in lithium-ion batteries, *J. Power Sources*. 338 (2017) 82–90. doi:10.1016/j.jpowsour.2016.11.026.
- [16] G. Nagasubramanian, K. Fenton, Reducing Li-ion safety hazards through use of non-flammable solvents and recent work at Sandia National Laboratories, *Electrochim. Acta*. 101 (2013) 3–10. doi:10.1016/j.electacta.2012.09.065.
- [17] G.G. Eshetu, S. Grugeon, H. Kim, S. Jeong, L. Wu, G. Gachot, S. Laruelle, M. Armand, S. Passerini, Comprehensive Insights into the Reactivity of Electrolytes Based on Sodium Ions, *ChemSusChem*. 9 (2016) 462–471. doi:10.1002/cssc.201501605.
- [18] J.K. Feng, X.P. Ai, Y.L. Cao, H.X. Yang, Possible use of non-flammable phosphonate ethers as pure electrolyte solvent for lithium batteries, *J. Power Sources*. 177 (2008) 194–198. doi:10.1016/j.jpowsour.2007.10.084.
- [19] E.P. Roth, C.J. Orendorff, How Electrolytes Influence Battery Safety, *Interface Mag.* 21 (2012) 45–49. doi:10.1149/2.F04122if.
- [20] M.S. Ding, K. Xu, S. Zhang, T.R. Jow, Liquid/Solid Phase Diagrams of Binary Carbonates for Lithium Batteries Part II, *J. Electrochem. Soc.* 148 (2001) A299. doi:10.1149/1.1353568.
- [21] K. Xu, Electrolytes and Interphases in Li-Ion Batteries and Beyond, *Chem. Rev.* 114 (2014) 11503–11618. doi:10.1021/cr500003w.
- [22] K. Xu, Nonaqueous Liquid Electrolytes for Lithium-Based Rechargeable Batteries,

- Chem. Rev. 104 (2004) 4303–4418. doi:10.1021/cr030203g.
- [23] T. Kawamura, A. Kimura, M. Egashira, S. Okada, J.I. Yamaki, Thermal stability of alkyl carbonate mixed-solvent electrolytes for lithium ion cells, *J. Power Sources*. 104 (2002) 260–264. doi:10.1016/S0378-7753(01)00960-0.
- [24] N. Katayama, T. Kawamura, Y. Baba, J. Yamaki, Thermal stability of propylene carbonate and ethylene carbonate–propylene carbonate-based electrolytes for use in Li cells, *J. Power Sources*. 109 (2002) 321–326. doi:10.1016/S0378-7753(02)00075-7.
- [25] V. Sharova, A. Moretti, T. Diemant, A. Varzi, R.J. Behm, S. Passerini, Comparative study of imide-based Li salts as electrolyte additives for Li-ion batteries, *J. Power Sources*. 375 (2018) 43–52. doi:10.1016/j.jpowsour.2017.11.045.
- [26] P. Ping, Q. Wang, J. Sun, H. Xiang, C. Chen, Thermal Stabilities of Some Lithium Salts and Their Electrolyte Solutions With and Without Contact to a LiFePO₄ Electrode, *J. Electrochem. Soc.* 157 (2010) A1170. doi:10.1149/1.3473789.
- [27] S. Santee, A. Xiao, L. Yang, J. Gnanaraj, B.L. Lucht, Effect of combinations of additives on the performance of lithium ion batteries, *J. Power Sources*. 194 (2009) 1053–1060. doi:10.1016/j.jpowsour.2009.06.012.
- [28] W. Li, B.L. Lucht, Inhibition of the Detrimental Effects of Water Impurities in Lithium-Ion Batteries, *Electrochem. Solid-State Lett.* 10 (2007) A115. doi:10.1149/1.2458913.
- [29] P. Murmann, X. Mönnighoff, N. von Aspern, P. Janssen, N. Kalinovich, M. Shevchuk, O. Kazakova, G.-V. Röschenthaler, I. Cekic-Laskovic, M. Winter, Influence of the Fluorination Degree of Organophosphates on Flammability and Electrochemical Performance in Lithium Ion Batteries: Studies on Fluorinated Compounds Deriving from Triethyl Phosphate, *J. Electrochem. Soc.* 163 (2016) A751–A757. doi:10.1149/2.1031605jes.
- [30] H.Y. Xu, S. Xie, Q.Y. Wang, X.L. Yao, Q.S. Wang, C.H. Chen, Electrolyte additive trimethyl phosphite for improving electrochemical performance and thermal stability of LiCoO₂ cathode, *Electrochim. Acta*. 52 (2006) 636–642. doi:10.1016/j.electacta.2006.05.043.
- [31] H. Ota, A. Kominato, W.-J. Chun, E. Yasukawa, S. Kasuya, Effect of cyclic phosphate

- additive in non-flammable electrolyte, *J. Power Sources*. 119–121 (2003) 393–398. doi:10.1016/S0378-7753(03)00259-3.
- [32] G.E. Blomgren, Liquid electrolytes for lithium and lithium-ion batteries, *J. Power Sources*. 119–121 (2003) 326–329. doi:10.1016/S0378-7753(03)00147-2.
- [33] J. Kalhoff, G.G. Eshetu, D. Bresser, S. Passerini, Safer Electrolytes for Lithium-Ion Batteries: State of the Art and Perspectives, *ChemSusChem*. 8 (2015) 2154–2175. doi:10.1002/cssc.201500284.
- [34] M.N. Golovin, Applications of Metallocenes in Rechargeable Lithium Batteries for Overcharge Protection, *J. Electrochem. Soc.* 139 (1992) 5. doi:10.1149/1.2069200.
- [35] Y. Deng, Effects of 2,4-difluorobiphenyl as an Electrolyte Additive to Enhance the Overcharge Protection of Cylindrical LiCoO₂/graphite Batteries, *Int. J. Electrochem. Sci.* 13 (2018) 5923–5937. doi:10.20964/2018.06.74.
- [36] S.L. Li, L. Xia, H.Y. Zhang, X.P. Ai, H.X. Yang, Y.L. Cao, A poly(3-decyl thiophene)-modified separator with self-actuating overcharge protection mechanism for LiFePO₄-based lithium ion battery, *J. Power Sources*. 196 (2011) 7021–7024. doi:10.1016/j.jpowsour.2010.09.111.
- [37] B.P. Matadi, S. Geniès, A. Delaille, T. Waldmann, M. Kasper, M. Wohlfahrt-Mehrens, F. Aguesse, E. Bekaert, I. Jiménez-Gordon, L. Daniel, X. Fleury, M. Bardet, J.-F. Martin, Y. Bultel, Effects of Biphenyl Polymerization on Lithium Deposition in Commercial Graphite/NMC Lithium-Ion Pouch-Cells during Calendar Aging at High Temperature, *J. Electrochem. Soc.* 164 (2017) A1089–A1097. doi:10.1149/2.0631706jes.
- [38] K. Liu, Y. Liu, D. Lin, A. Pei, Y. Cui, Materials for lithium-ion battery safety, *Sci. Adv.* 4 (2018) eaas9820. doi:10.1126/sciadv.aas9820.
- [39] <http://webbook.nist.gov/chemistry/name-ser.html>.
- [40] <http://www.chemrtp.com/>.
- [41] S.J. Harris, A. Timmons, W.J. Pitz, A combustion chemistry analysis of carbonate solvents used in Li-ion batteries, *J. Power Sources*. 193 (2009) 855–858. doi:10.1016/j.jpowsour.2009.04.030.
- [42] S. Hess, M. Wohlfahrt-Mehrens, M. Wachtler, Flammability of Li-Ion Battery

- Electrolytes: Flash Point and Self-Extinguishing Time Measurements, *J. Electrochem. Soc.* 162 (2015) A3084–A3097. doi:10.1149/2.0121502jes.
- [43] C.J. Orendorff, G. Nagasubramanian, T.N. Lambert, R. Kyle, C.A. Apblett, C.R. Shaddix, M. Geier, E. Peter, *Advanced Inactive Materials for Improved Lithium-Ion Battery Safety*, Albuquerque, New Mexico, 2012. <http://prod.sandia.gov/techlib/access-control.cgi/2012/129186.pdf>.
- [44] M.A. MacDonald, T.M. Jayaweera, E.M. Fisher, F.C. Gouldin, Inhibition of nonpremixed flames by phosphorus-containing compounds, *Combust. Flame.* 116 (1999) 166–176. doi:10.1016/S0010-2180(98)00034-0.
- [45] N. Bouvet, G.T. Linteris, V.I. Babushok, F. Takahashi, V.R. Katta, R. Krämer, A comparison of the gas-phase fire retardant action of DMMP and Br₂ in co-flow diffusion flame extinguishment, *Combust. Flame.* 169 (2016) 340–348. doi:10.1016/j.combustflame.2016.04.023.
- [46] J. Green, A Review of Phosphorus-Containing Flame Retardants, *J. Fire Sci.* 14 (1996) 353–366. doi:10.1177/073490419601400504.
- [47] T.A. Bolshova, V.M. Shvartsberg, O.P. Korobeinichev, A.G. Shmakov, A skeletal mechanism for flame inhibition by trimethylphosphate, *Combust. Theory Model.* 20 (2016) 189–202. doi:10.1080/13647830.2015.1115556.
- [48] M. Rakotomalala, S. Wagner, M. Döring, Recent Developments in Halogen Free Flame Retardants for Epoxy Resins for Electrical and Electronic Applications, *Materials (Basel)*. 3 (2010) 4300–4327. doi:10.3390/ma3084300.
- [49] V.I. Babushok, G.T. Linteris, V.R. Katta, F. Takahashi, Influence of hydrocarbon moiety of DMMP on flame propagation in lean mixtures, *Combust. Flame.* 171 (2016) 168–172. doi:10.1016/j.combustflame.2016.06.019.
- [50] F. Takahashi, V.R. Katta, G.T. Linteris, V.I. Babushok, Numerical study of gas-phase interactions of phosphorus-containing compounds with co-flow diffusion flames, *Proc. Combust. Inst.* 000 (2018) 1–9. doi:10.1016/j.proci.2018.06.140.
- [51] F. Takahashi, V. Katta, G. Linteris, V. Babushok, Numerical Simulations of Gas-Phase Interactions of Phosphorus-Containing Compounds with Cup-Burner Flames, in: *Fire Sci. Technol.* 2015, Springer Singapore, Singapore, 2017: pp. 751–758.

- doi:10.1007/978-981-10-0376-9_77.
- [52] M.M. Velencoso, A. Battig, J.C. Markwart, B. Schartel, F.R. Wurm, Molecular Firefighting-How Modern Phosphorus Chemistry Can Help Solve the Challenge of Flame Retardancy, *Angew. Chemie Int. Ed.* 57 (2018) 10450–10467. doi:10.1002/anie.201711735.
- [53] T.A. Bolshova, O.P. Korobeinichev, Promotion and inhibition of a hydrogen—oxygen flame by the addition of trimethyl phosphate, *Combust. Explos. Shock Waves*. 42 (2006) 493–502. doi:10.1007/s10573-006-0081-z.
- [54] O.P. Korobeinichev, A.G. Shmakov, V.M. Shvartsberg, Chemical Transformations in Inhibited Flames over Range of Stoichiometry, in: A. Innocenti (Ed.), *Stoichiom. Mater. Sci. - When Numbers Matter*, IntechOpen, 2012. doi:10.5772/33856.
- [55] O.P. Korobeinichev, S.B. Ilyin, V.M. Shvartsberg, A.A. Chernov, The destruction chemistry of organophosphorus compounds in flames—I: quantitative determination of final phosphorus-containing species in hydrogen-oxygen flames, *Combust. Flame*. 118 (1999) 718–726. doi:10.1016/S0010-2180(99)00030-9.
- [56] J. Liu, X. Song, L. Zhou, S. Wang, W. Song, W. Liu, H. Long, L. Zhou, H. Wu, C. Feng, Z. Guo, Fluorinated phosphazene derivative – A promising electrolyte additive for high voltage lithium ion batteries: From electrochemical performance to corrosion mechanism, *Nano Energy*. 46 (2018) 404–414. doi:10.1016/j.nanoen.2018.02.029.
- [57] B. Schartel, Phosphorus-based Flame Retardancy Mechanisms—Old Hat or a Starting Point for Future Development?, *Materials (Basel)*. 3 (2010) 4710–4745. doi:10.3390/ma3104710.
- [58] E.-G. Shim, T.-H. Nam, J.-G. Kim, H.-S. Kim, S.-I. Moon, Electrochemical performance of lithium-ion batteries with triphenylphosphate as a flame-retardant additive, *J. Power Sources*. 172 (2007) 919–924. doi:10.1016/j.jpowsour.2007.04.088.
- [59] C.L. Campion, W. Li, B.L. Lucht, Thermal Decomposition of LiPF₆-Based Electrolytes for Lithium-Ion Batteries, *J. Electrochem. Soc.* 152 (2005) A2327. doi:10.1149/1.2083267.
- [60] G.G. Botte, R.E. White, Z. Zhang, Thermal stability of LiPF₆-EC:EMC electrolyte for lithium ion batteries, *J. Power Sources*. 97–98 (2001) 570–575. doi:10.1016/S0378-

7753(01)00746-7.

- [61] M. Hietaniemi, Thermal stability of chemicals used in lithium-ion batteries, University of Oulu, 2015. <http://jultika.oulu.fi/files/nbnfioulu-201512032229.pdf>.
- [62] G.G. Eshetu, S. Jeong, P. Pandard, A. Lecocq, G. Marlair, S. Passerini, Comprehensive Insights into the Thermal Stability, Biodegradability, and Combustion Chemistry of Pyrrolidinium-Based Ionic Liquids, *ChemSusChem*. 10 (2017) 3146–3159. doi:10.1002/cssc.201701006.
- [63] X. Chen, W. Xu, M.H. Engelhard, J. Zheng, Y. Zhang, F. Ding, J. Qian, J.-G. Zhang, Mixed salts of LiTFSI and LiBOB for stable LiFePO₄-based batteries at elevated temperatures, *J. Mater. Chem. A*. 2 (2014) 2346. doi:10.1039/c3ta13043f.
- [64] H. Yang, G. V. Zhuang, P.N. Ross, Thermal stability of LiPF₆ salt and Li-ion battery electrolytes containing LiPF₆, *J. Power Sources*. 161 (2006) 573–579. doi:10.1016/j.jpowsour.2006.03.058.
- [65] C.L. Campion, W. Li, B.L. Lucht, Thermal Decomposition of LiPF₆-Based Electrolytes for Lithium-Ion Batteries, *J. Electrochem. Soc.* 152 (2005) A2327. doi:10.1149/1.2083267.
- [66] Z. Lu, L. Yang, Y. Guo, Thermal behavior and decomposition kinetics of six electrolyte salts by thermal analysis, *J. Power Sources*. 156 (2006) 555–559. doi:10.1016/j.jpowsour.2005.05.085.
- [67] A. Guéguen, D. Streich, M. He, M. Mendez, F.F. Chesneau, P. Novák, E.J. Berg, Decomposition of LiPF₆ in High Energy Lithium-Ion Batteries Studied with Online Electrochemical Mass Spectrometry, *J. Electrochem. Soc.* 163 (2016) A1095–A1100. doi:10.1149/2.0981606jes.
- [68] G.G. Eshetu, S. Grugeon, G. Gachot, D. Mathiron, M. Armand, S. Laruelle, LiFSI vs. LiPF₆ electrolytes in contact with lithiated graphite: Comparing thermal stabilities and identification of specific SEI-reinforcing additives, *Electrochim. Acta*. 102 (2013) 133–141. doi:10.1016/j.electacta.2013.03.171.
- [69] M. Dahbi, F. Ghamouss, F. Tran-Van, D. Lemordant, M. Anouti, Comparative study of EC/DMC LiTFSI and LiPF₆ electrolytes for electrochemical storage, *J. Power Sources*. 196 (2011) 9743–9750. doi:10.1016/j.jpowsour.2011.07.071.

- [70] E.-S. Hong, S. Okada, T. Sonoda, S. Gopukumar, J. Yamaki, Thermal Stability of Electrolytes with Mixtures of LiPF₆ and LiBF₄ Used in Lithium-Ion Cells, *J. Electrochem. Soc.* 151 (2004) A1836. doi:10.1149/1.1802136.
- [71] E.M. Fahmi, A. Ahmad, N.N.M. Nazeri, H. Hamzah, H. Razali, M.Y.A. Rahman, Effect of LiBF₄ salt concentration on the properties of poly(ethylene oxide)-based composite polymer electrolyte, *Int. J. Electrochem. Sci.* 7 (2012) 5798–5804. <http://www.electrochemsci.org/papers/vol7/7075798.pdf>.
- [72] H.-B. Han, S.-S. Zhou, D.-J. Zhang, S.-W. Feng, L.-F. Li, K. Liu, W.-F. Feng, J. Nie, H. Li, X.-J. Huang, Lithium bis(fluorosulfonyl)imide (LiFSI) as conducting salt for nonaqueous liquid electrolytes for lithium-ion batteries: Physicochemical and electrochemical properties, *J. Power Sources.* 196 (2011) 3623–3632. doi:10.1016/j.jpowsour.2010.12.040.
- [73] T. Kawamura, S. Okada, J. Yamaki, Decomposition reaction of LiPF₆-based electrolytes for lithium ion cells, *J. Power Sources.* 156 (2006) 547–554. doi:10.1016/j.jpowsour.2005.05.084.
- [74] M.E. Karp, Flammability limits of lithium-ion battery thermal runaway vent gas in air and the inerting effects of Halon 1301, Rutgers University, 2016. doi:<https://doi.org/doi:10.7282/T38P62PJ>.
- [75] <https://www.dekra-process-safety.co.uk/instruments/process-safety-instruments/ctl19-auto-ignition-test-apparatus-ait>.
- [76] https://commons.wikimedia.org/wiki/File:Bomb_Calorimeter.png.
- [77] T. Tsujikawa, K. Yabuta, T. Matsushita, T. Matsushima, K. Hayashi, M. Arakawa, Characteristics of lithium-ion battery with non-flammable electrolyte, *J. Power Sources.* 189 (2009) 429–434. doi:10.1016/j.jpowsour.2009.02.010.
- [78] X. Li, W. Li, L. Chen, Y. Lu, Y. Su, L. Bao, J. Wang, R. Chen, S. Chen, F. Wu, Ethoxy (pentafluoro) cyclotriphosphazene (PF₅PN) as a multi-functional flame retardant electrolyte additive for lithium-ion batteries, *J. Power Sources.* 378 (2018) 707–716. doi:10.1016/j.jpowsour.2017.12.085.
- [79] T. Dagger, C. Lürenbaum, F.M. Schappacher, M. Winter, Electrochemical performance evaluations and safety investigations of pentafluoro(phenoxy)cyclotriphosphazene as a

- flame retardant electrolyte additive for application in lithium ion battery systems using a newly designed apparatus for improved self-exting, *J. Power Sources*. 342 (2017) 266–272. doi:10.1016/j.jpowsour.2016.12.007.
- [80] S.-T. Fei, H.R. Allcock, Methoxyethoxyethoxyphosphazenes as ionic conductive fire retardant additives for lithium battery systems, *J. Power Sources*. 195 (2010) 2082–2088. doi:10.1016/j.jpowsour.2009.09.043.
- [81] ASTM D5306-92(2013), Standard Test Method for Linear Flame Propagation Rate of Lubricating Oils and, ASTM International, West Conshohocken, PA, 2013. doi:10.1520/D5306.
- [82] C. Arbizzani, G. Gabrielli, M. Mastragostino, Thermal stability and flammability of electrolytes for lithium-ion batteries, *J. Power Sources*. 196 (2011) 4801–4805. doi:10.1016/j.jpowsour.2011.01.068.
- [83] H. Nakagawa, Y. Fujino, S. Kozono, Y. Katayama, T. Nukuda, H. Sakaebe, H. Matsumoto, K. Tatsumi, Application of nonflammable electrolyte with room temperature ionic liquids (RTILs) for lithium-ion cells, *J. Power Sources*. 174 (2007) 1021–1026. doi:10.1016/j.jpowsour.2007.06.133.
- [84] C. Beyler, Flammability Limits of Premixed and Diffusion Flames, in: *SFPE Handb. Fire Prot. Eng.*, Springer New York, New York, NY, 2016: pp. 529–553. doi:10.1007/978-1-4939-2565-0_17.
- [85] M.G. Zabetakis, *Flammability Characteristics of Combustible Gases and Vapors*, Washington, DC; United States, 1965.
- [86] P.M. Osterberg, J.K. Niemeier, C.J. Welch, J.M. Hawkins, J.R. Martinelli, T.E. Johnson, T.W. Root, S.S. Stahl, Experimental Limiting Oxygen Concentrations for Nine Organic Solvents at Temperatures and Pressures Relevant to Aerobic Oxidations in the Pharmaceutical Industry, *Org. Process Res. Dev.* 19 (2015) 1537–1543. doi:10.1021/op500328f.
- [87] W. Li, H. Wang, Y. Zhang, M. Ouyang, Flammability characteristics of the battery vent gas: A case of NCA and LFP lithium-ion batteries during external heating abuse, *J. Energy Storage*. 24 (2019) 100775. doi:10.1016/j.est.2019.100775.
- [88] P.-L. Kuo, C.-H. Tsao, C.-H. Hsu, S.-T. Chen, H.-M. Hsu, A new strategy for

- preparing oligomeric ionic liquid gel polymer electrolytes for high-performance and nonflammable lithium ion batteries, *J. Memb. Sci.* 499 (2016) 462–469.
doi:10.1016/j.memsci.2015.11.007.
- [89] G. Ikeda, Oxygen Index Tests to Evaluate the Suitability of a Given Material for Oxygen Service, in: B.L. Werley (Ed.), *Flammability Sensit. Mater. Oxyg. Atmos.* ASTM STP 812, ASTM International, 1983: pp. 56–67. doi:10.1520/STP35206S.
- [90] R.F. Simmons, H.G. Wolfhard, Some limiting oxygen concentrations for diffusion flames in air diluted with nitrogen, *Combust. Flame.* 1 (1957) 155–161.
doi:10.1016/0010-2180(57)90042-1.
- [91] ISO 4589-2 Plastics Determination of burning behaviour by oxygen index, 1996.
- [92] Y. Konno, N. Hashimoto, O. Fujita, Downward flame spreading over electric wire under various oxygen concentrations, *Proc. Combust. Inst.* 37 (2019) 3817–3824.
doi:10.1016/j.proci.2018.05.074.
- [93] K. Miyamoto, X. Huang, N. Hashimoto, O. Fujita, C. Fernandez-Pello, Limiting oxygen concentration (LOC) of burning polyethylene insulated wires under external radiation, *Fire Saf. J.* 86 (2016) 32–40. doi:10.1016/j.firesaf.2016.09.004.
- [94] L. Hu, Y. Zhang, K. Yoshioka, H. Izumo, O. Fujita, Flame spread over electric wire with high thermal conductivity metal core at different inclinations, *Proc. Combust. Inst.* 35 (2015) 2607–2614. doi:10.1016/j.proci.2014.05.059.
- [95] X. Huang, S. Link, A. Rodriguez, M. Thomsen, S. Olson, P. Ferkul, C. Fernandez-Pello, Transition from opposed flame spread to fuel regression and blow off: Effect of flow, atmosphere, and microgravity, *Proc. Combust. Inst.* 37 (2019) 4117–4126.
doi:10.1016/j.proci.2018.06.022.
- [96] M.C. Johnston, J.S. T'ien, Gravimetric measurement of solid and liquid fuel burning rate near and at the low oxygen extinction limit, *Fire Saf. J.* 91 (2017) 140–146.
doi:10.1016/j.firesaf.2017.03.027.
- [97] J.W. Marcum, P. Rachow, P. V Ferkul, S.L. Olson, Low Pressure Flame Blowoff from the Forward Stagnation Region of a Blunt-nosed Cast PMMA Cylinder in Axial Mixed Convective Flow, in: 10th U. S. Natl. Combust. Meet., Eastern States Section of the Combustion Institute, College Park, Maryland, 2017: pp. 3–8.

- <https://ntrs.nasa.gov/archive/nasa/casi.ntrs.nasa.gov/20170003880.pdf>.
- [98] P.B. Sunderland, J.G. Quintiere, G.A. Tabaka, D. Lian, C.-W. Chiu, Analysis and measurement of candle flame shapes, *Proc. Combust. Inst.* 33 (2011) 2489–2496. doi:10.1016/j.proci.2010.06.095.
 - [99] Q. Wang, L. Hu, A. Palacios, S.H. Chung, Burning characteristics of candle flames in sub-atmospheric pressures: An experimental study and scaling analysis, *Proc. Combust. Inst.* 37 (2019) 2065–2072. doi:10.1016/j.proci.2018.06.113.
 - [100] L. Hu, Y. Lu, K. Yoshioka, Y. Zhang, C. Fernandez-Pello, S.H. Chung, O. Fujita, Limiting oxygen concentration for extinction of upward spreading flames over inclined thin polyethylene-insulated NiCr electrical wires with opposed-flow under normal- and micro-gravity, *Proc. Combust. Inst.* 36 (2017) 3045–3053. doi:10.1016/j.proci.2016.09.021.
 - [101] H.F. Xiang, Q.Y. Jin, C.H. Chen, X.W. Ge, S. Guo, J.H. Sun, Dimethyl methylphosphonate-based nonflammable electrolyte and high safety lithium-ion batteries, *J. Power Sources.* 174 (2007) 335–341. doi:10.1016/j.jpowsour.2007.09.025.
 - [102] R. Morford, D. Welna, C. Kellamiii, M. Hofmann, H. Allcock, A phosphate additive for poly(ethylene oxide)-based gel polymer electrolytes, *Solid State Ionics.* 177 (2006) 721–726. doi:10.1016/j.ssi.2006.01.014.
 - [103] F. Larsson, P. Andersson, P. Blomqvist, B.-E. Mellander, Toxic fluoride gas emissions from lithium-ion battery fires, *Sci. Rep.* 7 (2017) 10018. doi:10.1038/s41598-017-09784-z.
 - [104] Y. Fu, S. Lu, L. Shi, X. Cheng, H. Zhang, Combustion Characteristics of Electrolyte Pool Fires for Lithium Ion Batteries, *J. Electrochem. Soc.* 163 (2016) A2022–A2028. doi:10.1149/2.0721609jes.
 - [105] G.G. Eshetu, J.-P. Bertrand, A. Lecocq, S. Grugeon, S. Laruelle, M. Armand, G. Marlair, Fire behavior of carbonates-based electrolytes used in Li-ion rechargeable batteries with a focus on the role of the LiPF₆ and LiFSI salts, *J. Power Sources.* 269 (2014) 804–811. doi:10.1016/j.jpowsour.2014.07.065.
 - [106] ASTM D1322-97, Standard Test Method for Smoke Point of Kerosine and Aviation Turbine Fuel, ASTM International, West Conshohocken, PA, 1997.

doi:10.1520/D1322-97.

- [107] C. Romero, X. Li, S. Keyvan, R. Rossow, Spectrometer-based combustion monitoring for flame stoichiometry and temperature control, *Appl. Therm. Eng.* 25 (2005) 659–676. doi:10.1016/j.applthermaleng.2004.07.020.
- [108] W. Yan, Y. Ya, F. Du, H. Shao, P. Zhao, Spectrometer-Based Line-of-Sight Temperature Measurements during Alkali-Pulverized Coal Combustion in a Power Station Boiler, *Energies*. 10 (2017) 1375. doi:10.3390/en10091375.
- [109] Y. Nakamura, K. Kizawa, S. Mizuguchi, A. Hosogai, K. Wakatsuki, Experimental Study on Near-Limiting Burning Behavior of Thermoplastic Materials with Various Thicknesses Under Candle-Like Burning Configuration, *Fire Technol.* 52 (2016) 1107–1131. doi:10.1007/s10694-016-0567-5.
- [110] O. Fujita, Solid combustion research in microgravity as a basis of fire safety in space, *Proc. Combust. Inst.* 35 (2015) 2487–2502. doi:10.1016/j.proci.2014.08.010.
- [111] S. Takahashi, T. Ebisawa, S. Bhattacharjee, T. Ihara, Simplified model for predicting difference between flammability limits of a thin material in normal gravity and microgravity environments, *Proc. Combust. Inst.* 35 (2015) 2535–2543. doi:10.1016/j.proci.2014.07.017.
- [112] A. Kumar, J. Tien, A computational study of low oxygen flammability limit for thick solid slabs, *Combust. Flame*. 146 (2006) 366–378. doi:10.1016/j.combustflame.2006.02.008.
- [113] M. Thomsen, X. Huang, C. Fernandez-Pello, D.L. Urban, G.A. Ruff, Concurrent flame spread over externally heated Nomex under mixed convection flow, *Proc. Combust. Inst.* 37 (2019) 3801–3808. doi:10.1016/j.proci.2018.05.055.
- [114] K. Maruta, K. Tsuboi, S. Takahashi, Limiting Oxygen Concentration of Flame Resistant Material in Microgravity Environment, *Int. J. Microgravity Sci. Appl.* 34 (2017) 340304. doi:10.15011/jasma.34.340304.
- [115] J.S. T'ien, M.P. Raju, Two-Phase Flow inside an Externally Heated Axisymmetric Porous Wick, *J. Porous Media*. 11 (2008) 701–718. doi:10.1615/JPorMedia.v11.i8.10.
- [116] M.S. Ding, K. Xu, T.R. Jow, Liquid-Solid Phase Diagrams of Binary Carbonates for Lithium Batteries, *J. Electrochem. Soc.* 147 (2000) 1688. doi:10.1149/1.1393419.

- [117] T.M. Jayaweera, C.F. Melius, W.J. Pitz, C.K. Westbrook, O.P. Korobeinichev, V.M. Shvartsberg, A.G. Shmakov, I.V. Rybitskaya, H.J. Curran, Flame inhibition by phosphorus-containing compounds over a range of equivalence ratios, *Combust. Flame*. 140 (2005) 103–115. doi:10.1016/j.combustflame.2004.11.001.
- [118] E.L. Charsley, R.A. Schulz, An apparatus for the measurement of critical oxygen index incorporating a paramagnetic oxygen analyser, *J. Phys. E*. 8 (1975) 147–149. doi:10.1088/0022-3735/8/2/024.
- [119] M. Sibulkin, M. Little, Propagation and extinction of downward burning fires, *Combust. Flame*. 31 (1978) 197–208. doi:10.1016/0010-2180(78)90129-3.
- [120] A. Alsairafi, S.-T. Lee, J.S. T'ien*, Modeling gravity effect on diffusion flames stabilized around a cylindrical wick saturated with liquid fuel, *Combust. Sci. Technol.* 176 (2004) 2165–2191. doi:10.1080/00102200490515038.
- [121] A. Kumar, J.S. T'ien, Numerical Modeling of Limiting Oxygen Index Apparatus for Film Type Fuels, *Int. J. Spray Combust. Dyn.* 4 (2012) 299–322. doi:10.1260/1756-8277.4.4.299.
- [122] H. Kooama, K. Miyasaka, A.C. Fernandez-Pello, Extinction and Stabilization of a Diffusion Flame on a Flat Combustible Surface with Emphasis on Thermal Controlling Mechanisms, *Combust. Sci. Technol.* 54 (1987) 37–50. doi:10.1080/00102208708947042.
- [123] C.-P. Mao, H. Kodama, A.C. Fernandez-Pello, Convective structure of a diffusion flame over a flat combustible surface, *Combust. Flame*. 57 (1984) 209–236. doi:10.1016/0010-2180(84)90058-0.
- [124] J.L. Torero, T. Vietoris, G. Legros, P. Joulain, Estimation of a total mass transfer number from the standoff distance of a spreading flame, *Combust. Sci. Technol.* 174 (2002) 187–203. doi:10.1080/713712953.
- [125] J.S. T'ien, M. Endo, Material Flammability: A Combustion Science Perspective, *Procedia Eng.* 62 (2013) 120–129. doi:10.1016/j.proeng.2013.08.049.
- [126] W.Y. CHAN, J.S. T'ien, An Experiment on Spontaneous Flame Oscillation Prior to Extinction, *Combust. Sci. Technol.* 18 (1978) 139–143. doi:10.1080/00102207808946845.

- [127] F. Guo, W. Hase, Y. Ozaki, Y. Konno, M. Inatsuki, K. Nishimura, N. Hashimoto, O. Fujita, Experimental study on flammability limits of electrolyte solvents in lithium-ion batteries using a wick combustion method, *Exp. Therm. Fluid Sci.* 109 (2019) 109858. doi:10.1016/j.expthermflusci.2019.109858.
- [128] N. Bouvet, G. Linteris, V. Babushok, F. Takahashi, V. Katta, R. Krämer, Experimental and numerical investigation of the gas-phase effectiveness of phosphorus compounds, *Fire Mater.* 40 (2016) 683–696. doi:10.1002/fam.2319.
- [129] J.S. T'ien, The possibility of a reversal of material flammability ranking from normal gravity to microgravity, *Combust. Flame.* 80 (1990) 355–357. doi:10.1016/0010-2180(90)90111-4.
- [130] S.H. Chung, Stabilization, propagation and instability of tribrachial triple flames, *Proc. Combust. Inst.* 31 (2007) 877–892. doi:10.1016/j.proci.2006.08.117.
- [131] BS EN ISO 4589-2:1999, *Plastics - Determination of burning behaviour by oxygen index - Part 2: Ambient-temperature test*, The British Standards Institution, 1999. doi:10.3403/01894062.
- [132] T.F. Guiberti, D. Durox, T. Schuller, Flame chemiluminescence from CO₂ - and N₂ - diluted laminar CH₄/air premixed flames, *Combust. Flame.* 181 (2017) 110–122. doi:10.1016/j.combustflame.2017.01.032.
- [133] T. Kathrotia, *Reaction Kinetics Modeling of OH*, CH*, and C₂* Chemiluminescence*, Heidelberg University, 2011. doi:10.11588/heidok.00012027.
- [134] T. García-Armingol, Y. Hardalupas, A.M.K.P. Taylor, J. Ballester, Effect of local flame properties on chemiluminescence-based stoichiometry measurement, *Exp. Therm. Fluid Sci.* 53 (2014) 93–103. doi:10.1016/j.expthermflusci.2013.11.009.
- [135] M.D. Huang, H. Becker-Ross, S. Florek, U. Heitmann, M. Okruss, Determination of phosphorus by molecular absorption of phosphorus monoxide using a high-resolution continuum source absorption spectrometer and an air–acetylene flame, *J. Anal. At. Spectrom.* 21 (2006) 338–345. doi:10.1039/B512986A.
- [136] P.A. Hamilton, T.P. Murrells, Mechanism for the chemiluminescence in oxygen-phosphorus system, *J. Phys. Chem.* 90 (1986) 182–185. doi:10.1021/j100273a041.
- [137] M.E. Fraser, D.H. Stedman, Spectroscopy and mechanism of chemiluminescent

- reactions between group V hydrides and ozone, *J. Chem. Soc. Faraday Trans. 1 Phys. Chem. Condens. Phases.* 79 (1983) 527. doi:10.1039/f19837900527.
- [138] S.A. Hashim, S. Karmakar, A. Roy, Combustion Characteristics of Boron-HTPB-Based Solid Fuels for Hybrid Gas Generator in Ducted Rocket Applications, *Combust. Sci. Technol.* 00 (2018) 1–19. doi:10.1080/00102202.2018.1544973.
- [139] P.J. Wakelyn, *Cotton Fiber Chemistry and Technology*, CRC Press, 2006. doi:10.1201/9781420045888.
- [140] G.I. Finch, S. Fordham, The effect of crystal-size on lattice-dimensions, *Proc. Phys. Soc.* 48 (1936) 85–94. doi:10.1088/0959-5309/48/1/312.

Appendix

Table A. 1 Specification of combustion chamber

Chamber inner diameter:	80 mm
Chamber outer diameter:	88 mm
Chamber height:	220 mm
Chamber material:	Pyrex glass, acrylic
Honeycomb outer diameter:	80 mm
Honeycomb central hole diameter:	8 mm
Honeycomb number:	2
Honeycomb thickness:	10 mm
Wick height:	7 mm \pm 0.5mm
Wick diameter:	4 mm
Stainless tube outer diameter:	8 mm
Stainless tube inner diameter:	6 mm
Axial flow velocity:	4 cm/s \sim 18 cm/s
Oxygen range:	Depends on flow velocity, 0~45% in 10cm/s

Table A. 2 Specification of temperature measurement devices

Camera:	Panasonic, HDC-TM70
Focus mode:	Manual focus (FM) on flame
White balance:	Same flame color as observation
Frame rate:	60 fps

Table A. 3 Specification of flame spectrometer

Spectrometer:	Hamamatsu mini Spectrometer C10082CA
Spectral response range:	200 \sim 800 nm
Spectral resolution:	4 nm
A/D resolution:	16 bits
Built-in sensor:	Back-thinned CCD image sensor
Number of total pixels:	2048 pixels

Table A. 4 Specification of temperature measurement devices

Thermocouple:	R-type
Wire diameter:	0.3 mm
Junction (molten ball) diameter:	0.7 mm
Temperature measurement error:	± 40 K
Measurable directions:	Axial and radial directions
Measurement interval:	3mm for axial; 1 mm for radial.
Data logger:	GRAPHTEC, midi LOGGER GL900
Measurement period:	15 s for once
Movable range:	Axial: 50 mm; radial: 25 mm

Achievements

Journal publications:

1. **F. Guo**, Y. Ozaki, K. Nishimura, N. Hashimoto, O. Fujita, Experimental study on flame stability limits of lithium ion battery electrolyte solvents with organophosphorus compounds addition using a candle-like wick combustion system, *Combust. Flame*. 207 (2019) 63–70. doi:10.1016/j.combustflame.2019.05.019.
2. **F. Guo**, W. Hase, Y. Ozaki, Y. Konno, M. Inatsuki, K. Nishimura, N. Hashimoto, O. Fujita, Experimental study on flammability limits of electrolyte solvents in lithium-ion batteries using a wick combustion method, *Exp. Therm. Fluid Sci.* 109 (2019) 109858. doi:10.1016/j.expthermflusci.2019.109858.
3. **F. Guo**, Y. Ozaki, K. Nishimura, N. Hashimoto, O. Fujita, Influence of lithium salts on the combustion characteristics of dimethyl carbonate-based electrolytes using a wick combustion method, *J. Hazard. Mater.* (2019) (submitted).
4. Y. Gao, G. Zhu, M. Yu, **F. Guo**, Y. Xia, W. An, Experimental study of welding region effects on upward flame spread over textile membranes, *Text. Res. J.* 89 (2019) 2041–2053. doi:10.1177/0040517518783368.
5. Y. Xia, G. Zhu, **F. Guo**, Y. Gao, H. Tao, Effect of DPK flame retardant on combustion characteristics and fire safety of PVC membrane, *Case Stud. Therm. Eng.* 10 (2017) 656–663. doi:10.1016/j.csite.2017.07.002.
6. Y. Xia, G. Zhu, Y. Gao, **F. Guo**, Use of Cone Calorimeter for Estimating Fire Behavior of PVC Membranes, *Procedia Eng.* 211 (2018) 810–817. doi:10.1016/j.proeng.2017.12.079.
7. **F. Guo**, G. Zhu, “Analysis on upward flame spread characteristics of EPS insulation system in specific scenarios,” *Fire Science and Technology*, 2015. 34(7): p. 853-856. (in Chinese)
8. **F. Guo**, G. Zhu, “Fire simulation of EPS exterior insulation system in L-shaped building,” *Fire Science and Technology*, 2015. 34(10): p. 1333-1341. (in Chinese)

Conference presentations:

1. **F. Guo**, Y. Ozaki, K. Nishimura, N. Hashimoto, O. Fujita, “Influence of three lithium salts on the flame behaviors and extinction limits of dimethyl carbonate-based electrolytes using a wick combustion method,” *12th Asia-Pacific Conference on Combustion*, Fukuoka, Japan, (2019.07, Oral presentation)
2. **F. Guo**, Y. Ozaki, K. Nishimura, N. Hashimoto, O. Fujita, “Flame stability limits of Li-ion battery electrolyte solvents with organophosphorus compounds addition on a wick-stabilized flame,” *56th Symposium (Japanese) on Combustion*, Sakai, Japan, (2018.11, Oral presentation)
3. **F. Guo**, K. Nishimura, N. Hashimoto, O. Fujita, “Low Oxygen Extinction Behavior of Li-ion Batteries Electrolyte with Phosphorus-based Flame Retardant in a Wick Combustion System,” *55th Symposium (Japanese) on Combustion*, Toyama, Japan, (2017.11, Oral presentation).
4. Y. Ozaki, **F. Guo**, O. Fujita, N. Hashimoto, K. Nishimura, “Deposition Analysis of residue after burning the electrolyte solvent adding Li-salt used in LIB,” *2019 JAFSE Annual Symposium*, Tokyo, Japan, (2019.05, Oral presentation)
5. Y. Ozaki, **F. Guo**, O. Fujita, N. Hashimoto, K. Nishimura, “Flammability change due to mixing of LIB electrolyte solvent by Wick-LOC method,” *47th Student Lecture of Graduation Research presented by JSME Hokkaido Branch*, Sapporo, Japan, (2018.03, Oral presentation)

Awards:

1. Selected as scholarship student supported from China Scholarship Council, China (2016.10).
2. Selected for the recipient of NITOE School Project Grant and Project Excellent Grant (a grant of JPY300,000 plus JPY200,000) from Frontier Foundation, Hokkaido University. (2018.10)